2004

Comparison studies of the mechanistic formation of polyhalogentaed dibenzo-p-dioxins and furans from the thermal degradation of 2-bromophenol and 2-chlorophenol

Catherine Spearing Evans
Louisiana State University and Agricultural and Mechanical College, cevans2@lsu.edu

COMPARISON STUDIES OF THE MECHANISTIC FORMATION OF POLYHALOGENATED DIBENZO-P-DIOXINS AND FURANS FROM THE THERMAL DEGRADATION OF 2-BROMOPHENOL AND 2-CHLOROPHENOL

A Dissertation

Submitted to the Graduate Faculty of the
Louisiana State University and
Agricultural and Mechanical College
in partial fulfillment of the
requirements for the degree of
Doctor of Philosophy

in

The Department of Chemistry

by
Catherine Spearing Evans
B. S., University of the South, Sewanee, Tennessee, 1998
December 2004

ACKNOWLEDGEMENTS

I would like to thank Dr. Barry Dellinger for all of his help and support during my studies and also giving me the opportunity to do this work.

I would never have accomplished all that I have without the constant wisdom, invaluable insight and understanding of Dr. Lavrent Khachatryan and Dr. Alexander Burcat.

I am also very grateful for the support of the Barry Dellinger Group, especially Slawo Lomnicki as well as Raphael Cueto. They helped considerably in assisting me in starting my research.

Thank you to my committee members for donating the time to read my thesis and their invaluable comments.

Finally, I would like to thank my family for their constant support and believing that I could accomplish something that is very different from what they expected.

TABLE OF CONTENTS

LIST OF TABLES

LIST OF FIGURES

ABSTRACT

Emissions of polychlorinated dibenzo-*p*-dioxins and furans (PCDD/Fs) and polybrominated dibenzo-*p*-dioxins and furans (PBDD/Fs) from hazardous waste incinerators, and many other sources for combustion have been considered environmentally hazardous and a major health threat. Recently, a growing number of materials containing brominated hydrocarbons, commonly used flame retardants, have been disposed in municipal and hazardous waste incinerators. This results in the increased potential for formation of PBDD/Fs and other hazardous combustion by-products. In contrast to chlorinated hydrocarbons, the reactions of brominated hydrocarbons have been studied only minimally. In fact, studies have shown that brominated phenols form higher yields of PBDD/Fs than the analogous chlorinated phenols form PCDD/Fs. For this study, the individual homogeneous, gas-phase oxidative and pyrolytic thermal degradations of 2-bromophenol and 2-chlorophenol were studied in a 1 cm i.d., fused silica flow reactor at a concentration of 88 ppm, with a reaction time of 2.0 s, and over a temperature range of 300 to 1000°C. In addition, 50:50 mixture of 2-chlorophenol and 2-bromophenol with a combined concentration of 88 ppm was studied under similar conditions. Also in order to compare previous work with 2-chlorophenol, the surface catalyzed gas-phase reactions for 2-bromophenol to form PBDD/Fs are described over a temperature range from 250 to 550°C. The results are compared and contrasted with each other in order to understand the roles oxygen, chlorine and bromine play in the formation of PCDD/Fs and PBDD/Fs. Reaction pathways to PCDD/F and PBDD/F products as well as all other products detected are proposed that are consistent with the experimental data for each condition. The presence of oxygen increases the formation of PBDFs and PCDFs. Presence of bromine increases the concentration of Cl radicals, which in turn increases chlorination and formation of 4,6-dichlorodibenzofuran (4,6-DCDF).

However the yields of the PCDFs and PBDFs are considerably less with the presence of both bromine and oxygen. The pool of •OH and concentration of the chlorine atoms is reduced and thus prevents these furans from becoming major products.

CHAPTER 1. INTRODUCTION

1.1 Introduction of the Presence of Brominated Hydrocarbons

Brominated hydrocarbons (BHCs) are useful in a variety of applications. Bromine is used as an alternative to chlorine in water purification in swimming pools. In addition, BHCs are used in agriculture as effective pesticides, important ingredients of many over the counter and prescription drugs, in batteries for electric cars and necessary for photo development and capturing sufficient light in photographs. However the largest use for BHCs is as flame retardants [1]. The purpose of the flame retardants is to hinder the ignition or reduce the propagation of a fire. Depending on their nature, flame retardants can act chemically and/or physically in the solid, liquid or gas phase. They interfere with combustion during a particular stage of this process, either during heating, decomposition, ignition or flame spread. Flame retardants are used in many appliances and electronic equipment such as computers, TVs, mobile phones, furniture, insulation boards, plastics and many others. Other flame retardants include chlorinated flame retardants, phosphorous-containing flame retardants, inorganic flame retardants and nitrogen-containing flame retardants. The choice of which flame retardant depends on the type of application, the material, fire safety standards, cost considerations and recyclability.

BHCs are the most effective flame retardants in comparison with the other flame retardant choices because they are cost effective in that lower quantities are needed to achieve the same fire resistancy [1]. In addition, brominated flame retardants (BFRs) are effective in that they work in the gas-phase of the combustion process by interfering with the radical chain mechanism in bromine removing the OH and H radicals and considerably slow or prevent the burning process [1- 2]. They also meet higher fire safety standards than the other flame

retardants [1]. They are especially ideal for plastics because they remain unaffected by the temperature at which the plastic is processed and they do not change the physical properties of the plastic [1-3].

There has been an increase in the use of brominated flame retardants (BFRs) in the recent years. In 1992 around 600,000 tons of flame retardants were used world wide and 25% of those compounds were BFRs [4-5]. The level of BFRs has increase to 39% in 1999 of the total world-wide production of flame retardants [1]. There are four major types of BFRs: polybrominated biphenyls (PBBs), polybrominated biphenyl ethers (PBDEs), tetrabromobisphenol – A (TBBPA) and hexabromocyclododecane (HBCD) (Figure 1.1). BFRs that are chemically bound to plastic

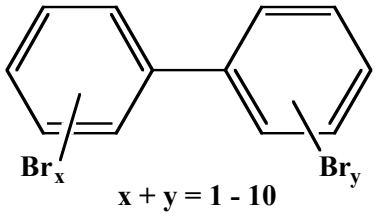

Polybrominated biphenyls (PBBs)

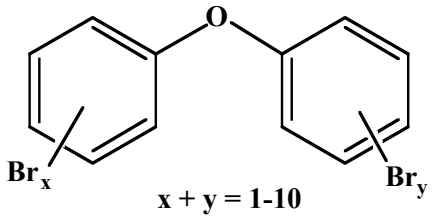

Polybrominated diphenyl ethers (PBDEs)

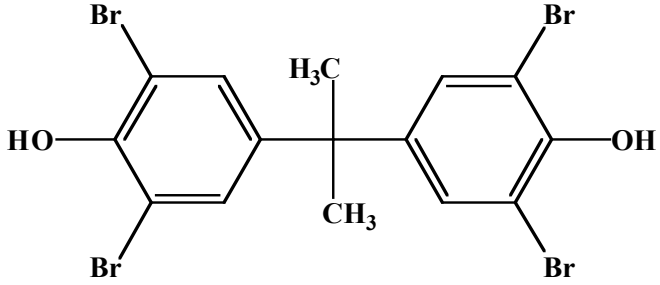

Tetrabromobisphenol A (TBBPA)

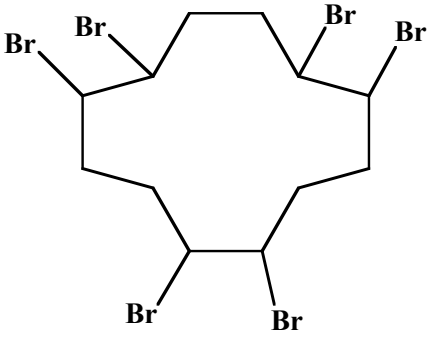

Hexabromocyclododecane (HBCD)

Figure 1.1 The Four Major Types of Brominated Flame Retardants

are called reactive while other BFRs mixed into polymers and not chemically bound are called additive. TBBPA is used as a reactive flame retardant in polyesters, epoxy resins and printed circuit boards. PBDEs, PBBs and HBCD are primarily used in plastics as additive flame retardants. TBBPA can also be used as an additive flame retardant in plastics as well. The chemical bonding of the BFR decides the mobility of the BFR in the material and affects the emission of the flame retardant into the environment.

PBDEs and TBBPA are the major BFRs used in various forms of plastic, paints, textiles, thermo sets and printed circuit boards [1-2]. In 1999, TBBPA was the major BFRs produced and accounted for 59% of the total production of BFRs [1]. PBDEs accounted for 33% of the total production of BFRs in 1999 [1]. In fact the United States has the highest concentrations of PBDEs emissions in the world [1]. The most commonly used PBDEs in descending order are decaBDE, octaBDE and pentaBDE. HBCD only accounted for about 8% of the total BFRs. Due to their similarity in toxicity to polychlorinated biphenyls (PCBs), PBBs are no longer used as BFRs [1-5].

Recently, there has also been an increase in the levels of PBDEs present in human blood [6-7], breast milk [8-9], fish [10-11] and other wildlife [13-14]. In Sweden, the concentrations of PBDEs found in breast milk have doubled every five years for the past 25 years [15]. A recent study in the San Francisco Bay Area found that women contained 3 times the concentration of PBDEs in their breast milk than the results observed in Sweden [16]. Evidence of BFRs have also been observed in sewage sludge, water, sediment, indoor air and dust [17-19]. In the cases for indoor air, some of the BFRs studied are seen at levels higher than the government health based guidelines [17-18]. With this increase in BHCs observed in numerous sources and their presence in humans and animals, the understanding of how they get from these sources to the

humans and animals is still undetermined [20]. However, it is generally considered that they originate from a combination of different sources mainly electronic waste recycling and combustion sources [6, 21-24].

Emissions of BHCs have been reported from various combustion sources [21-24]. Materials containing BFRs and other brominated materials are also subject to accidental fires [25]. Because the presence of bromine inhibits combustion, the conditions in these accidental fires will be sufficient to inhibit complete combustion, thus increasing the likelihood of formation of products of incomplete combustion (PICs). This results in increased concern over potential emissions of PICs, mainly polybrominated dibenzo-*p*-dioxins and dibenzofurans (PBDD/Fs). Similarly brominated phenols as well as PBDEs have been identified as precursors to PBDD/Fs [26-28]. In fact, brominated phenols are also intermediates to formation of PBDEs, PBBs and TBBPA as well. Some studies have shown that brominated phenols may form more PBDD/Fs than the analogous chlorinated phenols form polychlorinated dibenzo-*p*-dioxins and dibenzofurans (PCDD/Fs) [26, 29]. Previous work has also shown that the addition of bromine during combustion increases the production of PBDD/Fs, PCDD/Fs, and mixtures of brominated and chlorinated dibenzo-*p*-dioxins and dibenzofurans [30-31]. Some research also suggests that bromination is 10 times more efficient than chlorination [26]. This has been attributed to the predominant form of bromine being Br_2 versus HCl for chlorine [30]. The addition of bromine not only increases bromination but also increases chlorination with bromine serving as a good leaving group for displacement by chlorine [30-32].

With this knowledge, it is interesting to note that the toxicity of the PBDD/Fs has been shown to be similar to the analogous PCDD/Fs [33-34]. Some PBDEs and PBDD/Fs are reported as known endocrine disruptors [34-35]. Endocrine disruptors are described as chemicals

that cause a hormonal imbalance by out-competing the body's natural hormones. PBDEs can cause liver and neurodevelopment toxicity, affect the thyroid hormone levels and disrupt the development of human and animal fetuses. TBBPA was also found to have a high potential in interfering with the natural thyroid hormone metabolism [35]. PentaBDEs are considered to have the greatest number of health effects. They are persistent, bio-accumulative and highly toxic to aquatic animals [36, 37]. The octa- and decaBDE have not been as extensively studied as pentaBDEs but these PBDEs can be debrominated by UV light to lower brominated PBDEs such as pentaBDE [38-39]. In addition to being possible endocrine disruptors, PBDD/Fs are considered potential carcinogens as well [33]. One study discovered that the PBDD/Fs have the potential to cause dermal, heptic and gastrointestinal toxicities in humans [33]. While at this present time the levels of the brominated hydrocarbons found in humans are not at high enough concentrations to be harmful to humans, the increase in the use of brominated hydrocarbons every year will only lead to an increase in levels that could be potentially become hazardous [6, 8-10].

Europe is leading the way in the regulations of numerous BFRs. The European Union (EU) parliament has already issued a ban of the use of pentaBDE and octaBDE in all applications by August 2004 with the intention of banning decaBDE by 2006 [1, 2, 37]. The EU is also in the process of providing risk assessments for decaBDE, HBDE and TBBPA as well [1, 37]. The use of PBBs as flame retardants was phased out in 2000 in Europe since they are potential endocrine disrupting chemicals [1-2]. The Brominated Flame Retardants Industry signed a Voluntary Industry Commitment (VIC) with Organization for Economic Co-operation and Development (OECD) in 1995 stating that PBBs will not be produced, imported or exported [1]. At the present time, the United States is utilizing the VIC in eliminating the production of

PBBs. Other than this voluntary ban, the United States does not currently have regulations on any BFRs. Though as of March 2004, a draft bill is under consideration that would prohibit the use of two PBDES, pentaBDE and octaBDE in the United States [1].

1.2 Previous Research on Formation of PCDD/F from Chlorophenols

The primary source of emission of PCDD/Fs and PBDD/Fs is the combustion of chlorinated and brominated waste [38-39]. The formation of PCDD/Fs has been detected from combustion sources including steel mills, copper smelters, hospital waste incinerators, automobiles and municipal waster incinerators [40-42]. Basically PCDD/Fs are formed in all combustion processes where carbon, oxygen and chlorine are present. Many factors that influence the formation of PCDD/Fs are temperature, residence time, chlorine input, percent oxygen and feed rate.

Numerous experimental and theoretical research on the formation of PCDD/Fs from various chlorophenols has been studied [29, 43-52]. Previous research has shown that the formation of PCDF was based primarily on the ortho-ortho coupling of chlorophenoxy radicals to form an intermediate of ortho, ortho dihydroxybiphenyl (DOBP) (Figure 1.2) [46-48, 51]. The

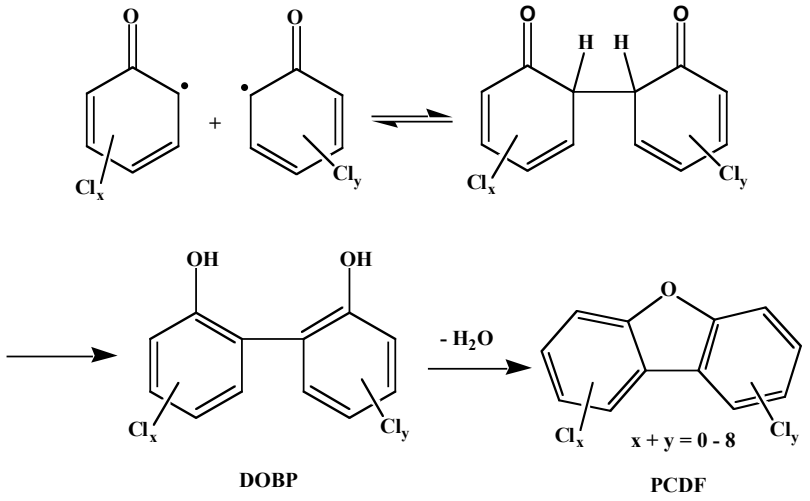

Figure 1.2 Proposed Mechanism to PCDF Formation

mechanisms involving PCDD formation were attributed to formation of ortho-phenoxyphenol (POP) intermediates (Figure 1.3) [49-50]. POP may be formed by a radical-radical or radical-

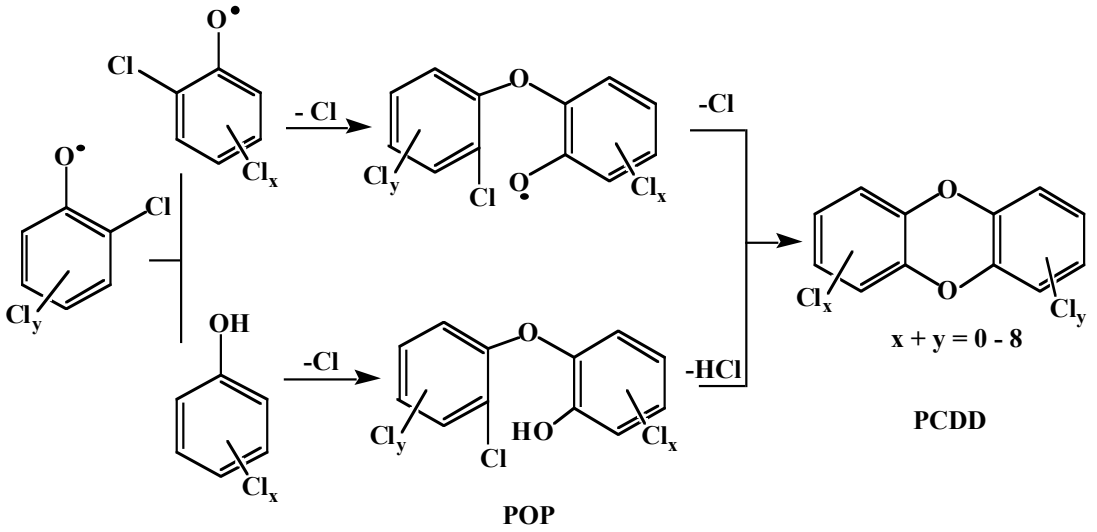

Figure 1.3 Proposed Mechanisms to PCDD Formation

molecule reaction pathway. Much of the results from previous research with chlorophenols were determined from a "slow combustion process", i.e. the residence time was between 10 and 10 minutes [46, 48-52]. Various chlorophenol precursors were used as well as different concentrations of oxygen. The many parameters were used to mimic conditions in the different flame zone areas. Table 1.1 depicts the previous research for PCDD/F formation from monochlorophenols.

Robert Louw's research group studied the slow combustion pyrolysis of the monochlorophenols [47]. At a residence time of 100 seconds and a temperature of 490°C, formation of a PCDD, unchlorinated dibenzo-*p*-dioxin (DD), was formed only when ortho-chlorophenol was present. The detected PCDD/F products for 2-chlorophenol were DD, 4,6-dichlorodibenzofuran (4,6-DCDF) and 4-chlorodibenzofuran (4-MCDF) with yields in μmol/h of 16.5, 5.2, and 0.7 at 500°C, respectively. For the meta and para chlorophenols, only various

Table 1.1 Previous Research Results on PCDD/F Detected from Pyrolysis and Oxidation of Monochlorophenols

Chlorophenol	PCDD/F Results	Reference
2-chlorophenol	Pyrolysis/100 seconds/ 490°C DD>4,6-DCDF>4-MCDF	[47]
	Pyrolysis/ 10 seconds/ 700°C DD>DF>MCDFs>DCDFs>	[51]
	Oxidation/ 80 seconds/ 550°C 4,6-DCDF>DD>4-MCDF	[46]
	Oxidation/ 10 minutes/ 375°C: 1-MCDD> 4,6-DCDF>DD>4-MCDF 500°C: 4,6-DCDF>DD>1-MCDD>4-MCDF	[49-50]
3-chlorophenol	Pyrolysis/100 seconds/ 490°C Only DCDFs detected	[47]
	Pyrolysis/ 10 seconds/ 700°C DCDFs>MCDFs> DF	[51]
	Pyrolysis/ 2 – 10 seconds/ 300 – 900°C 1,7-DCDF >3,7-DCDF > 1,9-DCDF	[52]
	Oxidation/ 2 – 10 seconds/ 300 – 900°C Higher yields DCDFs over pyrolysis	[52]
	Catalysis/ 2 – 10 seconds/ 300 – 600°C 1,7- DCDF >>1,9-DCDF	[52]
4-chlorophenol	Pyrolysis/ 100 seconds/ 490°C Only DCDFs detected	[47]
	Pyrolysis/ 10 seconds/ 700°C DCDFs>MCDFs> DF	[51]

isomers of PCDFs were detected. Thus it was determined that the presence of chlorine in the ortho position is essential for the formation of PCDDs. However, another study with the residence time of 79 seconds and in the presence of oxygen showed 4,6-DCDF was the major product for 2-chlorophenol [46]. They continued to study the effect of the location of the chlorine at the ortho position by looking at 2-chlorophenol, 2,4,6-trichlorophenol and pentachlorophenol [46]. These studies determined that the radical-radical reactions of chlorophenols to form PCDD/Fs are more favorable reactions than the radical-molecule reactions [46, 48].

Yang, Mulholland, and Akki also reported the pyrolysis of 2-chlorophenol with a residence time of 10 seconds over a temperature range of 350 to 750°C [51]. Yields of dioxin products were reported only at 700°C. DD, 4,6-DCDF, 4-MCDF and dibenzofuran (DF) were observed, with percent yields, on a carbon feed basis, of 0.218, 0.024, 0.04 and 0.092, respectively. They also found from their results with 3-chlorophenol and 4-chlorophenol that only PCDFs were detected in higher yields and no PCDDs were observed [51]. Naphthalene was also observed at much higher yields than the PCDD/Fs for all three monochlorophenols [51]. Another study with Mulholland, Akki, Yang and Ryu observed the oxidative, pyrolytic and catalytic thermal degradation of 3-chlorophenol [52]. The studies were performed between 300 and 900°C at residence times between 2 and 10 seconds. In descending order, 1,7-dichlorodibenzofuran (1,7-DCDF), 3,7-dichlorodibenzofuran (3,7-DCDF) and 1,9-dichlorodibenzofuran (1,9-DCDF) were the PCDFs detected for the gas-phase oxidative and pyrolytic conditions. However for the catalytic conditions 1,7- DCDF was seen at higher yields than the gas-phase conditions and only a minor fraction of 1,9-DCDF was observed. The results suggested that steric factors associated with the geometries of the different DOBPs play an important role in determining the distribution of the PCDF product isomers [52].

Weber and Hagenmaier reported the oxidation of 2-chlorophenol with a residence time of 10 minutes and a temperature range of 330 to 600°C [49-50]. Initially at 375°C, 1-chlorodibenzo-*p*-dioxin (1-MCDD) was the highest yield PCDD/F product. However between 400 and 500°C, 4,6-DCDF was the highest yield PCDD/F. These studies suggest that reaction temperature, molecular oxygen and oxygen containing radicals, i.e. hydroxyl radical, are playing a large role in the product distribution and PCDD/F ratio.

Kinetic models on the formation of PCDDs from 2,4,6-trichlorophenol were developed in order to compare with the experimental results shown by Sidhu, Maqsud and Dellinger [29, 43-45]. The kinetic model included reactions that were absent in the Shaub and Tsang model [43-45]. Particularly, the radical-radical recombination reactions of 2,4,6-trichlorophenol radicals were added to the model. In addition, the rate of reaction of O_2 with 2,4,6-trichlorophenol was determined to be five orders of magnitude slower than the previous Shaub and Tsang model [43, 53]. Thus the contributions for gas-phase pathways were underestimated and should be given more consideration.

Various other chlorinated phenols were studied in addition to the monochlorophenols [29, 46, 48, 52]. The most popular chlorophenol studied was 2,4,6-trichlorophenol. The major PCDD/F products detected for 2,4,6-trichlorophenol from all the studies were 1,3,7,9-tetrachlorodibenzo-*p*-dioxin (1,3,7,9-TCDD) and 1,3,6,8-tetrachlorodibenzo-*p*-dioxin (1,3,6,8-TCDD) [58, 65, 67]. Sidhu and Dellinger studied the thermal oxidation of 2,4,6-trichlorophenol over a temperature range of 300 to 800°C with a residence time of 2 seconds [29]. The experimental results showed that the original theoretical model for PCDD formation significantly underestimated the contribution of the gas-phase formation of PCDDs [29, 43]. Waiter-Protas and Louw also studied the gas-phase thermal degradation of 2,4,6-trichlorophenol over at temperature of 550°C and a residence time of 79 seconds [46]. In addition to 2,4,6-trichlorophenol, pentachlorophenol, phenol and 2-chlorophenol were all included in the study [46]. PCDD/F products observed from the thermal oxidation of phenol and pentachlorophenol observed in decreasing yields were DF, 1,2,3,4-tetrachlorodibenzofuran (1,2,3,4-TCDF), 1,2,3,4-tetrachlorodibenzo-*p*-dioxin (1,2,3,4-TCDD), octachlorodibenzo-*p*-dioxin (OCDD), pentachlorodibenzo-*p*-dioxin (PCDD), pentachlorodibenzofuran (PCDF), heptachlorodibenzo-*p*-

dioxin (HpCDD), hexachlorodibenzo-*p*-dioxin (HCDD), hexachlorodibenzofuran (HCDF), heptachlorodibenzofuran (HpCDF). It was determined that as long as an ortho-hydrogen is present the PCDFs rather than PCDDs are the major products [46]. Another study of 2,4,6-trichlorophenol by Louw and Ahonkhai determined that the bond strength of the O-H bond on 2,4,6-trichlorophenol was determined to be 5 kcal/mol weaker than the O-H bond in phenol itself [48].

Mulholland, Akki, Yang and Ryu studied the formation of PCDD/Fs from one other polychlorinated phenol, 2,6-dichlorophenol, under oxidative, pyrolytic and catalytic conditions [52]. The studies were performed between 300 and 900°C at residence times between 2 and 10 seconds. Because chlorines occupy both ortho sites, only PCDDs, 1,6-dichlorodibenzo-*p*-dioxin (1,6-DCDD) and 1,9-dichlorodibenzo-*p*-dioxin (1,9-DCDD), were formed. 1,6-DCDD was observed at higher yields than 1,9-DCDD for all three conditions.

1.3 Previous Research on Formation of PBDD/F from Brominated Hydrocarbons

Considerably less research has been performed on the mechanistic formation of PBDD/Fs from bromophenols [29, 54]. However there have been a few studies on the formation of PBDD/Fs and PBDEs from various brominated flame retardants [23-24, 27-28, 30, 55-58]. With the increase in the presence of brominated hydrocarbons present, research on the effect of bromine on the formation of PCDD/Fs has also been considered [55, 62-63]. Table 1.2 depicts a complete list of all previous research conducted on the formation of PBDD/Fs from brominated hydrocarbons.

Borojovich and Azenshtat studied the thermal behavior of various brominated compounds, particularly ortho and para bromophenol as well as 2,6-dibromophenol and 2,4,6-tribromophenol [54]. They also conducted a study with other common brominated hydrocarbons

Table 1.2 Previous Research on PBDD/Fs Resulting from Various Brominated Hydrocarbons

Brominated Hydrocarbon	Significant Results	Reference
2-bromophenol	600°C/pyrolysis/ 1 hour DD> DF>phenol	[54]
	600°C/oxidation/ 1 hour DD>DBDF	[54]
4-bromophenol	600°C/pyrolysis/1 hour phenol>DBDF> DF	[54]
	600°C/oxidation/hour no PBDD/Fs formed	[54]
2,6-dibromophenol	600°C/ pyrolysis/ 1 hour DD> MBDD > DBDDs> DF	[54]
2,4,6-tribromophenol	600°C/pyrolysis/ 1hour MBDD>TBDDs>TrBDD>DBDDs	[54]
	600–900°C/pyrolysis/max at 800°C PBDDs and brominated benzenes	[56]
	300-800°C/ 2.0 seconds pyrolysis-no PBDD/Fs/ oxidation-TBDDs	[58]
	300-800°C/oxidation/2.0 seconds 1,3,6,8-& 1,3,7,9-TBDD-max% yields 31 & 25	[29]
Pentabromophenol	600-900°C/pyrolysis brominated benzenes, naphthalenes, PBDDs	[56]
Bromohexane	600°C/ pyrolysis/ 1 hour benzene, toluene, bromopentane - no PBDD/Fs	[57]
Bromonaphthalene	600°C/ pyrolysis/ 1 hour benzene, toluene, dibromonaphthalene, bromopentane- no PBDD/Fs	[57]
TBBA	600°C/ pyrolysis/ 10 sec – 1 hour brominated phenols, bromopentane – minor [PBDD/Fs]	[57]
TBBPA	Pilot scale/ Br/Cl ratio-1:1/ O_2%-8.2 PBCDD/Fs > PCDD/Fs> TBDD/Fs	[30]
	Pilot scale/ combustion 40 minutes T- 900°C/ cooling 2 seconds T- 200°C/ [input] = 0.5 kg/h [PBDD/Fs] = 53 – 230 ng/N m^3	[24]
	700- 900°C/ pyrolysis maximum yield of PBDD/Fs at 800°C	[55]

(Table 1.2 continued)

(Table 1.2 continued)

HBCD	Pilot scale/ Br/Cl ratio-1:1/ O_2%-8.3 PBCDD/Fs > PCDD/Fs> TBDD/Fs	[30]
DecaDBE	Pilot scale/ Br/Cl ratio-1:1/ O_2%-9.6 PBCDD/Fs > PCDD/Fs> TBDD/Fs	[30]
Hexabrombiphenyl	600-900°C/ pyrolysis bromobenzenes, bromobiphenyls,	[56]
Tetrabromophthalic Anhydride	700- 900°C/ pyrolysis absence of polybrominated products	[55]
BTBPE	300-800°C/ 2.0 seconds pyrolysis- no PBDD/Fs/ oxidation - TBDDs	[58]
PBDEs	1:1 mixture of PBDEs/ 300-800°C/ 2.0 s pyrolysis-DBDF, TrBDF, no PBDDs/ oxidation-DBDD, TrBDD, TBDD	[58]
	Pilot scale/combustion 40 minutes T- 900°C/ cooling 2 seconds T- 200°C/ [input] = 0.5 kg/h [PBDD/Fs] = 43-990 ng/N m^3	[24]
	510-600°C/ dissolved in toluene maximum yield = 10% at 630°C	[27]
TV waste	Pilot scale/combustion 40 minutes T- 900°C/ cooling 2 seconds T- 200°C PBDD/Fs > PCDD/Fs	[24]
Circuit board waste	Pilot scale/combustion 40 minutes T- 900°C/ cooling 2 seconds T- 200°C PBCDD/Fs > PBDD/Fs> PCDD/Fs	[24]

to observe the thermal behavior of the C-Br bond [57]. All studies were performed at 600°C under pyrolytic conditions and the reaction time ranged from 10 seconds to 1 hour. In the case where the brominewas located in the ortho position, PBDDs were formed. Ortho-bromophenol formed high concentrations of DD, 2,6-dibromophenol formed DD, monobromodibenzo-*p*-dioxin (MBDD) and dibromodibenzo-*p*-dioxins (DBDDs), and 2,4,6-tribromophenol formed DD, MBDD, DBDDs and tribromodibenzo-*p*-dioxins (TrBDDs) and tetrabromodibenzo-*p*-dioxins (TBDD). However all brominated phenols formed PBDFs. However, the other study with bromohexane, bromonaphthalene and 4,4-isopropylline bis (2,6-dibromophenol) (TBBA) detected PBDD/Fs in very minute concentrations and the exact isomers where not identified [57].

Thus concluding that the presence of brominated phenols causes higher concentrations of PBDD/Fs.

In 1986, Hans-Rudolf Buser first found PBDD/Fs from the thermolysis of three common PBDE flame retardants [27]. It was determined that the maximum yield at 630°C of PBDD/Fs was 10%. Three common brominated flame retardants, decaBDE, TBBPA and HBCD, were combusted in a pilot scale incinerator by Soderstrom and Marklund [30]. The brominated flame retardants were combusted with a chlorine content that mimics ordinary waste, 0.75%, as well as varying levels of bromine content, 0.5 to 1.7%. More bromination was observed over chlorination and the levels of chlorination were increased with the presence of bromine. Both PCDD/Fs and PBDD/Fs as well as polybromochlorodibenzo-*p*-dioxins and furans (PBCDD/Fs) were detected with PBCDD/Fs being the favored products. Theoretical calculations also showed that bromine was mainly found in the form of Br_2 and chlorine as HCl.

Hutzinger and Thoma with others published numerous studies on the formation of PBDD/Fs from brominated flame retardants [22, 55-56]. 2,4,6-tribromophenol, pentabromophenol, hexabromobiphenyl, TBBPA, and tetrabromophthalic anhydride were pyrolyzed from 700 to 900°C and resulted in the formation of numerous PBDD/Fs where the maximum yields were detected at 800°C [55]. Numerous brominated benzenes, naphthalenes and PBDEs were detected as well [55]. Pyrolysis of polymers containing various brominated flame retardants also yielded the formation of numerous PBDD/Fs between 600 and 800°C [56]. Higher yields of PBDFs were seen relative to the PBDDs detected.

Striebich et al. studied the high-temperature degradation of three flame retardants under both oxidative and pyrolytic conditions [58]. The three polybrominated flame retardants, 2,4,6-tribromophenol, 1,2-bis(tribromophenoxyl) ethane (BTBPE), and a 1:1 mixture of two

commercial PBDEs, were studied between 300 and 800°C. Under oxidative conditions, all three formed PBDDs. However only the PBDEs formed PBDFs under both pyrolytic and oxidative conditions.

Incineration of three different wastes samples containing brominated flame retardants from a pilot scale incinerator were also examined by Sakai et al [24]. The samples used consisted of PBDEs and TBBPA, waste TV casing materials and waste printed circuit boards. In all cases PBDD/Fs, PCDD/Fs and PBCDD/Fs were detected. The increase in chlorine concentration introduced to the input sample reduced the ratio of PBDDs to PBDFs and increased the ratio of PCDDs to PCDFs. Also the amount of PBDD/Fs released dominated the total amount of dioxins released.

Sidhu, Masqud and Dellinger studied the gas-phase thermal oxidation of 2,4,6-trichlorophenol and 2,4,6-tribromophenol as direct precursors to formation of PCDDs and PBDDs [29]. The 1,3,6,8- TCDD and 1,3,7,9- TCDD were the dominant isomers observed for 2,4,6-trichlorophenol and the analogous tetrabrominated isomers were observed for 2,4,6-tribromophenol at maximum yields that were around 500 times higher. These results were used in modifying the original gas-phase formation model of Shaub and Tsang [43]. Grotheer and Louw continued this research by studying the reactions of phenoxyl radicals with bromobenzene and chlorobenzene [59]. The results determined that the radical-radical reactions of (ortho)-halogenated phenoxyl radicals were the dominant source for the formation of PCDD/Fs and PBDD/Fs.

1.4 Summary of Present Study

This study describes the gas-phase oxidative and pyrolytic thermal degradations of 2-bromophenol and 2-chlorophenol individually and in a 50:50 mixture of the two for a reaction

time of 2.0 seconds over the temperature range of 300 to 1000°C. In addition, the surface mediated gas-phase oxidation and pyrolysis reactions for 2-bromophenol to form PBDD/Fs are described over a temperature range from 250 to 550°C. These conditions are used to mimic conditions in the post-flame zone of combustion systems. 2-Chlorophenol and 2-bromophenol were chosen because they are simple model precursors to PCDD/F and PBDD/F formation, which simplifies the mechanistic interpretation of the results.

The purpose in undertaking this study is to develop data under conditions relevant to combustion. This data could then be used to develop a detailed model of PCDD/F and PBDD/F formation in incinerators and thermal processes. The results also complement and expand upon the previously published studies of other chlorinated phenols and brominated phenols under slow combustion conditions at lower temperatures and reaction times between 10 seconds to 1 hour [46-47, 49-51, 54]. In addition, comparisons between the two conditions, oxidative and pyrolysis, are made as well as the effect bromine has on the formation of both PCDD/Fs and PBDD/Fs. The surface mediated gas-phase thermal degradation of 2-bromophenol is described for comparison with previous similar studies with 2-chlorophenol [60-61]. Reaction pathways to PCDD/F and PBDD/F products are proposed that are consistent with the experimental data for each condition. Pathways to all other products detected are also analyzed and the intermediates in these pathways are discussed in their relation to formation of PCDD/Fs and PBDD/Fs.

1.5 References

1. Bromine Science and Environmental Forum (BSEF), *An Introduction to Brominated Flame Retardants*, Bromine Science and Environmental Forum, Brussels, Belgium, 19.10.2000, www.bsef.com.

2. Danish Environmental Protection Agency, *Brominated Flame Retardants*, Environmental Project no. 494 1999, www.mst.dk/homepage.

3. de Witt, C. *An Overview of Brominated Flame Retardants in the Environment*, Chemosphere, 2002, **46**: 583.

4. World Health Organization (WHO), *Environmental Health Criteria 192, Flame Retardants: A General Introduction*, World Health Organization, Geneva Switzerland, 1997.

5. *Selected Brominated Flame Retardants, Risk Reduction Monograph 3*: Organization for Economic Cooperation and Development (OECD), Environment Directorate: Paris, France, 1994.

6. Thomsen, C.; Lundanes, E.; Becher, G. *Brominated Flame Retardants in Plasma Samples from Three Different Occupational Groups in Norway*, Journal of Environmental Monitoring, 2001, 366.

7. Schroter-Kermani, C; Helm, D.; Herrman, T; Papke, O. *The German Environmental Specimen Bank-Application in Trend Monitoring of Polybrominated Diphenyl Ethers in Human Blood*, Organohalogen Compounds, 2000, **47**: 45.

8. Noren, K; Meironyte, D. *Certain Organochlorine and Organobromine Contaminants in Swedish Human Milk in Perspective of Past 20–30 Year*, Chemosphere, 2000, **40**: 1111.

9. Ryan, J. J.; Patry, B *Recent Trends in Levels of Brominated Diphenyl Ethers (BDEs) in Human Milk from Canada*, Organohalogen Compounds, 2002, **58**: 173.

10. Asplund, L.; Hornung, M.; Peterson, R. E.; Thuresson, K. ; Bergman, A. *Levels of Polybrominated Diphenyl Ethers (PBDEs) in Fish from the Great Lakes and Baltic Sea*, Organohalogen Compounds, 1999, **40**: 351.

12. Alaee, M.; Luross, J.; Sergeant, D.; Muir, D.; Whittle, D.; Solomon, K. *Distribution of Polybrominated Diphenyl Ethers in the Canadian Environment*, Organohalogen Compounds, 1999, **40**: 347.

13. Haglund, P.; Zook, D.; Buser, H.; Hu, J. *Identification and Quantification of Polybrominated Diphenyl Ethers and Methoxy-Polybrominated Diphenyl Ethers in Baltic Biota***,** Environmental Science and Technology, 1997, **31**: 3281.

14. Lindstrom, G.; Wingfors, H.; Dam, M.; van Bavel, B. *Identification of 19 Polybrominated Diphenyl Ethers (PBDEs) in Long-Finned Pilot Whale (Globicephala melas) from the Atlantic***,** Archives of Environmental Contamination Toxicology, 1999, **36**: 355.

15. Hooper, K; McDonald, T. *The PBDES: An Emerging Environmental Challenge and Another Reason for Breast-Milk Monitoring Programs*, Environmental Health Perspectives, 2000, **100**: 387.

16. She, J.; Petreas, M.; Ninkler, j.; Vista, P.; McKinney, M.; Kepec, D. *PBDEs in the San Fransisco Bay Area: Measurements in Harbor Seal Blubber and Human Adipose Tissue*, Chemosphere, 2002, **46**: 697.

17. Rudel, R. A.; Camann, D.; Spengler, J.; Korn, L.; Brody, J. *Phthalates, Alkylphenols, Pesticides, Polybrominated Diphenyl Ethers, and Other Endocrine-Disrupting Compounds in Indoor Air and Dust*, Environmental Science and Technology, 2003, **37**: 4543.

18. Sjodin, A.; Carlson, H.; Thuresson, K.; Sjolin, S.; Bergman, A.; Ostman, C.**,** *Flame Retardants in Indoor Air at an Electronics Recycling Plant and at Other Work Environments*, Environmental Science and Technology, 2001, **35**: 448.

19. Litten, S.; McChesney, D.; Hamilton, M.; Fowler, B. *Destruction of the World Trade Center and PCBs, PBDEs, PCDD/Fs, PBDD/Fs, and Chlorinated Biphenylenes in Water, Sediment, and Sewage Sludge*, Environmental Science and Technology, 2003, **37**: 5502.

20. World Health Organization (WHO), *Environmental Health Criteria 162*, *Brominated Biphenyl Ethers*, World Health Organization, Geneva, Switzerland, 1994.

21. Oberg, T.; Warman, K.; Bergstrom, S. *Brominated Aromatics from Combustion*, Chemosphere, 1987, **16**: 2451.

22. Dumlar, R.; Thoma, H.; Lenoir, D.; Hutzinger, O. *PBDF and PBDD from the Combustion of Bromine Containing Flame Retarded Polymers: A Survey*, Chemosphere, 1989, **19**:2023.

23. Sakai, S. *Thermal Behavior of Brominated Flame Retardants and PBDDs/DFs*, Organohalogen Compounds, 2000, **47**: 210.

24. Sakai, S.; Watanbe, J.; Honda, Y.; Takatsuku, H.; Aoki, I.; Futamatsu, M.; Shiozaki, K.; *Combustion of Brominated Flame Retardants and Behavior of its Byproducts*, Chemosphere, 2001, **42**: 519.

25. Wilken, M.; Schanne, L. *Brominated Dioxins – A Potentially Greater Hazard in Fires than PCDD and PCDF?*, Schriftenreiche WAR, 1994**, 74**: 109.

26. Kanters, J.; Louw, R. *Thermal and Catalysed Halogenation in Combustion Reactions*, Chemosphere, 1996, **32**: 89.

27. Buser, H.R. *Polybrominated Dibenzofurans and Dibenzo-p-dioxins: Thermal Reaction Products of Polybrominated Diphenyl Ether Flame Retardants*, Environmental Science and Technology, 1986, **20**: 404.

28. Dumler, R.; Thoma, H.; Lenoir, D.; Hutzinger, O. *Thermal Formation of Polybrominated Dibenzodioxins (PBDD) and Dibenzofurans (PBDF) from Bromine Containing Flame Retardants*, Chemosphere, 1989, **19**: 305.

29. Sidhu, S.S., Maqsud, L., Dellinger, B., *The Homogeneous, Gas-Phase Formation of Chlorinated and Brominated Dibenzo-p-dioxins from 2,4,6-Trichlorophenol and 2,4,6-Tribromophenols*, Combustion and Flame, 1995, **100**: 11.

30. Soderstrom, G.; Marklund, S. *PBCDD and PBCDF from Incineration of Waste-Containing Brominated Flame Retardants*, Environmental Science and Technology, 2002, **36**: 1959.

31. Lemieux, P. M.; Ryan, J. V. *Enhanced Formation of Dioxins and Furans from Combustion Devices by Addition of Trace Quantities of Bromine*, Waste Management, 1998, **18**: 361.

32. McMillen, D. F.; Golden, D. M. *Hydrogen Bond Dissociation Energies*, Annual Review of Physical Chemistry, 1982, **33**: 493.

33. Mennear, J. H.; Lee, C.C. *Polybrominated Dibenzo-p-dioxins and Dibenzofurans: Literature Review and Health Assessment*, Environmental Health Perspective, 1994, **102:** 265.

34. Weber, L. W.; Greim, H. *The Toxicology of Brominated and Mixed-Halogenated Dibenzo-p-dioxins and Dibenzofurans: An Overview*, Journal of Toxicology and Environmental Health, 1997, **50**: 195.

35. Meerts, I. A. T. M.; van Zanden, J. J.; Luijks, E. A. C.; Van Leeuwen-Bol, I.; Marsh, G.; Jakobsson, E.; Bergman, A.; and Brouwer, A. *Potent Competitive Interactions of Some Brominated Flame Retardants and Related Compounds with Human Transthyretin in Vitro*,Toxicology Science, 2000, **56**: 95.

36. EU Draft Risk Assesment biphenylether, pentabromo derivatives, UK October 1998a.

37. The Swedish National Chemicals Inspectorate, *Phase-out of PBDEs and PBBs*, Report on a Governmental Commission, March 15, 1999.

38. Karasek, F. W.; Hutzinger, O. *Dioxin Danger from Garbage Incineration*, Analytical Chemistry, 1986, **58**; 633A.

39. Rappe, C. In Banbury Report 35: *Biological Basis for Risk Assessment of Dioxins and Related Compounds*, Cold Spring Harbor Press, Cold Springs Harbor, NY, 1990.

40. Öberg, T.; Allhammar, G. *Chlorinated Aromatics from Metallurgical Industries - Process Factors Influencing Production and Emissions*, Chemosphere, 1989, **19**: 711.

41. Marklund, S.; Andersom, R.; Tysklind, M.; Rappe, C.; Egeback, K. E.; Bjorkman, E.; Grigoriadis, V. *Emissions of PCDDs and PCDFs in gasoline and diesel fueled cars*, Chemosphere, 1990, **20**: 553.

42. Nestrick, T. J.; Lamparski, L. L. *Isomer-specific Determination of Chlorinated Dioxins for Assessment of Formation and Potential Environmental Emission from Wood Combustion* Analytical Chemistry, 1982, **54**: 2292.

43. Shaub, W. M.; Tsang, W. *Dioxin Formation in Incinerators*, Environmental Science and Technology, 1983, **17**: 721.

44. Khachtrayan, L.; Burcat, A.; Dellinger, B. *An Elementary Reaction-Kinetic Model for the Gas-Phase Formation of 1,3,6,8- and 1,3,7,9-Tetrachlorinated Dibenzo-p-dioxins from 2,4,6-Trichlorophenol*, Combustion and Flame, 2003**, 132**: 406.

45. Khachtrayan, L.; Asatrayan, R.; Dellinger, B. *Development of Expanded and Core Kinetic Models for the Gas Phase Formation of Dioxins from Chlorinated Phenols*, Chemosphere, 2003, **52**: 695.

46. Waiter-Protas, I.; Louw, R. *Gas-Phase Chemistry of Chlorinated Phenols – Formation of Dibenzofurans and Dibenzodioxins in Slow Combustions*, European Journal of Organic Chemistry, 2001, 3945.

47. Born, J.G.P.; Louw, R.; Mulder, P. *Formation of Dibenzodioxins and Dibenzofurans in Homogeneous Gas-Phase Reactions of Phenols*, Chemosphere, 1989, **19**: 401.

48. Louw, R.; Ahonkhai, S. T., *Radical/radical vs Radical/molecule Reactions in the Formation of PCDD/Fs from (Chloro)phenols in Incinerators* Chemosphere, 2002, **46**: 1273.

49. Weber, R.; Hagenmaier, H.; *Mechanism of the Formation of Polychlorinated Dibenzo-p-dioxins and Dibenzofurans from Chlorophenols in Gas Phase Reactions*, Chemosphere, 1999, **38**: 529.

50. Weber, R.; Hagenmaier, H. *On the Mechanism of the Formation of Polychlorinated Dibenzofurans from Chlorophenols*, Organohalogen Compounds**,** 1997, **31**: 480.

51. Yang, Y.; Mulholland, J.A.; Akki, U. *Formation of Furans by Gas-Phase Reactions of Chlorophenols*, 27th Symposium (International) on Combustion, The Combustion Institute, 1998, 1761.

52. Mulholland, J. A.; Akki, U.; Yang, Y.; Ryu, J. *Temperature Dependence of DCDD/F Isomer Distributions from Chlorophenol Precursors*, Chemosphere, 2001, **42**: 719.

53. NIST Chemical Kinetics Database 17, Gaithersburg, MD, 1998.

54. Borojovich, E.; Aizenshtat, Z. J. *Thermal Behavior of Brominated and Polybrominated Compounds II: Pyroproducts of Brominated Phenols as Mechanistic Tools*, Analytical and Applied Pyrolysis, 2002, **63**: 129.

55. Thoma, H.; Rist, S.; Hauschultz, O. *Polybrominated Dibenzodioxins and –furans from the Pyrolysis of Some Flame Retardants*. Chemosphere, 1986, **15**: 649.

56. Thoma, H.; Hutzinger, O. *Pyrolysis and GC/MS-analysis of Brominated Flame Retardants in On-line Operation*. Chemosphere, 1987, **18**: 1047.

57. Borojovich, E.; Aizenshtat, Z. J. *Thermal Behavior of Brominated and Polybrominated Compounds I: Closed Vessel Conditions*, Journal of Analytical and Applied Pyrolysis, 2002, **63**: 105.

58. Striebech, R. C.; Rubey, W. A.; Tirey, D. A.; Dellinger, B. *High-Temperature Degradation of Polybrominated Flame Retardant Materials*, Chemosphere, 1991, **23**:1197.

59. Grotheer, H. H.; Louw, R. *The Gas-Phase Reaction of Phenoxy Radicals with Bromobenzene* Combustion Science and Technology, 1998, **134**: 45.

60. Lomnicki, S.; Dellinger, B. *Formation of PCDD/F from the Pyrolysis of 2-Chlorophenol on the Surface of Dispersed Copper Oxide Particles*, 29th Symposium (International) on Combustion, The Combustion Institute, 2003, in press.

61. Lomnicki, S.; Dellinger, B. *A Detailed Mechanism of the Surface-Mediated Formation of PCDD/F from the Oxidation of 2-Chlorophenol on a CuO/Silica Surface*, Journal of Physical Chemistry A, 2003, **107**: 4387.

CHAPTER 2. EXPERIMENTAL

2.1 System for Thermal Diagnostic Studies

The System of Thermal Diagnostic Studies (STDS) was designed for studying the thermal behavior of virtually any organic material under various conditions [1]. This system is ideal for studying various hazardous waste incineration concerns as well as other thermal behavior studies of organic materials. The STDS contains individual units consisting of the thermal reactor compartment, cryogenic trapping, product separation and detection that can be modified or replaced in order to accommodate different experimental parameters.

The STDS was designed as a closed, continuous system. Ideally this allows for the quantitative transport of the sample and its products to the GC/MS for detection. Essentially, the STDS is composed of a high-temperature fused silica flow reactor that is equipped with an in-line gas chromatograph/mass spectrometer (GC/MS) (Figure 2.1). The flow reactor is

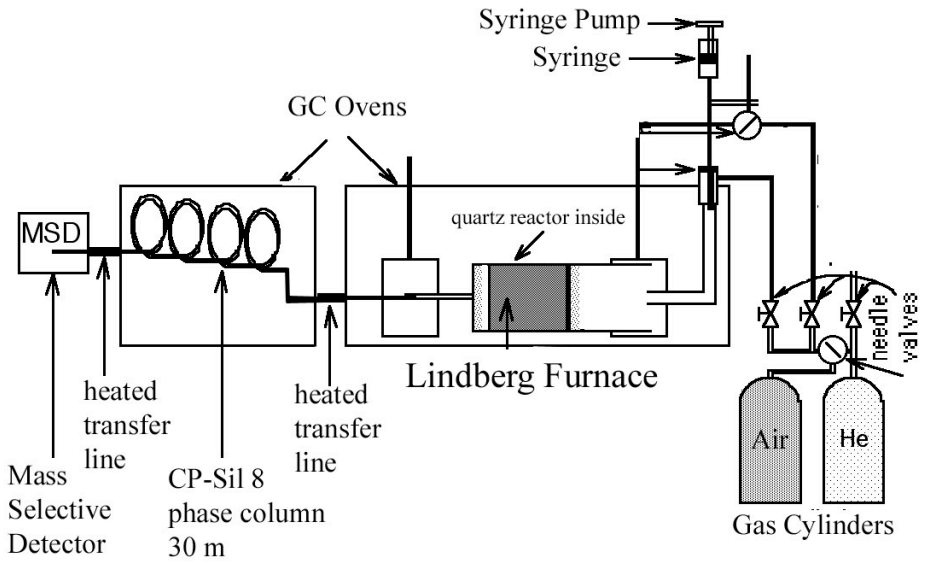

Figure 2.1 System for Thermal Diagnostic Studies (STDS)

located inside the thermal reactor compartment. The flow reactor is where the experimental thermal reactions take place. A Lindberg furnace houses the flow reactor and controls the temperature of the thermal reactions (Figure 2.2). The furnace is housed inside a gas chromatograph (GC) so that the surrounding temperatures for the connections are controlled. Downstream of the reactor is the inline GC/MS which is capable of cryogenic trapping, product separation and detection.

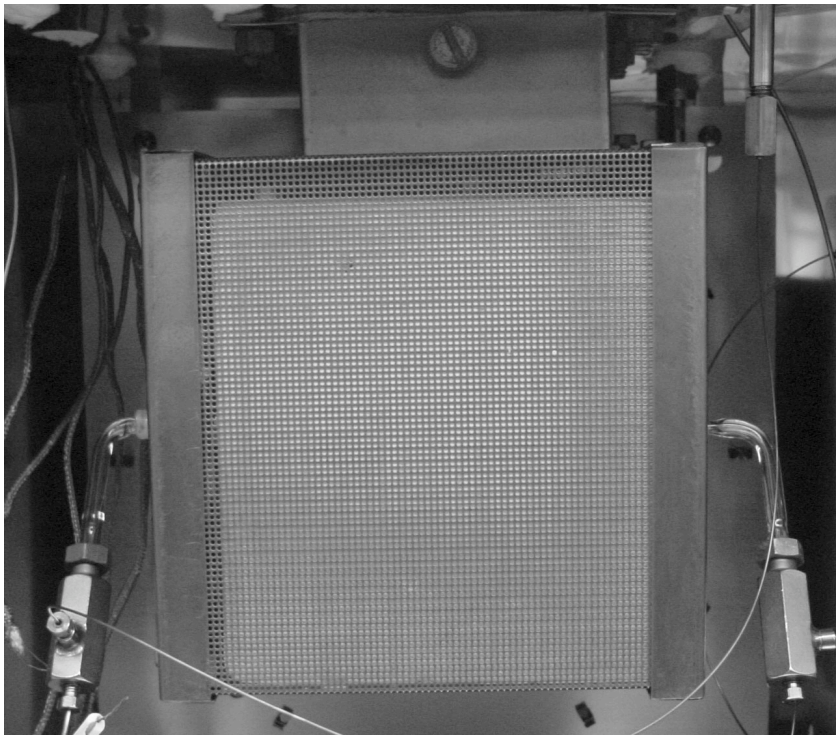

Figure 2.2 Lindberg Furnace that Houses the Flow Reactor

The GC used for the thermal reactor compartment was a Varian Vista 6000 Series. Since chromatography was not involved in this aspect of the system, the Varian does not contain a GC column or detector. This GC is designed to act as a temperature control that maintain the temperature of the lines coming from the injection port to the reactor and the line going from the reactor to the heated transfer line in order for the sample to remain a gas. A Lindberg furnace specifically designed for maintaining the extreme temperatures around the

reactor necessary for the experiments is installed inside this GC (Figure 2.2). This furnace is controlled by a separate temperature controller where the temperature could be maintain inside the furnace up to 1200°C.

The quartz reactor located inside this furnace is the location where the thermal reactions occur. The connections to the quartz reactor outside the furnace are all composed of fused silica in order to maintain an inert atmosphere. The flow path of the gas sample is maintained to be chemically inert by allowing contact with the sample to be only quartz surfaces. The flow rate of the Helium gas was maintained by a mass flow controller that can control flows up to 5 liter/minute. These high flow rates were needed to maintain a constant residence time of the sample inside the reactor. A syringe pump was used to control the rate and concentration at which the initial sample was introduced into the STDS. The STDS is maintained so that the sample and its products remain in a well-controlled and programmable thermal environment.

Any number of types of reactors can be used inside the STDS. For the purpose of the gas phase experiments, a 1 cm i.d quartz helical tubular flow reactor was used. Figure 2.3 depicts the design of this reactor. A straight 1 mm i.d. quartz tube that contained 1 mg of the surface catalyst was used for the surface mediated experiments. A more detailed description of each is described in Section 2.2.

The fused silica connection that connects the reactor to the inline analysis device or the Varian Saturn GC/MS maintains its temperature by heated transfer line that can be controlled up to 450°C. There is also a split in the transfer line that causes some of the effluent to split off to a charcoal trap. The rest of the flow or sample is trapped onto the head

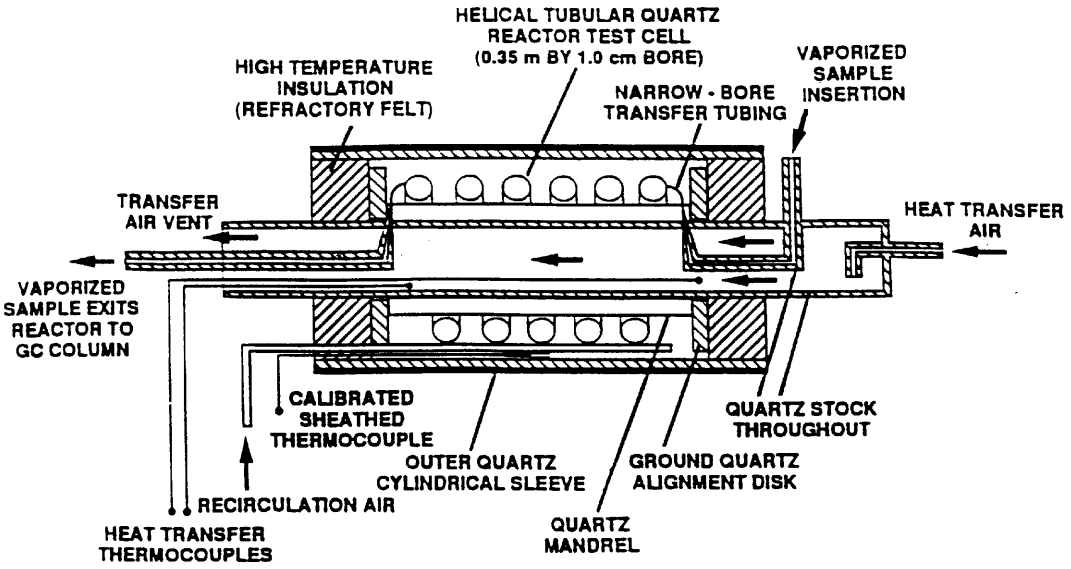

Figure 2.3. Gas-Phase Quartz Reactor Design

of the GC column for analysis. The reasoning behind the splitter is so that the pressure inside the reactor will remain at a constant pressure of around 1 atm and so that the GC/MS is not overloaded with the sample. This splitter is controller by a needle nose value and pressure gauge. The percentage of the flow that is split is measured for each run in order to know quantitatively the amount of sample trapped onto the head of the column.

A mass flow controller maintains the flow inside the system up to 5 liter/minute. By controlling the flow, the temperature and the pressure inside the reactor, the residence time inside the reactor can remain a constant for each run of the entire study. This is important in order to have uniformity for all experimental runs. With the uniformity, a better comparison between the sample experiments is achieved.

There is a wide variety of ways in which the sample can be introduced into the reactor. Gas and Liquid samples are introduced through a standard GC injection port. Since all

samples introduced into the reactor should be in gas-phase, the samples are vaporized in the injector before entering the reactor. Solid sample are introduced by a pyroprobe that is inserted into the injection port and is vaporized to a gas that then enters into the reactor. Since the experiments performed for this study only used liquid samples, the samples were inserted into the reactor via a liquid syringe. The injection port contained a straight tube quartz glass insert and thus maintaining the inert atmosphere inside the STDS. The flow rate of the injection was controlled by a syringe pump in order to maintain a constant concentration for each run.

A Varian Saturn 2000 GC/MS was used for the cryogenic trapping, separation and detection of the parent sample and its products. The sample was trapped onto the head of the CP-Sil 8 phase capillary column (30 m, 0.25 m i.d., 0.25 film thickness) cryogenically at a temperature of –60°C. In order to separate the individual products, the column was temperature programmed from –60 to 300°C at 15°C/min and held at 300°C. Detection and quantification of the products were obtained using the Varian Saturn MS that operated on a full-scan mode (10-650 amu) for the duration of the GC run. The MS ion trap oven was held at 200°C and the transfer line from the GC to the MS was held at 280°C.

2.2 Quartz Reactor Design

The quartz reactor was designed for the purpose of studying the thermal decomposition of organic materials. Figure 2.3 depicts the basic design of a tubular quartz cell reactor that was used for gas-phase experiments. The basic design of the reactor is to have the high temperature portion of the reactor encompasses a short length of the furnace. This allows for any axial temperature gradients within the furnace to be minimized. The design allows for

a relatively large temperature difference between the transport temperature and the actual exposure temperature; thus the gas phase sample is exposed to a square-wave thermal pulse where the jump to the exposure temperature is no greater than 5 ms.

The diameter of the reactor inside the furnace was designed to minimize the surface to volume ratio and thus lower the amount of surface initiation reactions. Previous work found that an inside diameter of 1 cm was acceptable in reducing the surface effects [2]. The volume of the reactor that is exposed to the high-temperature inside the furnace is 2.7×10^{-5} m^3.

In order to maintain continuity between temperature runs of the sample, a standard residence time inside the reactor was held constant at 2 seconds for each run. The residence time was held constant by varying the flow of the gas with the change in temperature. This relation is based on the ideal gas law where $V_2P_2/T_2 = V_0P_0/T_0$ where V is the volume, P is pressure and T is temperature. The subscript 2 denotes the quartz reactor interior and the subscript 0 denotes the ambient outlet conditions. By substituting the V_2 with the volume of the reactor $\pi r^2 L$ and the volume (V_0) is equal to F_0t_0 where F_0 is the flow though the reactor and t_0 is the residence time inside the reactor, the equation then becomes $\pi r^2 LP_2/T_2 = F_0t_0P_0/T_0$. Now the differential pressure (P_d) can be described as $P_2 - P_0$ if the resistance to the gas flow of the quartz tube reactor is much less than the sum of the downstream resistances to the gas flow (i.e. the transfer lines and the trap). Thus, the mean residence time can be described as

$$t_0 = (\pi r^2 L/ F_0)(T_2/ T_0)(1 + P_d/ P_0) \qquad \text{(Equation 1)}$$

Equation 1 was used to determine the flow needed for each temperature in order to maintain a residence time of 2 seconds. The time of 2 seconds was chosen in order to better duplicate

incineration conditions. Table 2.1 depicts the flow rate needed for each temperature based on the above equation.

Table 2.1. Helium Flow Rate for Each Gas-Phase Experimental Temperature

Temperature (°C)	Flow Rate (mL/min)
300	484.3
350	445.5
400	412.4
450	383.9
500	359.0
550	337.2
600	317.9
650	300.7
700	285.2
750	271.3
800	258.7
850	247.2
900	236.6
950	226.9
1000	218.0

A different quartz reactor was used for the surface catalyzed experiments. This reactor was simplified to a straight quartz tube with a 1 mm inside diameter. The surface catalyst, 1 mg, was placed inside the quartz tube and held in place on either side by quartz wool. The total volume of the reactor was based on the area that the surface catalyst occupied inside the reactor minus the surface area that the surface catalyst occupied. Thus the volume of the open space volume was 1.25×10^{-9} m^3. This volume was used in the calculations to obtain the flow needed to maintain a constant time of the sample to have contact with the catalytic surface. This contact time (t_{cc}) was decided to be 0.01 seconds in order to maintain a consistency with previous surface catalysis work performed by other members of the group with 2-chlorophenol [3-4]. Again equation 1 was used to determine the flow

rate based on the t_{cc} = 0.01 second and Table 2.2 represents the flow rates used for each temperature. Clearly the t_{cc} is different from the t_0 in that the t_{cc} only deals with the time at which the gas sample, i.e. 2-chlorophenol or 2-bromophenol, has contact with the surface.

Table 2.2 Helium Flow Rate for Each Surface-Catalyzed Experimental Temperature

Temperature (°C)	Flow Rate (mL/min)
200	5.43
250	4.91
300	4.49
350	4.13
400	3.82
450	3.55
500	3.33
550	3.12
600	2.94

2.3 Sample Preparation

Once the calculations for the flow rates inside the reactor are calculated, the next step is to determine the flow rates of the sample in order to maintain a constant concentration inside the quartz reactor. In this section, these calculations are discussed. The preparation of the CuO in Silica catalyst bed for the surface mediated reactions is also described.

2.3.1 2-Chlorophenol and 2-Bromophenol Preparations

In order to maintain a constant concentration of the sample inside the reactor, a syringe pump was used to control the flow rate of the sample as well as vary the flow rate with the change in temperature inside the reactor. The total amount of liquid injected into the STDS was chosen to be 0.135 μL for 2-bromophenol (2-MBP) and 0.120 μL for 2-chlorophenol (2-MCP) in order to have the total number of moles of each sample injected to be the same. A concentration present inside the reactor of 88 ppm was selected as the constant

concentration used for all experiments. This concentration and the amount of liquid injected were chosen based the signal strength obtained for the sample from the GC/MS. The GC/MS signal for this concentration was ideal in that it did not overload the column nor was it too small such that the products formed from the sample could not be detected.

The injection rate for the sample was determine based on the flow rate of the helium through the reactor depicted in Table 2.1 and 2.2. The rate ratio of the injection flow (R_i) to the rate of the helium (Flow Rate) should equal 88 ppm for all temperatures (R_i/Flow Rate = 88 ppm). From this we can obtain the flow rate of the sample needed. However this is the flow rate of the gas phase of the sample and since a liquid is injected this R_i needs to be converted to a rate for the liquid. Therefore R_i is converted to R_i(liq) in mL/min for the liquid by the following equation 2.

$$\{[R_i\,(\text{L/min})/22.414\,(\text{L/mol})] * FW_s\,(\text{g/mol})\}/\,VP_s\,(\text{g/mL}) = R_i(\text{liq})\,(\text{mL/min}) \qquad \text{(Equation 2)}$$

where FW_s is the formula weight of the sample and VP_s is the vapor pressure of the sample. Table 2.3 depicts the flow rates used for 2-MBP in the gas phase experiments.

Table 2.3 R_i(liq) used for each Experimental Temperature

Temperature (°C)	R_i(liq) (μL/h)
300	13.34
400	11.36
450	10.57
500	9.89
550	9.29
600	8.76
650	8.28
700	7.86
750	7.47
800	7.12
900	6.52
950	6.25
1000	6.00

2.3.2 CuO/Silica Bed Preparation for the Surface Catalyzed Reactions

The catalytic material was prepared by the method of incipient wetness. A water solution of copper(II) nitrate with a concentration chosen to obtain a 5% copper in Silica system was used as the active phase precursor. Silica powder (Aldrich - 500 m2/g) was introduced into the equivalent volume of precursor solution for incipient wetness to occur. The solution was well mixed and dried at 120°C for 24 hours. For the surface catalyzed reactions, 1 mg of this catalytic material was placed between quartz wool plugs in the 1 mm i.d. fused silica reactor in the STDS. Prior to each flow-reactor experiment, the catalytic material was oxidized *in situ* at 500°C for 1 hour with a 20% O_2/He flow rate of 5.5 cc/min to convert the copper nitrate to CuO.

Recent works for the surface catalyzed pyrolysis and oxidation of the model precursor, 2-chlorophenol, proposed possible mechanisms for PCDD/F formation [3-4]. In these works the model surface used was 5% copper (II) oxide on a silica surface. By using a simplified surface as a model for fly ash, the effects of other unknown cations present in fly-ash will be avoided. It is also known that copper and iron ions are probably the most active metals in PCDD/F formation [5]. Also instead of using purely copper oxide, the mixture with silica allows the study of small surface domains for well-dispersed CuO species.

2.4 Detailed Procedure

A detailed step by step procedure is described. Initially the STDS must be completely cleaned and baked out prior to use each day. In order to do this, it is best to bake out the transfer line and GC oven and Lindberg furnace overnight with the transfer line disconnected from the Varian Saturn GC/MS. For the bake out, the temperature of the transfer line is set to

450°C; the oven is set to 500°C, the injection port to 400°C, and the Lindberg furnace to 800°C. The flow inside the reactor is switched from the helium gas cylinder to the air gas cylinder where the flow rate is kept at around 30 mL/min. The transfer line is disconnected from the GC/MS to prevent the column from burning out and prevent air from entering the MS, which would burn out the filament. This usually cleans out the entire system except the GC/MS. The Varian Saturn GC/MS has a separate cleaning procedure. The GC column is cleaned using the bake out procedure where the column temperature is set and held at 300°C for 1 hour then returned to 120°C for the rest of the night. The bake out for the column is usually performed once or twice every week as needed. The mass spectrometer is usually baked out every weekend. The computer that controls the Varian GC/MS handles this procedure. There is a bake out panel in the computer system control program where the ion trap temperature is set at 250°C and the transfer line is set at 300°C. This bake out is set to last for 6 hours. After the bake out is complete, calibration of the GC/MS is needed. This calibration is also preformed by the computer system control through the autotune panel. It is important to note that the air and water measurements must be taken before the calibration as well as before using the GC/MS each morning. The GC/MS must not be used if the air and water levels are too high. High levels of air and water will burn out the filament. The air/water autotune is also located in the autotune panel in the computer system control program.

It is important to make sure every morning before experimental runs that the sample is quantitatively transported to the GC/MS. This will test for leaks and make sure that the STDS was cleaned out properly the night before. To do this, keep all temperatures inside STDS uniform and at a temperature that keeps the sample in the gas-phase but will not degrade. (This would probably be the lowest temperature of the range of temperatures studied.) If the

sample is not quantitatively transported, most probably there are leaks in the STDS. At this point, disconnect the transfer line from the GC/MS and turn off all heating inside the STDS. Test for leaks at all connections using the leak detector. If leaks are found, very carefully tighten the connections. Be very gentle when tightening the connections around the quartz reactor. Applying too much pressure can easily break the quartz. If no leaks are found, it is possible that the transfer line has a build up of products inside and therefore needs to be replaced. After replacing the transfer line turn on all the temperatures again and perform another quantitative run of the sample.

Once bake out is complete and quantitative transport of the sample is maintained, the experimental runs can begin. The following steps describe the exact procedure for running a single temperature run.

1. Set GC oven (the one that houses the reactor) temperature to the temperature needed to maintain the sample in gas-phase through out the STDS.
2. Set injection port temperature to the temperature that will convert the liquid sample to a gas sample.
3. Set Transfer line temperature to the desired temperature that will keep all products in the gas-phase to transport to the GC/MS.
4. Set Lindberg furnace temperature to desired temperature needed for experiments.
5. Switch to Helium Gas and set flow rate to desired flow rate for the experimental temperature. The flow rate is determined by equation 1.
6. Monitor the flow rate of the splitter from the reactor and the flow rate from the transfer line. The flow is monitored by a digital flowmeter connected to the output flow from the splitter. This is useful for measuring the percentage of flow reaching the GC/MS,

maintaining a constant pressure inside the reactor of 1 atm and checking for leaks in the STDS.

7. Once there are no leaks, meaning the initial flow into the STDS is equal to the combined output flows of the splitter and the transfer line, open the liquid nitrogen value for the Varian GC/MS. The GC temperature will begin to drop to –60°C or the desired temperature needed for cryogenically trapping the products on the head of the column.
8. Setup the GCMS run. -60°C (hold for 5 minutes) to 300°C at 15 °C/min. The MS is set for full scan mode (10 to 650 amu) for 40 minutes. (Note: this setup is used for the gas-phase experiments only) This setup changes for different samples and for the surface reactions as well.
9. Monitor temperatures surrounding the reactor with the thermal couples inside the GC to make sure the reactor inside the furnace and the surrounding temperatures are is at the desired temperatures.
10. Setup the syringe pump to the desired injection rate for the experimental run. The injection rate is determined by equation 2.
11. Once the GC/MS has reached the initial temperature of -60°C for cryogenic trapping, then insert the transfer line into the injection port of the GC/MS.
12. If all temperatures are stabilized and the flow rate is constant, then the sample is ready to be injected. Draw up desired amount of sample into syringe and place syringe in syringe pump.
13. Insert Syringe with syringe pump into inject port and start the syringe pump and immediately start the GC/MS run as well.

14. Once sample injection is complete, remove syringe pump from injection port and remove transfer line from injection port of the GC/MS.
15. Switch the gas cylinder from the helium to the air and set the furnace to the next experimental temperature desired. (To clean out the STDS between runs)
16. Once the GC/MS run is complete, repeat the steps for the next run.

2.5 Identification and Calculations of Products

For each run, the computer generates a gas chromatograph of the entire products detected and mass spectrum for each product. The identification of each product is based on the mass spectrum, the NIST library database and the standards of the products. The concentrations of the products calculated were based on the calibrations with standards of the products (Aldrich and Cambridge Isotope Lab) and the peak area counts from the chromatogram.

Standards for PBDD/Fs with less than four bromines were not available. Concentrations of observed PBDD/Fs are reported based on calibrations for the analogous PCDD/F. This is a reasonably accurate approach as the peak area counts for various chlorinated and brominated aromatics and PCDD/Fs and PBDD/Fs were compared, and it was found that the difference in calibration factors for brominated aromatic hydrocarbons and chlorinated aromatic hydrocarbons varied less than 10%. The only products detected that did not have available standards were 1-bromodibenzo-*p*-dioxin, dibromodibenzo-*p*-dioxin, tribromodibenzo-*p*-dioxin, 4-bromodibenzofuran, 4,6-dibromodibenzofuran and 4-bromo-6-chlorodibenzofuran. The mass spectral library match qualities for each of these species were 264, 343, 422, 248, 326, and 282, respectively. These products are the same PBDD/Fs that

were anticipated based on the predicted pathways from the observed formation of the PCDD/Fs from the analogous 2-chlorophenol. In the 2-chlorophenol study, the PCDD/F standards were available to confirm the identifications based on GC retention time and mass spectral pattern. Although standards were not available to confirm the identifications with PBDD/F standards, there is confidence in the assignments based on the combination of mechanistically anticipated product formation; comparison of GC retention times, mass spectral response, and mass spectral patterns of chlorinated and brominated hydrocarbons; and the results from the formation of PCDD/F from 2-chlorophenol.

Once the calibrations of all the product standards were taken, the percent yield of each product is calculated based on the following equation.

$Y = \{([Product])/[2\text{-}MXP]_0\} * 100$

[Product] is the concentration of the particular product formed (in moles) and $[2\text{-}MXP]_0$ is the initial concentration (in moles) of the sample, i. e. 2-MCP or 2-MBP, injected into the reactor. When equal parts of 2-MCP and 2-MBP were mixed, the combined total initial concentration was kept the same as the individual experiments. Thus all experiments had the same total concentration inside the reactor of 88 ppm. For the mixture of 2-MCP and 2-MBP experiments, the above equation for calculating the percent yield of each product is changed to the following:

$Y = \{[Product])/([2\text{-}MBP]_0 + [2\text{-}MCP]_0\}*100$

where $[2\text{-}MBP]_0$ is the initial concentration of 2-MBP (in moles) injected into the reactor and $2\text{-}[MCP]_0$ is the initial concentration of 2-MCP (in moles) injected into the reactor. Multiple runs were performed for each temperature to insure the repeatability of the experiments.

Once the experimental procedure was fully developed, the repeatability of the experiments was within 10%.

2.6 Theoretical Calculations

The heats of reaction, ΔH_{rxn}, for key steps in product formation pathways were calculated using AM1, semiempirical molecular orbital methods. The calculations were performed using the MOPAC computation program that is contained within the Chem3D Pro computer application. With this program, the user can draw a 3D model of each radical and molecule involved for each pathway in question. Once the 3D models are drawn, AM1 calculations are performed for each molecule to obtain the heat of formation (ΔH_f) for each radical and molecule. The ΔH_f for the small radicals and molecules involved, i. e. Cl•, HCl, Br•, HBr, •OH, H• are all obtained from Alexander Burat's thermochemical database [6]. The ΔH_{rxn} for each reaction is determined from all the ΔH_fs calculated for each molecule and radical for each pathway. Without experimental benchmarks, the calculated ΔH_{rxn} cannot be considered to be completely accurate. They are shown to assess the likelihood of potential parallel pathways.

Pseudo-equilibrium calculations were performed to estimate the concentrations of reactive species such as •OH, O•, H•, Br• and Cl• for all gas-phase conditions with 2-MCP and 2-MBP. The Chemkin Equil program was used to calculate the concentrations of these species over a range of reaction temperatures from 570 to 1270 K. The Chemkin Equil program predicts the equilibrium state of systems containing ideal gas mixtures. In order to run the Equil program, thermodynamic data is needed for all possible species including the two staring products, 2-MCP and 2-MBP. The thermodynamic data over a certain temperature

range must be fit in the form required for the database. Thus they need to be stored as polynomial fits to specific heat (cp/R), enthalpy (H/RT) and entropy (S/R). There are seven coefficients for each temperature. Thus for a temperature range, there are a total of 14 coefficients in all for each species. The majority of this thermodynamic data is found in the JANAF tables and from the compilation from Burcat [6-7]. Though generally the data is already available in the required format as the input data files available in Chemkin. The other input file needed consists of the initial conditions involved in the problem. These conditions are the concentrations of the starting products, the type of conditions for the problem, the starting temperature for the solution, the estimate of the equilibrium temperature, and the starting pressure of the solution. The initial inputs for the calculations were the same as each of the experimental runs. As an example input Equil file, below is the input file used for the oxidation of 2-MCP.

```
REAC C6H5CLO 8.8E-5
REAC N2 0.79
REAC O2 0.20
HP
TEMP 570
TEST 2000
PRES 1
END
```

Where REAC is the reactant concentration, HP stands for constant pressure and enthalpy conditions, TEMP is the starting temperature in Kelvin, TEST is the estimate of the equilibrium temperature in Kelvin, and PRES is the starting pressure in atmospheres of the solution. This input is repeated for several temperatures desired between the temperature ranges in question.

Once both input files are loaded into the Chemkin Equil program an output file of the mole fractions for species formed is generated for each condition. The major products species resulting in the calculation for this example with the oxidation of 2-MCP were CO_2, H_2O, HCl and Cl_2. Other species included were •OH, O•, H•, H_2, HO_2, H_2O_2, CO and Cl•.

These calculations are used for comparison of the rates of reactions identified in each respective experiment, which will be discussed later in Chapter 4. All output files for all conditions are available in Appendix 2.

2.7 References

1. Rubey, W. A.; Grant, R.A. *Design Aspects of a Modular Instrumentation System for Thermal Diagnostic Studies*, Review of Scientific Instruments, 1988, **59**:265.

2. Taylor, P.H.; Tirey, D. A.; Dellinger, B. *The High Temperature Pyrolysis of 1,3-Hexachlorobutadiene*, Combustion and Flame, 1996, **106**: 1.

3. Lomnicki, S.; Dellinger, B. *A Detailed Mechanism of the Surface-Mediated Formation of PCDD/F from the Oxidation of 2-Chlorophenol on a CuO/Silica Surface*, Journal of Physical Chemistry A, 2003, **107**: 4387.

4. Lomnicki, S.; Dellinger, B. *Formation of PCDD/F from the Pyrolysis of 2-Chlorophenol on the Surface of Dispersed Copper Oxide Particles*, 29th Symposium (International) on Combustion, The Combustion Institute, 2003, in press.

5. Stieglitz, L.; Vogg, H.; Zwick, G.; Beck, J.; Bautzx, H. *On Formation Conditions of Organohalogen Compounds from Particulate Carbon of Fly Ash*, Chemosphere, 1991, **23**: 1255.

6. Burcat, A.; Third Millenium Ideal Gas and Condensed Phase Thermochemical Database for Combustion, Report TEA867, January 2001.

7. JANAF, *Themochemical Tables, National Standards Reference Data Series* Report NSRDS-NBS 37: also Dow Chemical Company, distributed by Clearing house for Federal Scientific and Technical Information, PB168370 (1965) and subsequent updates., 1965.

CHAPTER 3. RESULTS

3.1 Gas-Phase, High-Temperature Pyrolysis

Results from the gas-phase high temperature pyrolysis were determined from conditions involved inside the STDS described in Chapter 2. The residence time inside the reactor was held at a constant 2.0 seconds for each temperature. The temperature range was maintained to be between 300 and 1000°C. In order to maintain pyrolytic conditions, the flow consisted of ultra-high purity helium. Two initial precursors were used, 2-chlorophenol (2-MCP) and 2-bromophenol (2-MBP). The concentrations of 2-MCP and 2-MBP for each experimental run was kept at 88 ppm for each temperature. However for the experiment involving the mixture of 2-MCP and 2-MBP, the initial concentration of each was held at 44 ppm so that the total initial concentration is 88 ppm. Thus the starting percent yield for 2-MCP and 2-MBP begins at 50%. The reasoning is to maintain a constant concentration of 88 ppm for all experiments.

3.1.1 Gas-Phase Pyrolysis of 2-Chlorophenol[1]

The temperature dependence of the thermal degradation of 2-MCP and the yield of polychlorinateddibenzo-*p*-dioxin and furan (PCDD/F) products are presented in figure 3.1 and table 3.1 for a reaction time of 2.0 s. The non-PCDD/F products are presented in figure 3.2 and table 3.1. Figures 3.1 and 3.2 are presented on a semi-logarithmic scale in which the percent yields of products (or percent of unconverted 2-MCP) are presented on a logarithmic scale versus temperature. The thermal degradation of 2-MCP gradually increased from 300 to 750°C, where the rate drastically accelerated, achieving 99 % destruction at 850°C.

[1] Reproduced in part with permission from Evans, C. S. and Dellinger, B. *Mechanisms of Dioxin Formation from the High-Temperature Pyrolysis of 2-Chlorophenol*, Environmental Science and Technology, 2003, **37**: 1325. Copyright 2003 American Chemical Society.

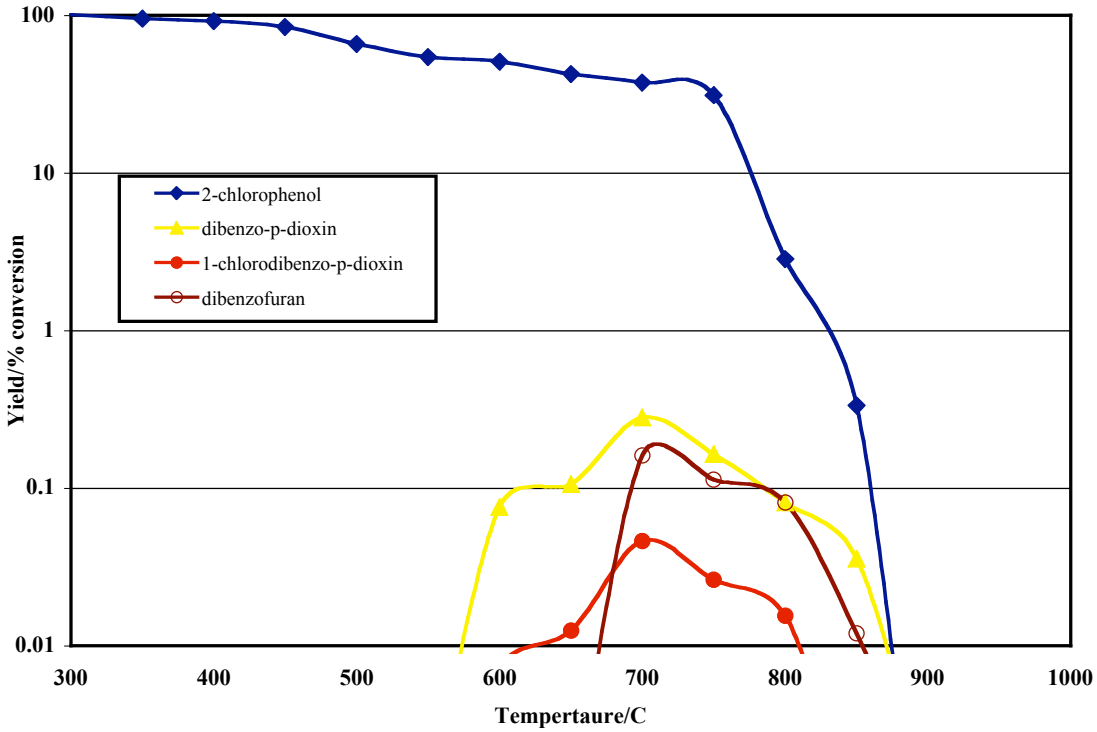

Figure 3.1 "Dioxin" Products from the Gas-Phase Pyrolysis of 2-Chlorophenol

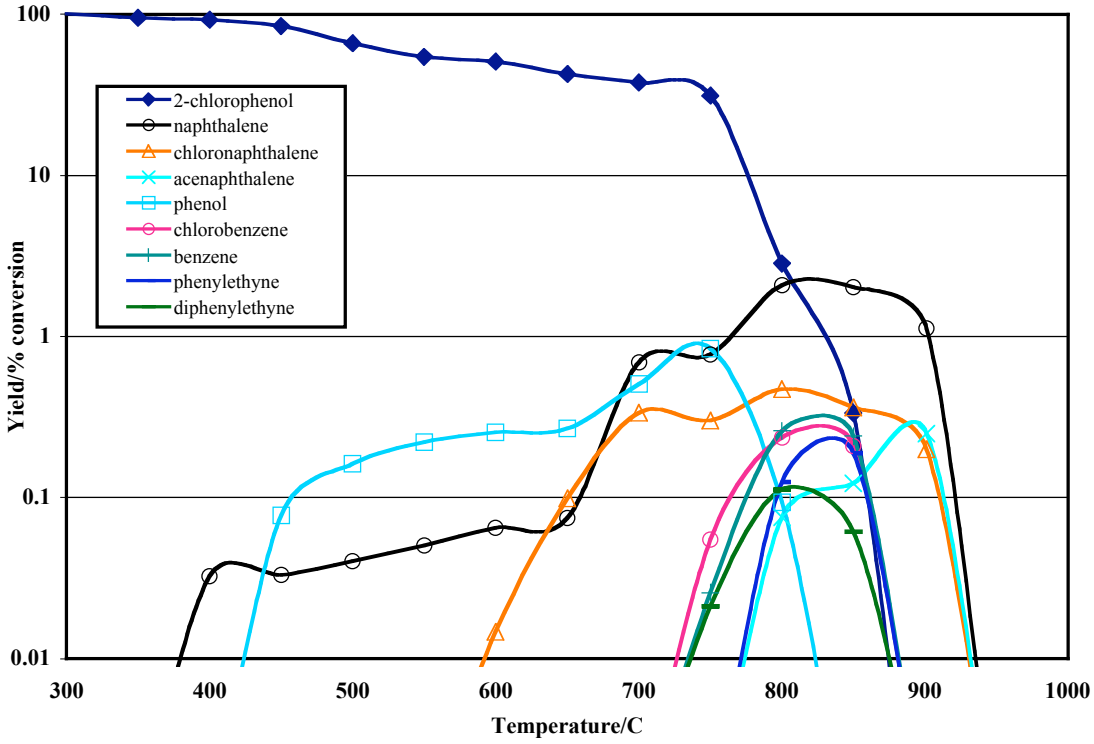

Figure 3.2 "Non- Dioxin" Products from the Gas-Phase Pyrolysis of 2-Chlorophenol

Table 3.1 Percent Yield of Products of Gas-Phase Pyrolysis of 2-Chlorophenol

Product	Temperature (° C)											
	300	**350**	**400**	**450**	**500**	**550**	**600**	**650**	**700**	**750**	**800**	**850**
2-Chlorophenol	100	95.0	92.2	84.6	65.8	54.4	50.9	42.6	37.6	31.2	2.84	1.18
Dibenzo-p-dioxin							0.08	0.11	0.28	0.16	0.08	0.03
1-Chlorodibenzo-p-dioxin							0.007	0.01	0.05	0.03	0.02	
Dibenzofuran									0.16	0.11	0.08	0.01
Naphthalene			0.03	0.03	0.04	0.05	0.06	0.08	0.69	0.77	2.09	2.01
Chloronaphthalene							0.01	0.10	0.34	0.30	0.47	0.36
Acenaphthalene											0.07	0.12
Phenol				0.08	0.16	0.22	0.25	0.27	0.51	0.84	0.09	
Benzene										0.03	0.26	0.24
Chlorobenzene										0.06	0.24	0.21
Phenylethyne											0.12	0.19
Diphenylethyne										0.02	0.11	0.06

* Percent Yield = {([Product])/ $[2\text{-MCP}]_0$}*100

Dibenzo-*p*-dioxin (DD), dibenzofuran (DF), and 1-chlorodibenzo-*p*-dioxin (1-MCDD) were observed between 575 and 900°C with maximum percent yields of 0.28, 0.16, and 0.05 at 700°C, respectively. The anticipated product, 4,6 dichlorodibenzofuran (4,6 DCDF) was not observed [1-2]. Unlike DD and 1-MCDD, which where detectable as low as 600°C, significant yields of DF were not observed until 700°C. Above 900°C no chlorinated aromatics were detected.

Non-dioxin products were also detected from the pyrolysis of 2-MCP. (cf. Figure 3.2 and table 3.1). Chlorinated products included chlorobenzene (maximum yield of 0.24 % at 800°C) and 1-chloronaphthalene (maximum yield of 0.47 % at 800°C). Other products included naphthalene, benzene, phenol, acenaphthalene, phenylethyne, and diphenylethyne. Naphthalene and phenol are the only products observed at lower temperatures. However phenol achieves its highest yield of 0.84% at 750°C and decomposes by 850°C whereas naphthalene achieves a maximum yield of 2.09% at 800 C. All other degradation products reach their maximum yield between 800°C and 850°C.

3.1.2 Gas-Pase Pyrolysis of 2-Bromophenol[2]

The temperature dependence of the thermal degradation of 2-MBP and the yield of polybrominateddibenzo-p-dioxin and furan (PBDD/F) products are presented in figure 3.3 and table 3.2 for a reaction time of 2.0 s. The non-PBDD/F products are presented in figure 3.4 and table 3.2. Figures 3.3 and 3.4 are presented on a semi-logarithmic scale in which the percent yields of products (or percent of unconverted 2-MBP) are presented on a logarithmic scale versus

[2] Reproduced in part with permission from Evans, C. S. and Dellinger, B. *Mechanismsof Dioxin Formation from the High-Temperature Pyrolysis of 2-Bromophenol*, Environmental Science and Technology, 2003, **37**: 5574. Copyright 2003 American Chemical Society.

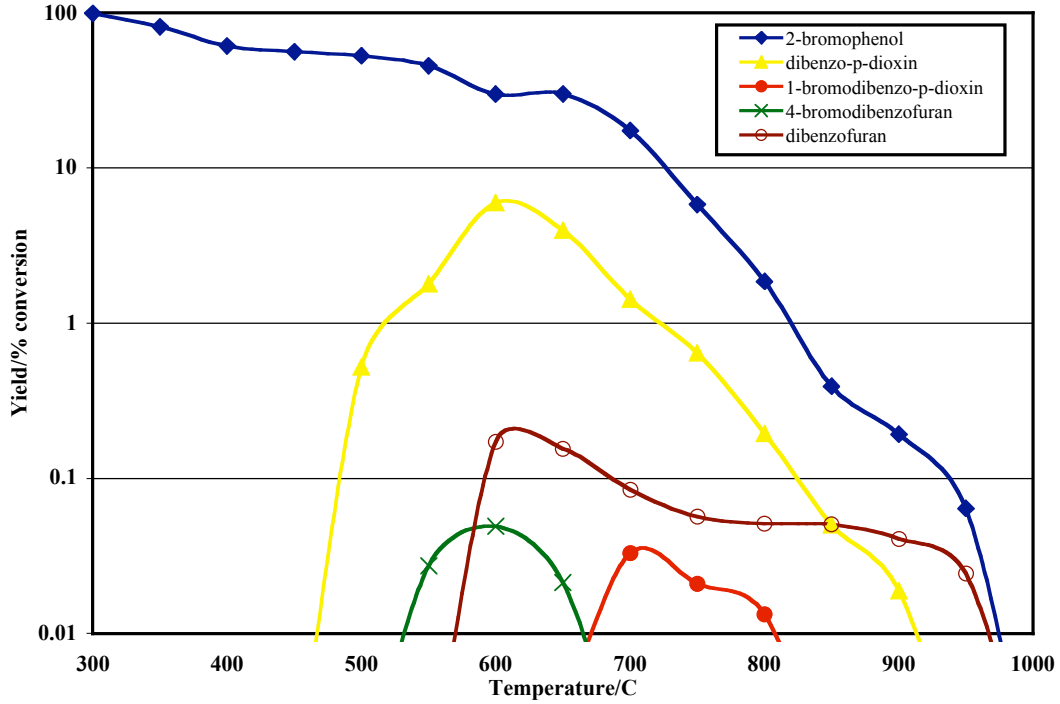

Figure 3.3 "Dioxin" Products from the Gas-Phase Pyrolysis of 2-Bromophenol

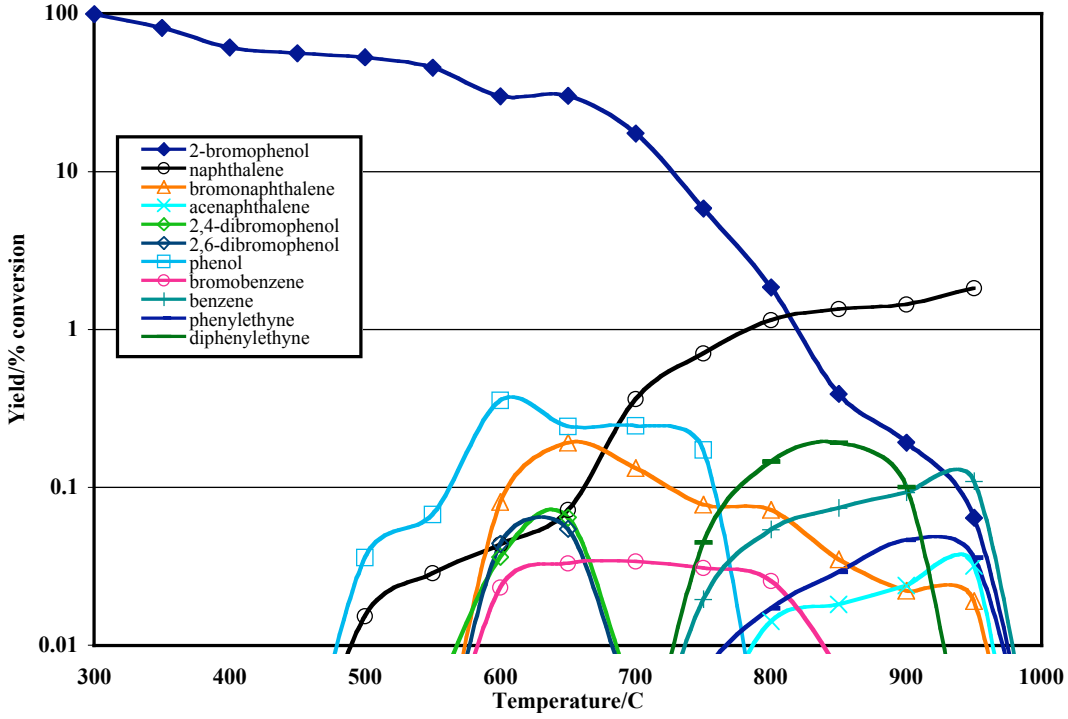

Figure 3.4 "Non-Dioxin" Products from the Gas-Phase Pyrolysis of 2-Bromophenol

Table 3.2 Percent Yield of Products of Gas-Phase Pyrolysis of 2-Bromophenol

Products	Temperature (°C)													
	300	**350**	**400**	**450**	**500**	**550**	**600**	**650**	**700**	**750**	**800**	**850**	**900**	**950**
2-Bromophenol	100	81.7	61.3	56.3	52.8	45.7	29.9	30.1	17.4	5.8	1.8	0.39	0.19	0.06
Dibenzo-p-dioxin					0.52	1.78	5.96	3.97	1.42	0.64	0.19	0.05	0.02	
1-Bromodibenzo-p-dioxin								0.003	0.03	0.02	0.01			
Dibenzofuran							0.17	0.15	0.08	0.05	0.05	0.05	0.04	0.02
4-Bromodibenzofuran						0.03	0.05	0.02						
Naphthalene					0.02	0.03	0.04	0.07	0.36	0.71	1.15	1.35	1.44	1.83
Bromonaphthalene							0.03	0.19	0.13	0.08	0.07	0.04	0.02	0.01
Acenaphthalene										0.002	0.01	0.02	0.02	0.03
Phenol					0.04	0.07	0.36	0.24	0.24	0.17				
2,4 Dibromophenol						0.004	0.04	0.06	0.004					
2.6 Dibromophenol							0.04	0.05	.003	0.001				
Benzene										0.02	0.05	0.07	0.09	0.10
Bromobenzene							0.02	0.03	0.03	0.04	0.03	0.006		
Phenylethyne										0.01	0.02	0.03	0.05	0.03
Diphenylethyne										0.04	0.15	0.19	0.10	

* Percent Yield = $\{([\text{Product}])/[\text{2-MBP}]_0\}*100$

temperature. The thermal degradation of 2-MBP gradually increased from 300 to 650°C, where the rate drastically accelerated, achieving 99 % destruction at 850°C.

DD, DF, 4-monobromodibenzofuran (4-MBDF) and 1-bromodibenzo-*p*-dioxin (1-MBDD) were observed between 500 and 900ºC. The anticipated product, 4,6-dibromodibenzofuran (4,6 DBDF) was not observed. Since previous results for the pyrolysis of 2-MCP resulted in the formation of 4,6-DCDF, the analogous 4,6-DBDF would also be likely to occur for the pyrolysis of 2-MBP [1-2]. However for this study, 4,6-DCDF was not detected for the pyrolysis of 2-MCP. Unlike DD and 4-MBDF, which were detectable as low as 500ºC, significant yields of 1-MBDD were not observed until 700ºC with a maximum yield of 0.03%. The major product, DD, was observed between 500 and 900ºC with a maximum yield of 6% at 600ºC. The other dioxin products, DF and 4-MBDF, were detected at much lower yields with maximums of 0.17 % and 0.05 % at 600ºC respectively. No brominated aromatics were detected above 950ºC.

Non-dioxin products were also detected from the pyrolysis of 2-MBP (cf. Figure 3.4and table 3.2). Brominated products included bromobenzene (maximum yield of 0.04 % at 750ºC), bromonaphthalene (maximum yield of 0.19 % at 650ºC), 2,4-dibromophenol and 2,6-dibromophenol (maximum yields of 0.06% and 0.05% at 650ºC respectively). Other products included naphthalene, benzene, phenol, acenaphthalene, phenylethyne, and diphenylethyne.

Initially naphthalene and phenol were observed at 500ºC followed by 2,4-dibromophenol, 2,6-dibromophenol and bromonapthalene at 600ºC. However phenol and bromonaphthalene achieved their highest yields of 0.36% and 0.19% at 600ºC and 650ºC respectively whereas naphthalene achieved a maximum yield of 1.83% at 950ºC. All other products were not detected until 750ºC and reached their maximum yields at 900ºC.

3.1.3 Gas-Phase Pyrolysis of a Mixture of 2-Chlorophenol and 2-Bromophenol[3]

The temperature dependence of the gas-phase pyrolytic thermal degradation of a 50/50 mixture of 2-MCP and 2-MBP and the yield of PCDD/F and PBDD/F products are presented in figure 3.5 and table 3.3. The remaining products are presented in figure 3.6 and table 3.3. Figure 3.5 and 3.6 are represented on a semi-logarithmic scale in which the percent yields of products (or percent yield of unconverted 2-MCP and 2-MBP) are presented on a logarithmic scale versus temperature. The thermal degradation of 2-MBP and 2-MCP gradually increased together from 350 to 700°C, where the rate drastically accelerated, achieving 99% destruction at 850°C.

Significant yields of DD were observed between 350 and 900ºC with a maximum yield of 1.16% at 700ºC. The remainder of the PCDD/F and PBDD/F products was observed between 600 and 900ºC. The only other PBDD product observed is 1-bromodibenzo-p-dioxin (1-MBDD) with a maximum of 0.02 at 750ºC. The PCDF and PBDF products observed were 4,6-dichlorodibenzofuran (4,6-DCDF) (maximum yield of 0.08 % at 700ºC), 4-bromodibenzofuran (4-MBDF) (maximum yield of 0.06 % at 700ºC), and 4-chlorodibenzofuran (4-MCDF) (maximum yield of 0.03 % at 750ºC). DF was detected as well between 650 and 900ºC with a maximum yield of 0.23 at 800ºC. 4-bromo-6-chlorodibenzofuran (4-B-6-CDF) was the only mixed bromo-chloro DD/F product observed with a maximum yield of 0.16 % at 700ºC. Above 950°C, no brominated or chlorinated aromatics were detected.

Many non-PCDD/F and non-PBDD/F products were also detected (cf. Figure 3.6 and table 3.3). Phenol and naphthalene were the only products observed with a maximum yield above 1% with naphthalene having the highest percent yield of 4.54 at 800ºC. Phenol was

[3] Reproduced in part with permission from Environmental Science and Technology, submitted for publication. Unpublished work copyright 2004 American Chemical Society.

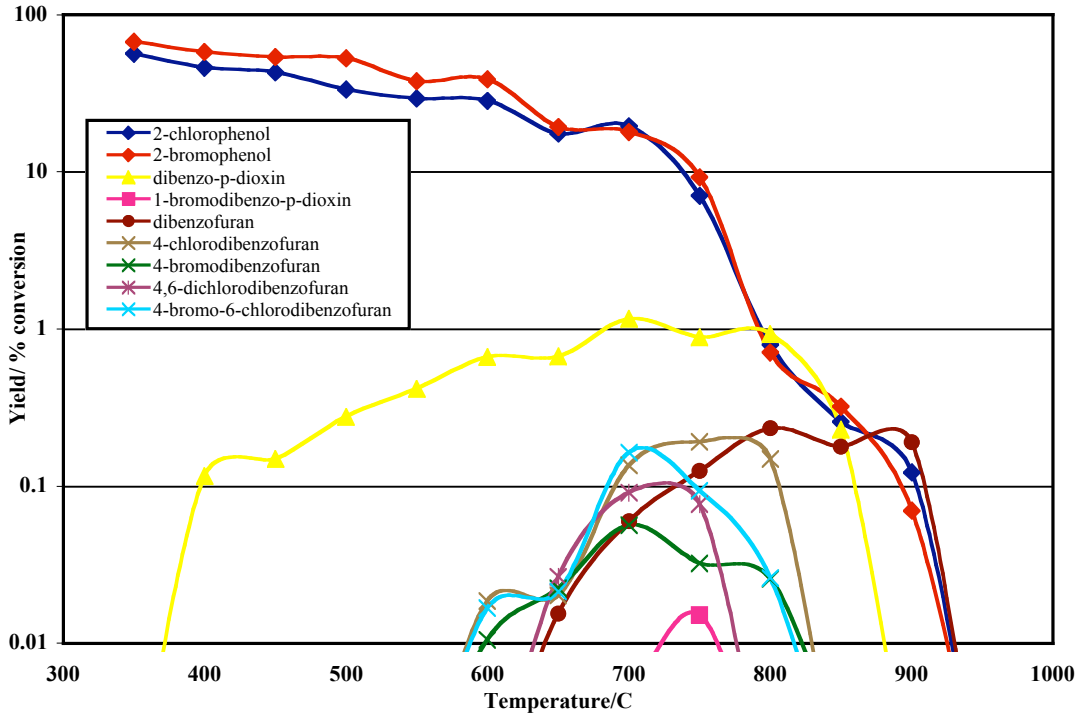

Figure 3.5 "Dioxin" Products from the Gas-Phase Pyrolysis of 2-Chlorophenol and 2-Bromophenol

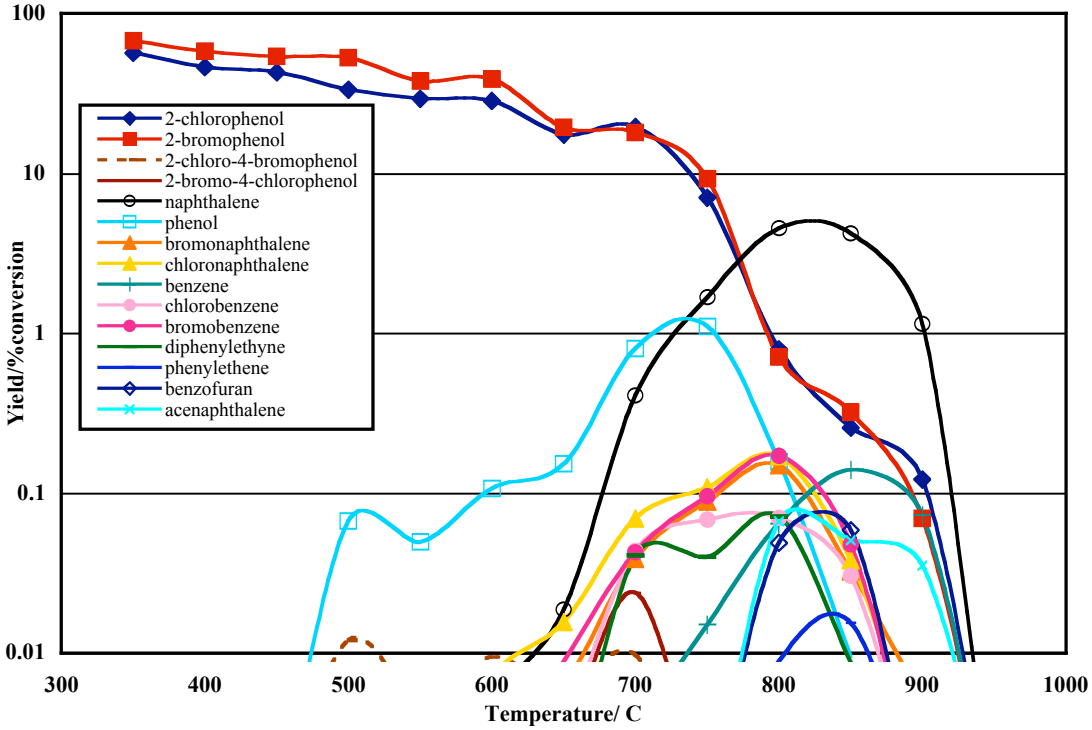

Figure 3.6 "Non-Dioxin" Products from the Gas-Phase Pyrolysis of 2-Chlorophenol and 2-Bromophenol

Table 3.3 Percent Yield of Products of Gas-Phase Pyrolysis of Mixture of 2-Bromophenol and 2-Chlorophenol

Products	Temperature (°C)											
	350	**400**	**450**	**500**	**550**	**600**	**650**	**700**	**750**	**800**	**850**	**900**
2-Chlorophenol	44.7	42.5	43.1	33.5	29.4	28.5	17.6	19.5	7.08	0.79	0.26	0.12
2-Bromophenol	53.2	53.2	53.9	52.9	38.9	37.8	19.3	18.0	9.29	0.71	0.32	0.07
Dibenzo-p-dioxin		0.11	0.15	0.28	0.42	0.66	0.67	1.16	0.89	0.94	0.23	
1-Bromodibenzo-p-dioxin							0.002	0.005	0.02			
Dibenzofuran							0.02	0.06	0.13	0.23	0.18	0.19
4-Chlorodibenzofuran						0.002	0.003	0.02	0.03	0.02	0.001	
4-Bromodibenzofuran						0.01	0.02	0.06	0.03	0.03	0.003	
4-Bromo-6-chlorodibenzofuran						0.02	0.02	0.16	0.09	0.03		
4,6-Dichlorodibenzofuran							0.03	0.09	0.08			
Phenol				0.07	0.05	0.11	0.15	0.81	1.10	0.16	0.009	
2-Chloro-4-bromophenol				0.01	0.005	0.009	0.006	0.009				
2-Bromo-4-chlorophenol				0.004			0.003	0.03				
2,4-Dibromophenol				0.005	0.005	0.005						
Naphthalene				0.001	0.001	0.005	0.02	0.41	1.68	4.54	4.23	1.14
Chloronaphthalene						0.007	0.02	0.07	0.11	0.17	0.04	0.002
Bromonaphthalene						0.003	0.006	0.04	0.09	0.15	0.03	0.005
Acenaphthalene										0.07	0.05	0.03
Benzene								0.003	0.02	0.06	0.14	0.07
Chlorobenzene						0.002	0.004	0.04	0.07	0.07	0.03	
Bromobenzene						0.001	0.008	0.04	0.09	0.17	0.05	
Phenylethyne										0.008	0.02	
Diphenylethyne								0.04	0.04	0.07	0.008	
Benzofuran										0.05	0.06	
Biphenylene									0.005			

* Percent Yield = {([Product])/ ([2-MBP]$_0$ + [2-MCP]$_0$)}*100

observed between 450 and 900°C with a maximum yield of 1.10 at 750°C. The chlorinated products included chlorobenzene (maximum yield of 0.07 at 750ºC) and chloronaphthalene (maximum yield of 0.17% at 800ºC). The analogous brominated products, bromobenzene and bromonaphthalene, were observed over a similar temperature range of 600 to 900ºC, with the maximum yields of 0.17 and 0.15 at 800ºC respectively. The other brominated product observed was 2,4-dibromophenol with a maximum yield of 0.006 at 550ºC. Products that contained both bromine and chlorine observed were 2-chloro-4-bromophenol and 2-bromo-4-chlorophenol over a temperature range of 500 to 700ºC with maximum yields of 0.01 and 0.03, respectively. The remaining products, which are decomposition and molecular growth products of 2-MCP and 2-MBP between 700 and 900°C, were acenaphthalene, benzene, phenylethyne, diphenylethyne, benzofuran and biphenylene.

3.2 Gas-Phase, High-Temperature Oxidation

Results from the gas-phase high temperature oxidation were determined from conditions involved inside the STDS. The residence time inside the reactor was held at a constant 2.0 seconds for each temperature. The temperature range was maintained to be between 300 and 1000°C. In order to maintain oxidative conditions, the flow consisted of 20% O_2 mixed in with UHP helium. Two initial precursors were used, 2-MCP and 2-MBP. The concentrations of 2-MCP and 2-MBP for each experimental run were kept at 88 ppm for each temperature. However for the experiment involving the mixture of 2-MCP and 2-MBP, the initial concentration of each was held at 44 ppm so that the total initial concentration is 88 ppm. Thus the starting percent yield for 2-MCP and 2-MBP begins at 50%. The reasoning is to maintain a constant concentration of 88 ppm for all experiments.

3.2.1 Gas-Phase Oxidation of 2-Chlorophenol[4]

The temperature dependence of the oxidative thermal degradation of 2-MCP and the yield of PCDD/F products are presented in figure 3.7 and table 3.4 for a reaction time of 2.0 s. The non-PCDD/F products are presented in figure 3.8 and table 3.4. Figures 3.7 and 3.8 are presented on a semi-logarithmic scale in which the percent yields of products (or percent of unconverted 2-MCP) are presented on a logarithmic scale versus temperature. The thermal degradation of 2-MCP initially increased gradually from 400 to 650°C, where the rate drastically accelerated, achieving 99 % destruction at 850°C.

The predicted PCDD/F products, DD, 1-MCDD and 4,6-DCDF were all observed for the oxidation of 2-MCP (cf. Figure 3.7 and Table 3.4). 4-MCDF and DF were the other PCDD/F products detected. Initially at 400°C, 1-MCDD was the only PCDD/F product observed and reached a maximum percent yield of 0.92% at 600°C. DD and 4,6 DCDF were detected between 500 and 900°C with maximum percent yields of 1.32 and 9.4% respectively. The other PCDD/F products, 4-MCDF and DF, were not observed until 650°C where they achieved maximum yields of 0.69 and 0.20% respectively. Above 900°C no chlorinated aromatics were detected.

Non-PCDD/F products were also detected from the oxidation of 2-MCP. (cf. Figure 3.8 and table 3.4). Chlorinated products included chlorobenzene (maximum yield of 0.03 % at 650°C), 1-chloronaphthalene (maximum yield of 0.10 % at 650°C), 2,4-dichlorophenol and 2,6-dichlorophenol (maximum yields of 0.28 and 0.59 respectively at 600°C). Other products included naphthalene, benzene and phenol. Naphthalene is the only non-PCDD/F product observed at 400°C and achieves a maximum yield of 0.22% at 700°C. However the percent yield

[4] Reproduced in part with permission from Environmental Science and Technology, submitted for publication. Unpublished work copyright 2004 American Chemical Society.

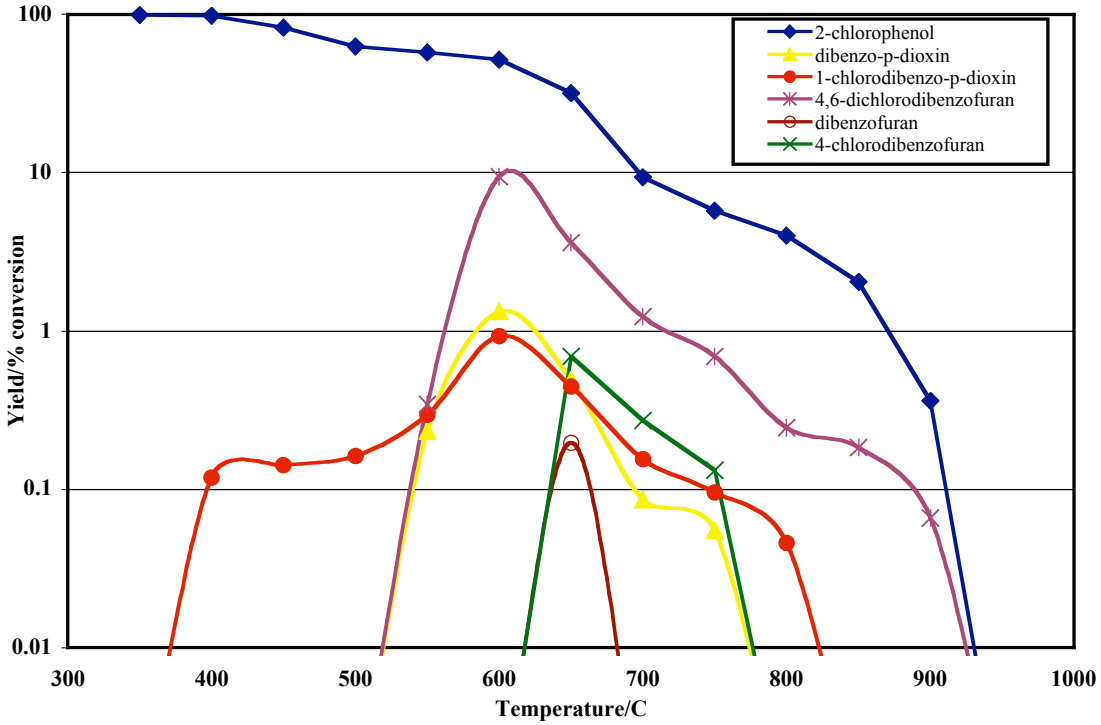

Figure 3.7 "Dioxin" Products from the Gas-Phase Oxidation of 2-Chlorophenol

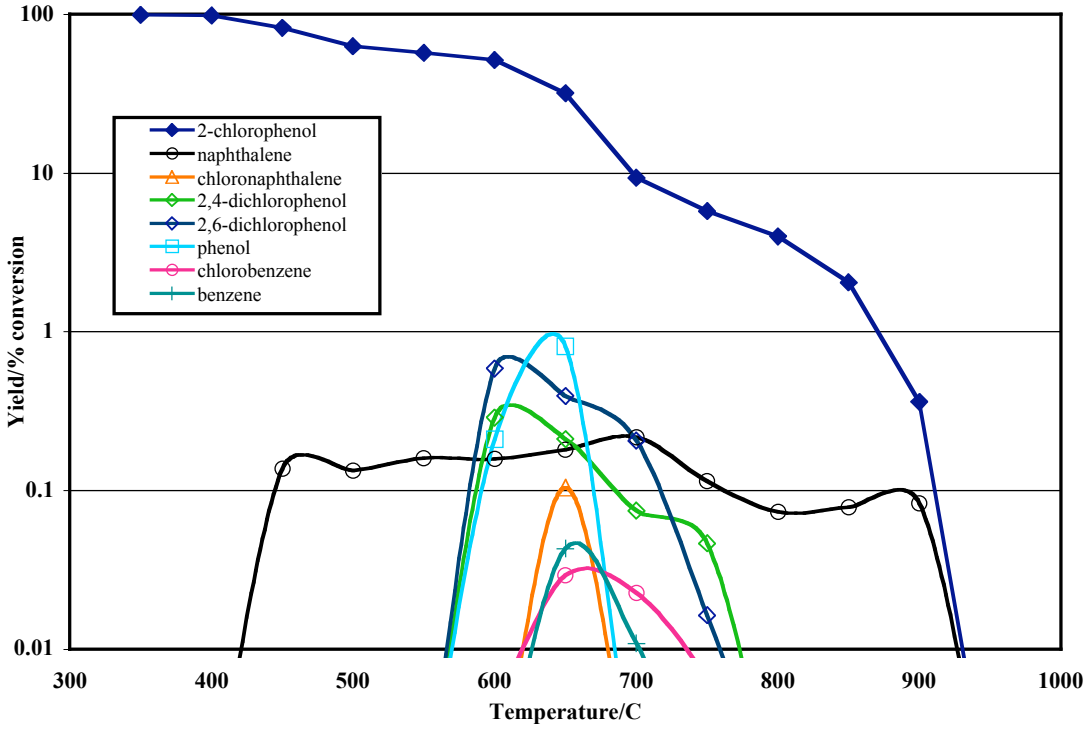

Figure 3.8 "Non-Dioxin" Products from the Gas-Phase Oxidation of 2-Chlorophenol

Table 3.4 Percent Yield of Products of Gas-Phase Oxidation of 2-Chlorophenol

Product	Temperature (° C)										
	400	**450**	**500**	**550**	**600**	**650**	**700**	**750**	**800**	**850**	**900**
2-Chlorophenol	98	82.1	62.7	57.2	51.6	31.8	9.34	5.74	3.99	3.52	0.36
Dibenzo-p-dioxin				0.23	1.32	0.49	0.09	0.05			
1-Chlorodibenzo-p-dioxin	0.12	0.14	0.16	0.29	0.92	0.44	0.16	0.09	0.05		
Dibenzofuran						0.20					
4-Chlorodibenzofuran						0.69	0.27	0.13			
4,6 Dichlorodibenzofuran				0.34	9.43	3.62	1.23	0.69	0.24	0.18	0.07
Naphthalene		0.14	0.13	0.16	0.16	0.18	0.22	0.11	0.08	0.08	0.07
Chloronaphthalene						0.10					
Phenol					0.21	0.81					
2,4 Dichlorophenol					0.28	0.21	0.07	0.05			
2,6 Dichlorophenol					0.59	0.39	0.21	0.02			
Benzene						0.04	0.01				
Chlorobenzene				0.004	0.005	0.03	0.02	0.006			

* Percent Yield = {([Product])/ $[2\text{-MCP}]_0$}*100

of naphthalene remains fairly consistent between 400°C and 900°C. All other products, benzene and phenol, achieve maximum yields at 650°C and were observed between 600 and 700°C.

3.2.2 Gas-Phase Oxidation of 2-Bromophenol[5]

The temperature dependence of the oxidative thermal degradation of 2-MBP and the yield of PBDD/F products are presented in figure 3.9 and table 3.5 for a reaction time of 2.0 s. The non-dioxin products are presented in figure 3.10 and table 3.5. Figures 3.9 and 3.10 are presented on a semi-logarithmic scale in which the percent yields of products (or percent yield of unconverted 2-MBP) are presented on a logarithmic scale versus temperature. The thermal degradation of 2-MBP initially increased gradually from 350 to 600°C, achieving 99% destruction at 800°C.

The predicted PBDD/F products, DD, 1-MBDD and 4,6-DBDF were all observed for the oxidation of 2-MBP (cf. Figure 3.9 and table 3.5). Other PBDD/F products detected where 4-MBDF and DF. The two PBDD products, DD and 1-MBDD, were observed between 400 and 850°C reaching a maximum yield of 22.2 and 0.15 at 550°C respectively. 4,6-DBDF and 4-MBDF were detected between 450 and 850°C reaching a maximum yield at 650°C of 2.40 and 0.82 respectively. The final product, DF, was not detected until 550°C and achieved a maximum yield of 0.90 at 650°C. No brominated aromatic products were detected above 900°C.

Non-PBDD/F products were also detected for the oxidation of 2-MBP (cf. Figure 3.10 and table 3.5). Initially at 400°C, 2,4-dibromophenol, 2,6-dibromophenol and naphthalene were observed. 2,4-dibromophenol and 2,6-dibromophenol achieved a maximum yield of 0.07 and 0.17 at 550°C respectively. Naphthalene remained at relatively constant yields from 400 to 700°C then decreased in yield to 900°C where it was no longer detected. Phenol, benzene, and

[5] Reproduced in part with permission from Environmental Science and Technology, submitted for publication. Unpublished work copyright 2004 American Chemical Society.

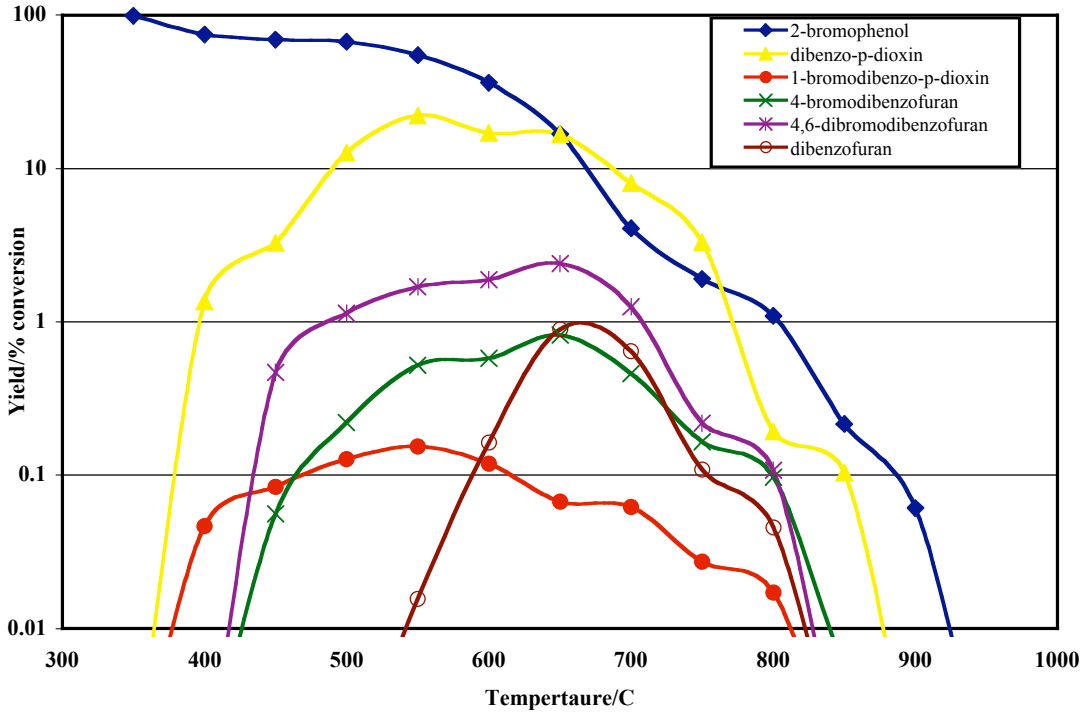

Figure 3.9 "Dioxin" Products from the Gas-Phase Oxidation of 2-Bromophenol

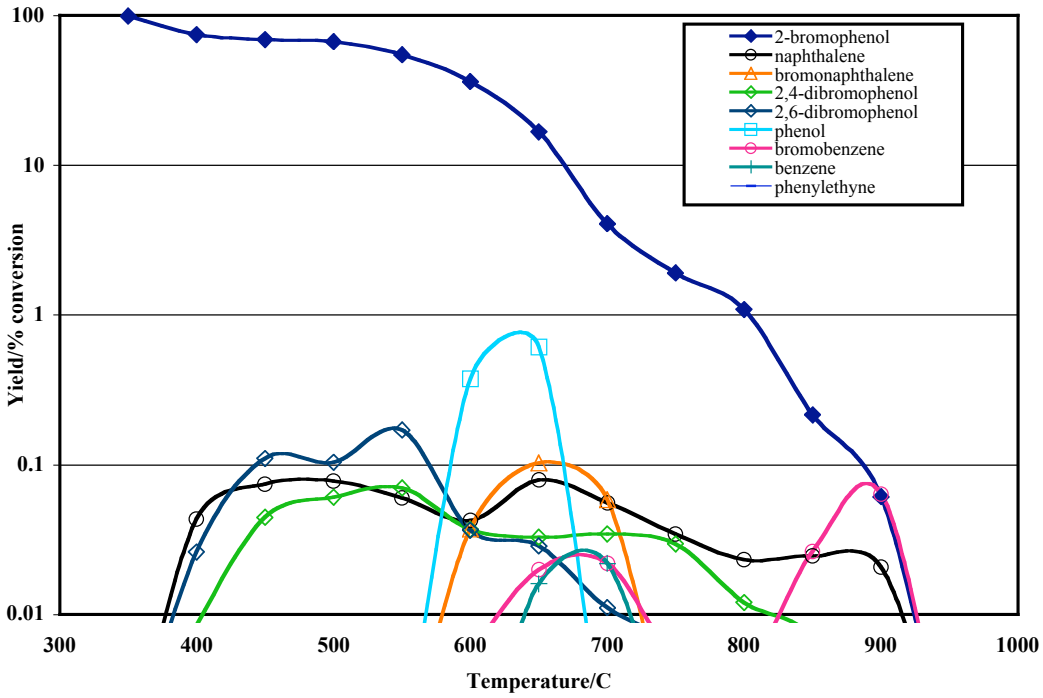

Figure 3.10 "Non-Dioxin" Products from the Gas-Phase Oxidation of 2-Bromophenol

Table 3.5 Percent Yield of Products of Gas-Phase Oxidation of 2-Bromophenol

Product	Temperature (° C)											
	350	400	450	500	550	600	650	700	750	800	850	900
2-Bromophenol	99.2	74.7	69.3	66.9	54.7	36.2	16.7	4.07	1.90	1.09	0.22	0.06
Dibenzo-p-dioxin		1.36	3.27	12.6	22.2	17.0	16.6	8.01	3.30	0.18	0.12	
1-Bromodibenzo-p-dioxin		0.04	0.08	0.13	0.15	0.12	0.07	0.06	0.03	0.02		
Dibenzofuran					0.02	0.16	0.90	0.64	0.11	0.05		
4-Bromodibenzofuran			0.06	0.22	0.52	0.58	0.82	0.46	0.17	0.10	0.005	
4,6-Dibromodibenzofuran			0.46	1.14	1.69	1.89	2.40	1.25	0.22	0.11		
Naphthalene		0.04	0.07	0.08	0.06	0.04	0.08	0.06	0.03	0.02	0.02	0.02
Bromonaphthalene						0.04	0.10	0.06				
Phenol						0.37	0.61					
2,4-Dibromophenol		0.008	0.04	0.06	0.07	0.04	0.03	0.03	0.03	0.03	0.01	0.006
2,6-Dibromophenol		0.03	0.11	0.10	0.17	0.04	0.03	0.01	0.007	0.005		
Benzene						0.002	0.02	0.02				
Bromobenzene						0.005	0.02	0.02	0.005	0.004	0.03	0.06
Phenylethyne							0.007	0.005				

* Percent Yield = {([Product])/ $[2\text{-MBP}]_0$}*100

phenylethyne, were detected between 550 and 750°C achieving their respective maximum yields of 0.61, 0.02, and 0.007 at 650°C. Bromobenzene was observed between 550 - 750°C and 825 – 925°C with local maximum yields of 0.02 at 650°C and 0.06 at 900°C.

3.2.3 Gas Phase Oxidation of a Mixture of 2-Chlorophenol and 2-Bromophenol[6]

The temperature dependence of the oxidative thermal degradation of a 50/50 mixture of 2-MCP and 2-MBP and the yield of PCDD/F and PBDD/F products are presented in figure 3.11 and table 3.6. The other products observed are presented in figure 3.12 and table 3.6. Figures 3.11 and 3.12 are represented on a semilogarithmic scale in which the percent yields of products (or percent yield of unconverted 2-MCP and 2-MBP) are presented on a logarithmic scale versus temperature. The thermal degradation of 2-MBP and 2-MCP gradually increased together from 350 to 600°C, where the rate drastically accelerated , achieving 99% destruction at 750°C.

DD, 1-chlorodibenzo-*p*-dioxin (1-MCDD) and 1-MBDD were initially observed at 350 C. 1-MBDD (maximum yield of 0.07% at 350°C) and 1-MCDD (maximum yield of 0.07% at 400°C) were detected at similar yields in a temperature range from 350 to 700°C. DD, the major product, was detected between 350 and 900°C and achieved a maximum yield of 8.7 % at 600°C. The remainder of the PBDD/F and PCDD/F products, 4-B-6-CDF (maximum yield of 0.91 % at 600°C), 4,6-DBDF (maximum yield of 0.53 % at 600°C), 4,6-DCDF (maximum yield of 0.43 % at 600°C), DF (maximum yield of 0.30 % at 650°C), 4-MBDF (maximum yield of 0.15 % at 600°C) and 4-MCDF (maximum yield of 0.11 % at 600°C) were detected between 500 and 750°C.

[6] Reproduced in part with permission from Environmental Science and Technology, submitted for publication. Unpublished work copyright 2004 American Chemical Society.

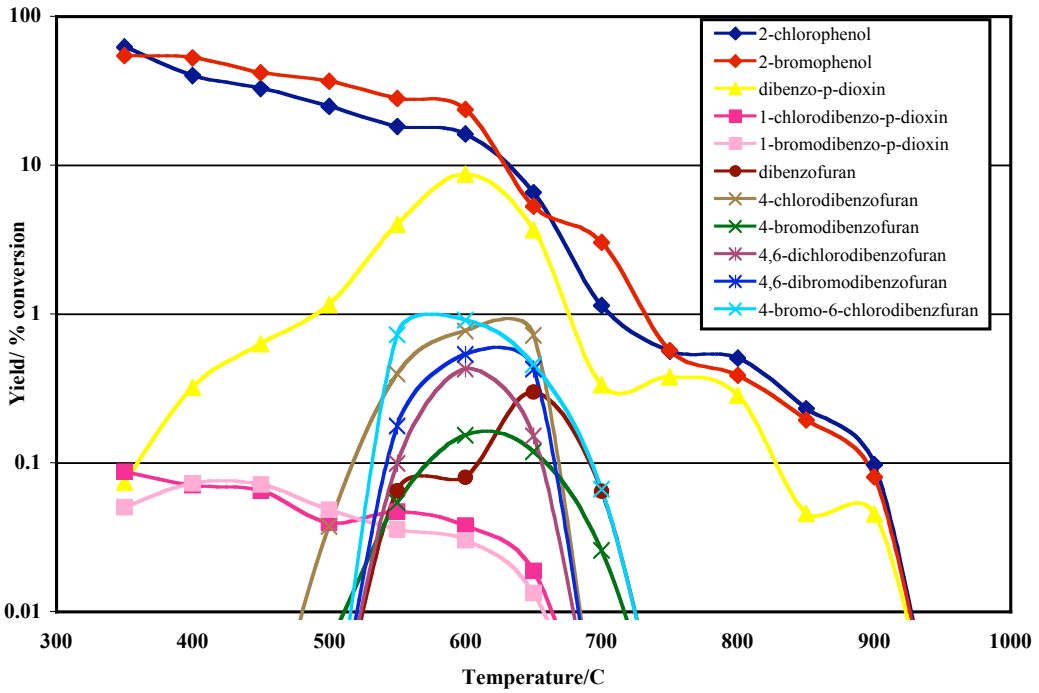

Figure 3.11 "Dioxin" Products from the Gas-Phase Oxidation of 2-Chlorophenol and 2-Bromophenol

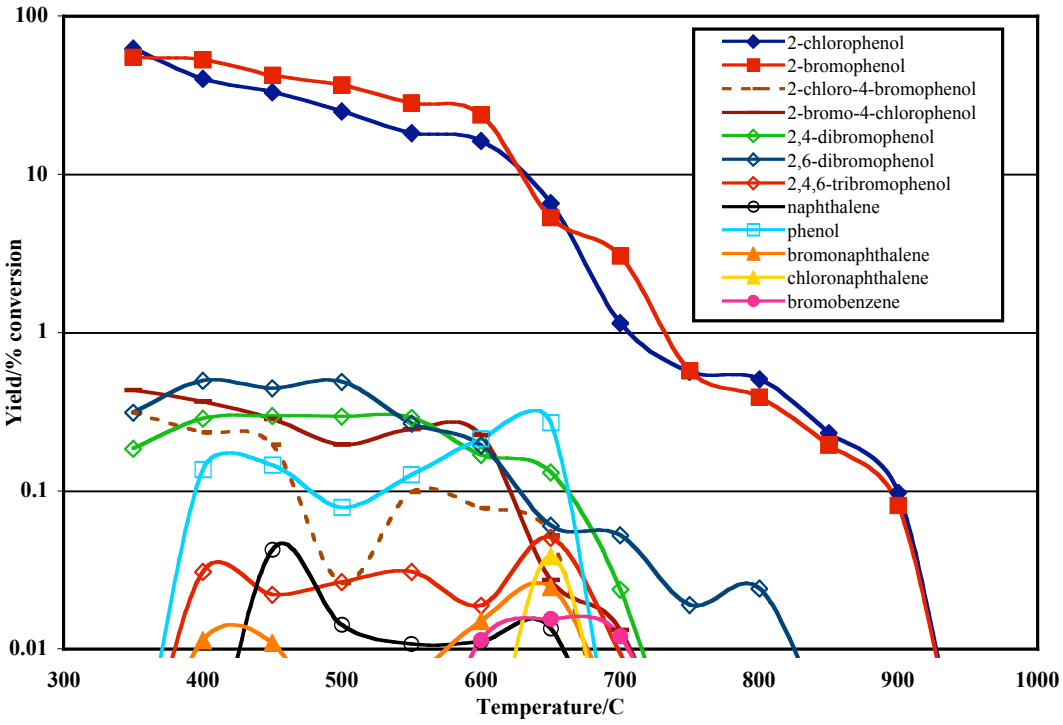

Figure 3.12 "Non-Dioxin" Products from the Gas-Phase Oxidation of 2-Chlorophenol and 2-Bromophenol

Table 3.6 Percent Yield of Products of Gas-Phase Oxidation of Mixture of 2-Bromophenol and 2-Chlorophenol

Products	Temperature (°C)											
	350	400	450	500	550	600	650	700	750	800	850	900
2-Chlorophenol	52.1	34.4	33.1	24.9	18.3	16.2	6.58	1.14	0.57	0.51	0.23	0.09
2-Bromophenol	45.5	45.4	42.1	36.7	28.2	23.8	5.32	3.04	0.57	0.38	0.19	0.08
Dibenzo-p-dioxin	0.06	0.28	0.63	1.16	4.02	8.71	3.70	0.33	0.38	0.20	0.05	0.05
1-Chlorodibenzo-p-dioxin	0.07	0.06	0.06	0.04	0.05	0.04	0.02					
1-Bromodibenzo-p-dioxin	0.04	0.06	0.07	0.05	0.04	0.03	0.01					
Dibenzofuran					0.06	0.08	0.30	0.06				
4-Chlorodibenzofuran				0.005	0.05	0.11	0.09					
4-Bromodibenzofuran				0.006	0.05	0.15	0.12	0.03				
4-Bromo-6-chlorodibenzofuran					0.73	0.91	0.46	0.07				
4,6 Dichlorodibenzofuran					0.10	0.43	0.15					
4,6 Dibromodibenzofuran					0.18	0.54	0.43					
Phenol		0.12	0.14	0.8	0.13	0.21	0.27					
2-Chloro-4-bromophenol	0.26	0.20	0.20	0.03	0.09	0.08	0.05					
2-Bromo-4-chlorophenol	0.36	0.31	0.29	0.20	0.24	0.22	0.03	0.01				
2,4 Dibromophenol	0.15	0.25	0.30	0.30	0.29	0.17	0.13					
2,6 Dibromophenol	0.26	0.43	0.45	0.49	0.26	0.17	0.06	0.05	0.02	0.02	0.003	
2,4,6 Tribromophenol		0.03	0.02	0.03	0.03	0.02	0.05	0.01				
Naphthalene			0.04	0.01	0.01	0.01	0.01					
Chloronaphthalene							0.04					
Bromonaphthalene		0.01	0.01	0.002	0.006	0.02	0.02	0.004				
Benzene						0.001	0.006	0.004				
Chlorobenzene						0.005	0.008	0.004				
Bromobenzene						0.01	0.02	0.01				
Chlorobenzofuran					0.11	0.14	0.13					
Benzofuran								0.09				

* Percent Yield = {([Product])/ ([2-MBP]$_0$ + [2-MCP]$_0$)}*100

Many other products were observed for the oxidation of the mixture of 2-MCP and 2-MBP (cf. Figure 3.12 and table 3.6 Phenolic products were observed between 350 and 770°C except 2,6-dibromophenol that persisted to 850°C. The phenolic products consist of phenol (maximum yield of 0.27 at 650°C); 2-chloro-4-bromophenol (maximum yield of 0.26 at 350°C); 2-bromo-4-chlorophenol (maximum yield of 0.36 at 350°C); 2,4-dibromophenol (maximum yield of 0.30 at 500°C); 2,6-dibromophenol (maximum yield of 0.49 at 500°C) and 2,4,6-tribromophenol (maximum yield of 0.05 at 650 °C).

Benzene (maximum yield of 0.006 at 650°C), chlorobenzene (maximum yield of 0.008 at 650°C) and bromobenzene (maximum yield of 0.02 at 650°C), were observed between 550 and 700°C. The remaining detected products were naphthalene (maximum yield of 0.04 at 650°C), bromonaphthalene (maximum yield of 0.02 at 650°C) and chloronaphthalene (maximum yield of 0.04 at 450°C).

3.3 Surface Catalyzed Thermal Degradation of 2-Bromophenol

Results from the gas-phase surface mediated reactions of 2-MBP were determined from various conditions involved inside the STDS. The surface used as a catalyst was composed of CuO and silica. The composition was setup so that the catalyst was composed of 5% copper. The contact time of the 2-MBP sample to the surface was 0.01 seconds. The temperature range for the experiments was from 250 to 600°C. In order to maintain pyrolytic conditions, the flow through the reactor was UHP Helium. To emulate oxidative conditions, 20% Oxygen was added to the Helium stream into the reactor.

3.3.1 Results from Pyrolytic Conditions[7]

The temperature dependence of the surface mediated pyrolytic thermal degradation of 2-MBP and the yield of PBDD/F products are presented in Figure 3.13 and Table 3.7. The remaining products detected are presented in Figure 3.14 and Table 3.7. Figures 3.13 and 3.14 are presented on a semi-logarithmic scale in which the percent yields of products (or percent yield of unconverted 2-MBP) are on a logarithmic scale versus temperature. The thermal degradation for 2-MBP increased rapidly from 250 to 550°C and 2-MBP achieved 99% destruction at 500°C.

DD, 1-MBDD, dibromodibenzo-*p*-dioxin (DBDD), 4-MBDF and DF were the PBDD/F products observed. DD, 1-MBDD and DBDD were all observed between 250 and 500°C with maximum yields of 1.90, 1.66 and 2.98 at 350°C respectively. 4-MBDF (maximum yield of 0.004% at 400°C) and DF (maximum yield of 0.04% at 450°C) were observed at a smaller temperature range of 350 to 450°C. TrBDD was also detected at 400°C at very low yields. No brominated aromatics were observed above 600°C.

Non-PBDD/F products were also detected from the surface-mediated pyrolysis of 2-MBP (Figure 3.14 and Table 3.7). The phenol products, 2,4-dibromophenol, 2,6-dibromophenol and 2,4,6-tribromophenol, were detected between 250 and 500°C. 2,6-dibromophenol achieved a maximum yield of 16.45 at 300°C, whereas 2,4-dibromophenol achieved its maximum yield of 9.99 at 350°C. 2,4,6-tribromophenol reached a maximum yield of 3.79 at 350°C as well. Bromobenzene (maximum yield of 0.09% at 400°C) and 1,2-dibromobenzene (maximum yield of 0.31% at 350°C) were detected between 250 and 475°C. 1,2,4-Tribromobenzene (maximum

[7] Reproduced in part with permission from Environmental Science and Technology, submitted for publication. Unpublished work copyright 2004 American Chemical Society.

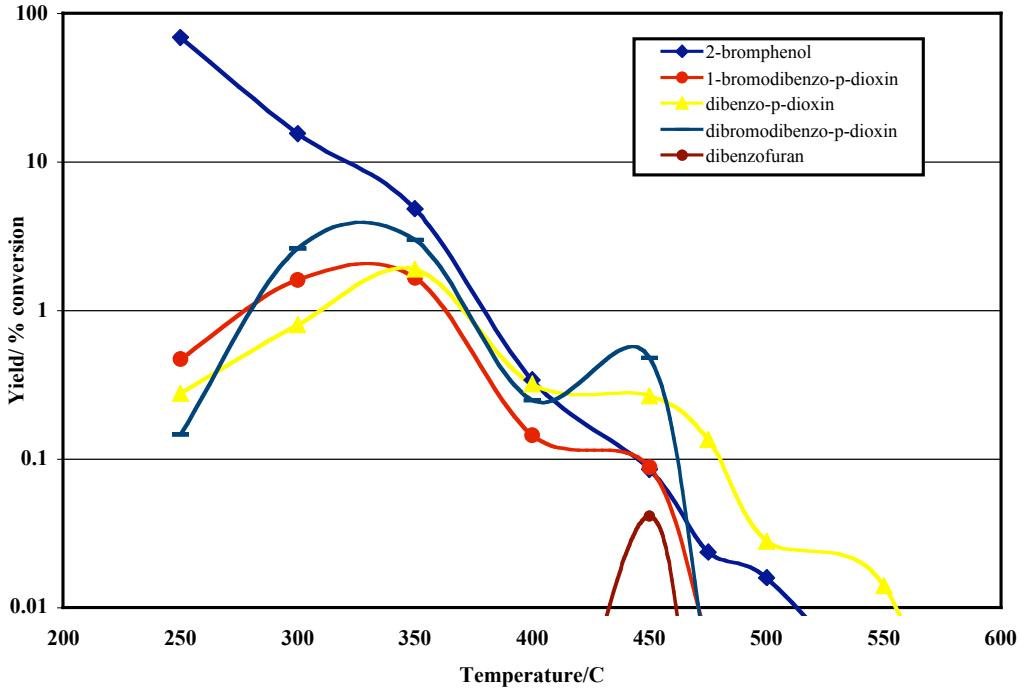

Figure 3.13 "Dioxin" Products from the Surface Catalyzed Pyrolysis of 2-Bromophenol

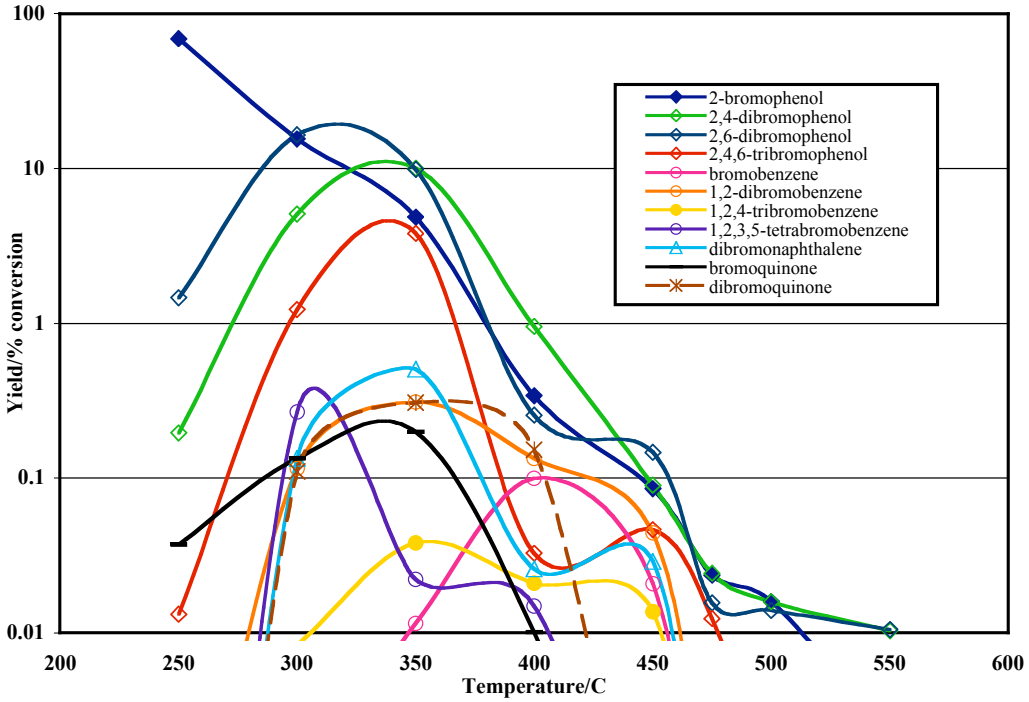

Figure 3.14 "Non-Dioxin" Products from the Surface Catalyzed Pyrolysis of 2-Bromophenol

Table 3.7 Percent Yield of Products of Surface Catalyzed Gas-Phase Pyrolysis of 2-Bromophenol

Products	Temperature (°C)								
	250	**300**	**350**	**400**	**450**	**475**	**500**	**550**	**600**
2-Bromophenol	68.9	15.5	4.84	0.34	0.08	0.02	0.02	0.002	
Dibenzo-*p*-dioxin	0.27	0.80	1.90	0.32	0.27	0.14	0.03		
1-Bromodibenzo-*p*-dioxin	0.47	1.60	1.66	0.14	0.09	0.006			
Dibromodibenzo-*p*-dioxin	0.14	2.62	2.98	0.24	0.48	0.003			
Dibenzofuran					0.04				
4-Bromodibenzofuran			0.002	0.004	0.002				
2,4-Dibromophenol	0.19	5.07	9.99	0.95	0.09	0.02	0.01	0.01	
2,6-Dibromophenol	1.46	16.45	9.85	0.25	0.15	0.02	0.01	0.01	
2,4,6-Tribromophenol	0.01	1.23	3.79	0.03	0.05	0.01			
Bromobenzene	0.001	0.001	0.01	0.09	0.02				
1,2-Dibromobenzene		0.12	0.30	0.13	0.04				
1,2,4-Tribromobenzene		0.008	0.03	0.02	0.01				
1,2,3,5-Tetrabromobenzene		0.27	0.02	0.02					
Bromoform	0.001	0.003	0.002						
Dibroonaphthalene		0.13	0.50	0.03	0.03				
Tribromoethane		0.004	0.009						
2,6 Dibromoquinone	0.04	0.13	0.19	0.01					

* Percent Yield = {([Product])/ $[2\text{-MBP}]_0$}*100

yield of 0.04% at 350°C) and 1,2,3,5-tetrabromobenzene (maximum yield of 0.26% at 300°C) were observed between 300 and 450°C. Dibromonaphthalene achieved a maximum yield of 0.50 at 350°C and as observed between 300 and 450°C. The bromoform, tribromoethane, bromoquinone, dibromoquinone were the remaining products detected between 300 and 400°C.

3.3.2 Results from Oxidative Conditions[8]

The temperature dependence of the surface-mediated thermal degradation of 2-MBP and the yields of PBDD/F products are presented in Figure 3.15 and Table 3.8. The other non PBDD/F products are presented in Figure 3.16 and Table 3.8. Figures 3.15 and 3.16 are given on a semi-logarithmic scale in which the percent yields of products (or percent yield of unconverted 2-MBP) are on a logarithmic scale versus temperature. The rate of the oxidative thermal degradation of 2-MBP drastically accelerated from 250 to 450°C and reached 99% destruction at 375°C.

DD, 1-MBDD, and one isomer of DBDD were detected between 250 and 550°C and achieved maximum percent yields of 14.44, 5.07 and 6.42 at 450°C respectively. A second isomer of dibromodibenzo-*p*-dioxin (DBDD(II)) reached a maximum yield of 1.26% at 500°C. One isomer of tribromodibenzo-*p*-dioxin (TrBDD) was observed between 250 and 500°C and reached a maximum yield of 1.83% at 450°C. A second isomer of tribromodibenzo-*p*-dioxin (TrBDD(II)) was detected between 350 and 500°C reaching a maximum yield of 0.91% at 450°C as well. The remaining PBDD/F product, 4-MBDF, was detected between 400 and 500°C and achieved a maximum yield of 0.20% at 450°C. No brominated aromatics were observed above 600°C.

[8] Reproduced in part with permission from Environmental Science and Technology, submitted for publication. Unpublished work copyright 2004 American Chemical Society.

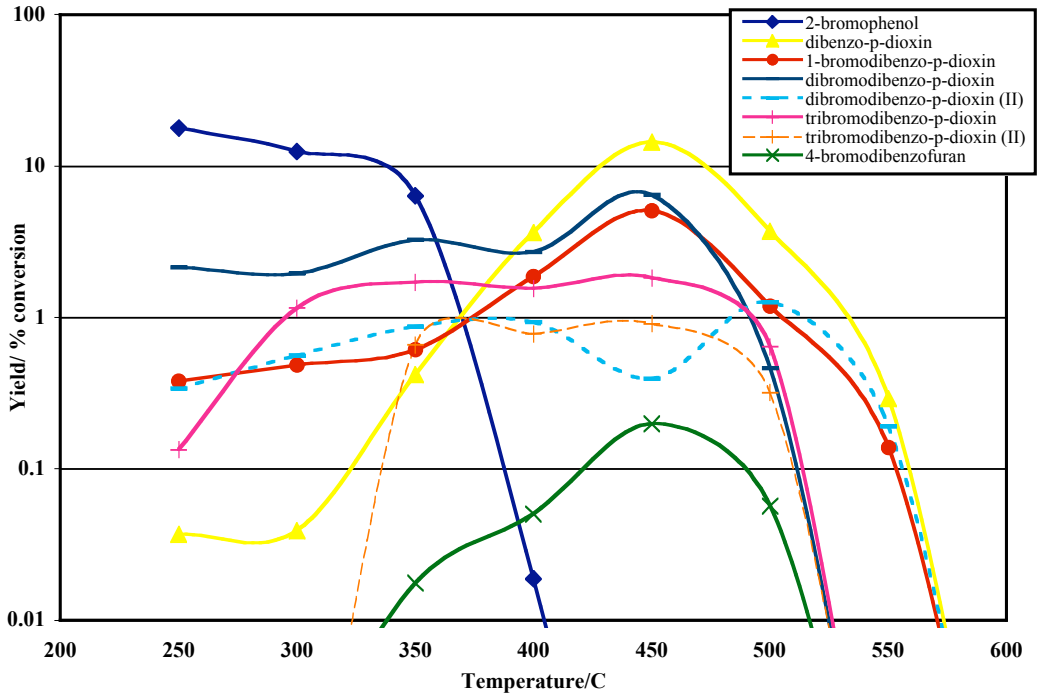

Figure 3.15 "Dioxin" Products from the Surface Catalyzed Oxidation of 2-Bromophenol

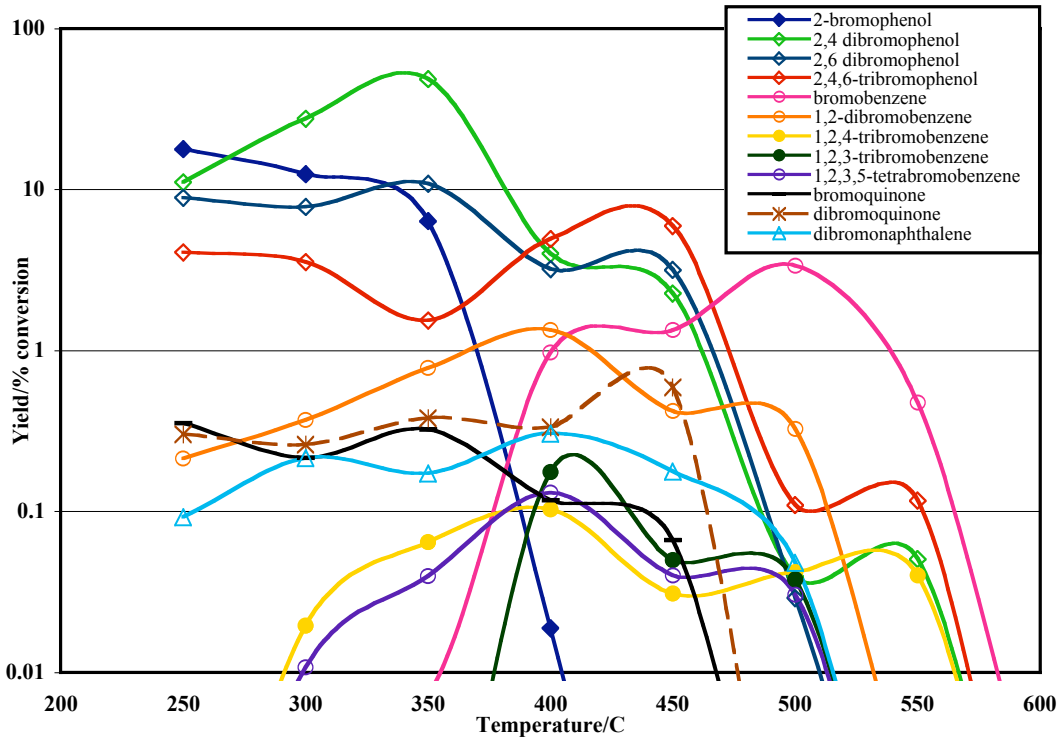

Figure 3.16 "Non-Dioxin" Products from the Surface Catalyzed Oxidation of 2-Bromophenol

Table 3.8 Percent Yield of Products of Surface Catalyzed Gas-Phase Oxidation of 2-Bromophenol

Products	Temperature (°C)						
	250	300	350	400	450	500	550
2-Bromophenol	17.94	12.52	6.39	0.02			
Dibenzo-p-dioxin	0.04	0.04	0.42	3.67	14.44	3.73	0.29
1-Bromodibenzo-p-dioxin	0.38	0.49	0.62	1.87	5.07	1.19	0.14
Dibromodibenzo-p-dioxin	2.14	1.96	3.26	2.71	6.42	0.46	
Dibromodibenzo-p-dioxin (II)	0.34	0.56	0.87	0.93	0.39	1.26	0.19
Tribromodibenzo-p-dioxin	0.13	1.16	1.72	1.56	1.83	0.64	
Tribromodibenzo-p-dioxin(II)			0.66	0.78	0.91	0.32	
4-Bromodibenzofuran			0.02	0.05	0.20	0.06	
2,4 Dibromophenol	11.15	27.78	48.93	4.02	2.28	0.04	0.05
2,6 Dibromophenol	8.94	7.86	10.92	3.22	3.18	0.03	
2,4,6 Tribromophenol	4.10	3.57	1.54	4.94	5.98	0.11	0.12
Bromobenzene	0.001	0.006	0.007	0.97	1.34	3.38	0.48
1,2-Dibromobenzene	0.21	0.37	0.78	1.35	0.42	0.33	0.001
1,2,4-Tribromobenzene		0.02	0.07	0.10	0.03	0.04	0.03
1,2,3-Tribromobenzene				0.18	0.05	0.04	
1,2,3,5-Tetrabromobenzene		0.01	0.04	0.13	0.05	0.03	
Bromoquinone	0.35	0.22	0.32	0.12	0.07		
Dibromoquinone	0.30	0.26	0.38	0.34	0.59		
Bromoform	0.04	0.04	0.08	0.14	0.03		
Dibromonaphthalene	0.09	0.22	0.17	0.31	0.18	0.05	
Tribromoethane	0.01	0.02	0.03	0.07	0.07	0.009	
Carbon Tetrabromide	0.004	0.005	0.01	0.02	0.02	0.06	

* Percent Yield = {([Product])/ $[2\text{-MBP}]_0$}*100

The non-PBDD/F products were also detected from the surface-mediated oxidation of 2-MBP. The brominated phenols, 2,4-dibromophenol (maximum yield of 48.93 at 350°C), 2,6-dibromophenol (maximum yield of 10.92 at 350°C) and 2,4,6-tribromophenol (maximum yield of 5.98 at 450°C), were observed between 250 and 550°C. Bromobenzene achieved its maximum yield of 3.38 at 500°C. Other detected brominated benzene products that were detected included: 1,2-dibromobenzene (maximum yield of 1.35 at 400°C), 1,2,3-tribromobenzene (maximum yield of 0.18 at 400°C), 1,2,4-tribromobenzene (maximum yield of 0.10 at 400°C) and 1,2,3,5-tetrabromobenzene (maximum yield of 0.13 at 400°C). Dibromonapthalene (maximum yield of 0.31 at 400°C) was detected between 250 and 500°C. The remaining detected products were bromoform, tribromoethane, bromoquinone, dibromoquinone and carbon tetrabromide and had yields of less than 1% at all temperatures.

3.4 References

1. Born, J.G.P.; Louw, R.; Mulder, P. *Formation of Dibenzodioxins and Dibenzofurans in Homogeneous Gas-Phase Reactions of Phenols*, Chemosphere, 1989, **19**: 401.

2. Yang, Y.; Muholland, J.A.; Akki, U. *Formation of Furans by Gas-Phase Reactions of Chlorophenols*, 27th Symposium (International) on Combustion, The Combustion Institute, 1998, 1761.

CHAPTER 4. DISCUSSION

4.1 Mechanisms from the Gas-Phase Pyrolysis of 2-Chlorophenol and 2-Bromophenol[1,2]

The formation of dioxin products (DD, 1-MCDD, 1-MBDD, 4-MBDF and DF) indicates that stable phenoxyl radicals are formed in significant yields through loss of the hydroxyl-hydrogen. The formation of aromatics (phenol, chlorobenzene, bromobenzene, and benzene) indicates that simple substitution reactions are occurring. The formation of 2,4 and 2,6-dibromophenol is evidence of bromination of 2-bromophenol. Minor evidence of chlorination is observed for the mixture of 2-MBP and 2-MCP with the presence of 2-bromo-4-chlorophenol. The formation of larger aromatic molecules at low temperatures (naphthalene, chloronaphthalene and bromonaphthalene) is the result of reactions involving the release of CO from the phenoxyl and bromophenoxyl radicals that will then recombine to form naphthalene, chloronaphthalene and bromonaphthalene. The formation of phenylethyne and diphenylethyne indicate fragmentation of the aromatic ring and reactions of even numbered radicals. All the heats of reaction, ΔH_{rxn}, AM1 semiempirical calculations for all key steps in the product formation pathways are located in appendix 1. Psuedo-equilibrium calculations performed to estimate the concentrations of H•, Cl• and Br• are located in appendix 2.

[1] Reproduced in part with permission from Evans, C. S. and Dellinger, B. *Mechanisms of Dioxin Formation from the High-Temperature Pyrolysis of 2-Chlorophenol*, Environmental Science and Technology, 2003, **37**: 1325. Copyright 2003 American Chemical Society.
[2] Reproduced in part with permission from Evans, C. S. and Dellinger, B. *Mechanismsof Dioxin Formation from the High-Temperature Pyrolysis of 2-Bromophenol*, Environmental Science and Technology, 2003, **37**: 5574. Copyright 2003 American Chemical Society.

4.1.1 2-Chlorophenol and 2-Bromophenol Decomposition

Decomposition of 2-chlorophenol (2-MCP) and 2-bromophenol (2-MBP) are both initiated by the loss of the phenoxyl hydrogen by unimolecular, bimolecular or possibly other low energy pathways (including heterogeneous reactions). Individually, the unimolecular decompositions of the oxygen-hydrogen bond for 2-MCP and 2-MBP are very similar to each other.

$C_6H_4ClOH \rightarrow C_6H_4ClO\bullet + H\bullet$ $\Delta H_{rxn} = 78$ kcal/mol (Reaction 1)

$C_6H_4BrOH \rightarrow C_6H_4BrO\bullet + H\bullet$ $\Delta H_{rxn} = 79$ kcal/mol (Reaction 2)

This is consistent with the activation energy for the reported rate coefficient for the decomposition of phenol, k_{phenol} (430 - 930°C) = $3.2 \times 10^{15}\exp(-86{,}500/RT)s^{-1}$ [1-2]. It has also been suggested by Louw that the activation energy for this reaction is 5 kcal lower for 2,4,6 trichlorophenol [3]. This suggests that the addition of Cl• will lower the activation energy causing reaction 1 to be more favorable for chlorinated phenols. Because of the relative similarity between 2-MBP and 2-MCP, 2-MBP is expected to behave in a similar manner. Studies have also shown that the O-H bond in 2-MBP is 0.10 kcal/mol weaker than the O-H bond the 2-MCP, and therefore H elimination is expected to be slightly faster for 2-MBP than for 2-MCP [4]. With the two, 2-MCP and 2-MBP, mixed together they are shown to decompose at the same rate. This rate is shown to be in between the individual rates of the pyrolysis of 2-MCP and 2-MBP being slightly faster than the pyrolysis of 2-MCP and slightly slower than the pyrolysis of 2-MBP.

Bimolecular propagation reactions under pyrolytic conditions include attack by H• and Br• and Cl•. Based on AM1 semiempirical molecular orbital calculations, thermodynamically feasible reactions of H• include: phenoxyl hydrogen abstraction (reaction 2a and 2b), chlorine or

bromine abstraction (reaction 3a and 3b), chlorine or bromine displacement (reaction 4a and 4b), and hydroxyl displacement (reaction 5a and 6 b) dependant on whether 2-MCP or 2-MBP is involved. Aromatic hydrogen abstraction however is thermodynamically unfavorable.

$C_6H_4ClOH + H\bullet \rightarrow C_6H_4ClO\bullet + H_2$ ΔH_{rxn} = -25 kcal/mol (Reaction 3a)

$C_6H_4BrOH + H\bullet \rightarrow C_6H_4BrO\bullet + H_2$ ΔH_{rxn} = -23 kcal/mol (Reaction 3b)

$C_6H_4ClOH + H\bullet \rightarrow \bullet C_6H_4OH + HCl$ ΔH_{rxn} = -14 kcal/mol (Reaction 4a)

$C_6H_4BrOH + H\bullet \rightarrow \bullet C_6H_4OH + HBr$ ΔH_{rxn} = -11 kcal/mol (Reaction 4b)

$C_6H_4ClOH + H\bullet \rightarrow C_6H_5OH + Cl\bullet$ ΔH_{rxn} = -17 kcal/mol (Reaction 5a)

$C_6H_4BrOH + H\bullet \rightarrow C_6H_5OH + Br\bullet$ ΔH_{rxn} = -29 kcal/mol (Reaction 5b)

$C_6H_4ClOH + H\bullet \rightarrow C_6H_5Cl + \bullet OH$ ΔH_{rxn} = 0 kcal/mol (Reaction 6a)

$C_6H_4BrOH + H\bullet \rightarrow C_6H_5Br + \bullet OH$ ΔH_{rxn} = 2 kcal/mol (Reaction 6b)

Chlorine atoms can also abstract phenoxyl hydrogens or aromatic hydrogens (Reactions 7a and 8a). Abstraction of phenoxyl hydrogens by bromine atoms is also favorable (Reaction 7b). In contrast, abstraction of chlorine or displacement of hydrogen is highly endothermic and unfavorable. The abstraction of an aromatic hydrogen by bromine (reaction 8b) for comparison to the analogous chlorine reaction, abstraction of bromine by bromine, displacement of hydrogen by bromine, and displacement of hydroxyl by bromine are highly endothermic and unfavorable.

$C_6H_4ClOH + Cl\bullet \rightarrow C_6H_4ClO\bullet + HCl$ ΔH_{rxn} = -25 kcal/mol (Reaction 7a)

$C_6H_4BrOH + Br\bullet \rightarrow C_6H_4BrO\bullet + HBr$ ΔH_{rxn} = -8 kcal/mol (Reaction 7b)

$C_6H_4ClOH + Cl\bullet \rightarrow \bullet C_6H_3ClOH + HCl$ ΔH_{rxn} = 1 kcal/mol (Reaction 8a)

$C_6H_4BrOH + Br\bullet \rightarrow \bullet C_6H_3BrOH + HBr$ ΔH_{rxn} = 19 kcal/mol (Reaction 8b)

Since the strength of the phenoxyl-hydrogen bonds in 2-MCP and 2-MBP are similar to that in non-halogenated phenol (ΔHrxn(phenoxyl---hydrogen) = 78 kcal mole), the rate coefficients are

based on analogous reactions with phenol for reactions 3, 4, 5 and 7 are k_3 (730-880°C) $=1.15x10^{14}exp(-12400/RT)$ $cm^3/mol/s$ [5], k_4 (800-1010°C) = $1.0x10^{13}exp(-11300/RT)$ $cm^3/mol/s$ [6], k_5 (800-1010°C)= $1.5x10^{13}exp(-7500/RT)$ $cm^3/mol/s$ [6], and k_7 (25°C) = $1.43x10^{14}$ $cm^3/mol/s$ [5], respectively.

Individually the formation of the chlorinated and/or brominated phenoxyl radical are initiated by reactions 1 and 2 with the abstraction of the phenoxyl hydrogen by H• (Reaction 3a,b) and Cl• (Reaction 7a) or Br• (Reaction 7b) being the dominant source of the phenoxyl radical formation. Reaction 5b is significant for 2-MBP and is faster than the analogous chlorine displacement in 2-MCP (Reaction 5a) because of the weaker carbon-bromine (80.5 kcal/mole) versus carbon-chlorine (95.7 kcal/mol) bond [7]. Reaction 7, hydrogen abstraction by a halogen atom, was found to be thermoneutral for 2-MCP and significantly endothermic and unfavorable for 2-MBP. Aromatic hydrogen atom abstractions by bromine atoms are not likely to play a role in the combustion chemistry of brominated hydrocarbons, as the resulting HBr is not highly stable.

In a previously studied mixed CHC/BHC system, BrCl was formed along with HCl, HBr, Br_2 and Cl_2 [8]. Equilibrium thermodynamic modeling of the mole fraction of these compounds formed in combustion processes suggests that BrCl is formed in higher yields than Cl_2 [8]. It was also calculated that in the presence of oxygen, Br_2 is the dominant molecular bromine species whereas HCl is the dominant chlorine species [8]. However, Br_2 readily dissociates at post-combustion temperatures, making Br• the dominant brominated species overall. Our pseudo equilibrium calculations show that for the pyrolysis of the mixture of 2-MCP and 2-MBP, Cl• appear at 700°C compared to the pyrolysis of pure 2-MCP where Cl• are not present (cf.

Appendix 2). This increase is due to Br• reacting with Cl_2 with a rate coefficient of k_4(293-333 K) = 4.5 x 10^{12}exp(-6.9 kcal/RT) cm^3/mol/s [5] to form more Cl• by reaction 4.

$Br• + Cl_2 \rightarrow BrCl + Cl•$ (Reaction 9)

We also attribute a slight increase in the rate of 2-MCP decomposition to the increase in Cl• and the resulting increase in the rate of hydrogen abstraction via reaction 8a. The decrease in the rate of 2-MBP decomposition is attributed to competition for reaction with the reactive radical pool with 2-MCP.

Because of the low activation energies for reaction of 2-MCP and 2-MBP, the purely gas-phase reactions described above can account for all the decomposition of 2-MCP and 2-MBP above 750ºC. We have previously shown that above 725°C, the purely gas-phase reactions of 2,4,6 trichlorophenol (2,4,6 TCP) can account for its decomposition behavior as well as observed dioxin products [9]. However the initiation of the decomposition of 2,4,6 TCP, 2-MBP and 2-MCP at temperatures as low as 400°C requires us to consider other possible low energy initiation pathways. Heterogeneous wall reactions may result in a wall collision assisted reaction analogous to reaction 1. Trace impurities may also result in low temperature decomposition. The potential contribution of these reactions have been previously analyzed for the oxidation of 2,4,6-trichlorophenol and been shown to not significantly impact subsequent propagation reactions [10].

4.1.2 Formation of Phenol, Chlorobenzene, Bromobenzene and Benzene

Based on the early onset of phenol formation at temperatures as low as 425°C for 2-MCP and 500°C for 2-MBP, the dominant source of phenol is due to the exothermic displacement of either chlorine or bromine by H• (Reaction 5a and 5b). Higher yields of phenol are observed and at lower temperatures for 2-MBP than 2-MCP. This is a result of the lower activation energy for

bromine displacement than chorine displacement. In the case where 2-MCP and 2-MBP are mixed, similar results were seen as well. The maximum yield observed for this study is similar to the maximum yield for 2-MCP in that they are both seen at the temperature of 750°C. The maximum yield for the results with 2-MBP was seen at 600°C. Based on the previous results, the lower temperature formation of phenol is probably due more to the displacement of bromine from 2-MBP because of the lower activation energy for bromine displacement than chlorine displacement. However, these results suggest that the less exothermic displacement of Cl• is occurring as well as the displacement of Br•.

Formation of chlorobenzene and benzene are at much lower yields and higher temperatures than phenol for the pyrolysis of 2-MCP. This is consistent with the more endothermic displacements of •OH from 2-MCP by H• to form chlorobenzene (reaction 6a) and the displacement of •OH by H• from phenol to form benzene (ΔH_{rxn} = 4 kcal/mol). Formation of bromobenzene occurs at much lower yields and higher temperatures than formation of phenol for the pyrolysis of 2-MBP as well. This is also consistent with the more endothermic displacements of the hydroxyl group by H• to form bromobenzene (reaction 6b) than the displacement of Br• to form phenol.

With the pyrolysis of 2-MBP, it is also notable that bromobenzene is initially produced at 600ºC while benzene is not formed until 750ºC. Bromobenzene is formed from 2-MBP at lower temperatures than chlorobenzene for 2-MCP. This is in part attributable to the earlier onset of decomposition of 2-MBP than 2-MCP; however, bromine (versus chlorine) substitution may also facilitate •OH displacement. Results from the mixture of 2-MBP and 2-MCP are similar to the inidividual pyrolysis results in that the reults are observed in the same temperature range as the individual pyrolytic results with 2-MCP and 2-MBP. However these results show bromobenzene

has a maximum yield that is 2.5 times higher than chlorobenzene suggesting that the presence of bromine facilitates displacement of the hydroxyl radical.

Considering the relatively high temperatures (725-875°C) for formation of benzene, chlorobenzene and bromobenzene and the formation of phenylethyne and diphenylethyne in the same temperature range, it is evident that 2-MBP and 2-MCP fragments into primarily C2 radicals (vinyl and ethynyl) and C2 molecules (ethylene and acetylene). Molecular growth pathways resulting in formation of benzene and substituted benzene involving C2 units are well documented in the literature [11-13].

4.1.3 Bromination and Chlorination of 2-Bromophenol and 2-Chlorophenol

2,4-Dibromophenol and 2,6-dibromophenol result from the bromination of 2-MBP. Previous research suggests that bromine predominantly exists as Br_2 while chlorine is mainly found as HCl [8]. In fact the psuedo-equilibrium calculations show a higher concentration of Br• over Cl• for the individual pyrolysis of each. With the excess Br_2, bromination can occur more readily than chlorination. It has also been noted that bromination is 10 times more efficient that chlorination [14]. Thus the evidence of bromination for 2-MBP is acceptable even though chlorination of 2-MCP was not evident for the pyrolysis of 2-MCP.

Since displacement of H• by Br• is endothermic, the direct reaction of Br• with 2-MBP is unlikely. The formation of dibromophenol is instead due to recombination of phenoxyl radicals and Br•. Figure 4.1 depicts the formation of 2,4-dibromophenol and 2,6-dibromophenol by Br• attack at the resonance-stabilized, ortho- or para- carbon sites of the bromophenoxyl radicals (ΔH_{rxn} = -29 kcal/mol). Subsequent tautomerization results in the formation of the respective dibromophenols (ΔH_{rxn} =-17 kcal/mol).

With 2-MCP and 2-MBP mixed, only 2,4-dibromophenol, 2-chloro-4-bromophenol and 2-bromo-4-chlorophenol were detected. 2,4-Dibromophenol and 2-chloro-4-bromophenol are formed from the bromination of 2-MBP. 2-Bromo-4-chlorophenol is formed from the chlorination of 2-MCP. Again, since displacement of H• by Br• or Cl• is endothermic, the direct reaction of Br• or Cl• with 2-MBP or 2-MCP is unlikely. The formations of 2,4-dibromophenol

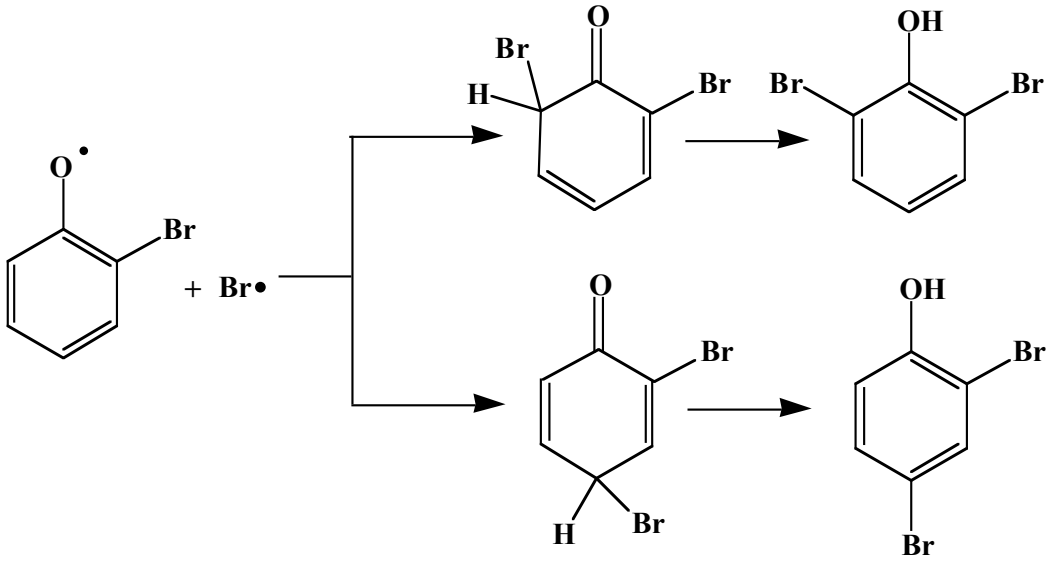

Figure 4.1 Reaction Mechanism for the Formation of 2,4-Dibromophenol and 2,6-Dibromophenol from the 2-Bromophenoxyl Radical

and 2-chloro-4-bromophenol are instead due to recombination of the respective para-carbon centred phenoxyl radicals and Br• and 2-bromo-4-chlorophenol is due to the recombination of the para-carbon centered bromophenoxyl radical with Cl•. Mechanisms for the formation of these products are analogous to the mechanisms for dibromophenol formation shown in Figure 4.1.

Bromination of 2-MBP was also evident for the pyrolysis of pure 2-MBP; however, chlorination was not observed for the pyrolysis of 2-MCP. This is attributed to chlorine be predominantly tied up as stable HCl, whereas HBr is much less stable and not a sink for bromine

atoms [8]. With the combination of 2-MCP and 2-MBP, there is evidence of chlorination with the formation of 2-bromo-4-chlorophenol. This is due largely appreciable to the presence of bromine that results in formation of BrCl that decomposes to release Cl• [8]. Also our theoritical psuedo equilibrium calculations show an increase in Cl• concentration with the presence of bromine (2-MBP) in the system. The other predicted isomers 2,6-dibromophenol and 2-bromo-6-chlorophenol remained undetected indicating a preference for halogenation at the para- site.

4.1.4 Formation of Naphthalene, Chloronaphthalene, Bromonaphthalene and Acenapthalene

Formation of polycyclics such as naphthalene, chloronaphthalene, and acenaphthalene are traditionally ascribed to molecular growth pathways involving largely C2 fragments [11-13]. However, the low temperature onset of formation of naphthalene for both 2-MCP and 2-MBP suggests a pathway that does not require the complete fragmentation of 2-MCP or 2-MBP and that is instead initiated at low temperatures.

Recently, resonantly stabilized cyclopentadienyl radicals have been recognized as potential precursors in the formation of naphthalene [15-16]. We have already discussed how 2-MCP or 2-MBP initially decomposes to the 2-chlorophenoxyl radical or the 2-bromophenoxyl radical, respectively. It is well documented that the thermal decomposition of a phenoxyl radical expels CO to form a cyclopentadienyl radical with a reported rate coefficient of k_{10} (730-1300°C) = $1x10^{11.4}exp(-22100+/-450/T)$ s^{-1} and the ΔH_f = 20 kcal/mol [2, 17]. Therefore, a similar elimination of CO from 2-chlorophenoxyl radical forms chlorocyclopentadienyl radical is also possible (Reaction 10):

$C_6H_4ClO• \rightarrow c\text{-}C_5H_4Cl• + CO$ (Reaction 10)

Recombination of two 2-chlorocyclopentadienyl radicals, followed by rearrangement and H• or Cl• elimination can result in formation of naphthalene if two Cl• are eliminated , chloronaphthalene if one Cl• and one H• are eliminated, and dichloronaphthalene if two H• are eliminated (cf. Figure 4.2). Formation of naphthalene, bromonaphthalene and dibromonaphthalene from 2-MBP occur via pathways analogous to pathways given for 2-MCP. The reported ΔH_{rxn} for the overall hydrocarbon reaction is 9.23 kcal/mol [15]. The dominance of naphthalene, lower concentration of chloronaphthalene and bromonapthalene, and absence of dichloronaphthalene and dibromonapthalene suggest that Cl• and Br• elimination is favored as

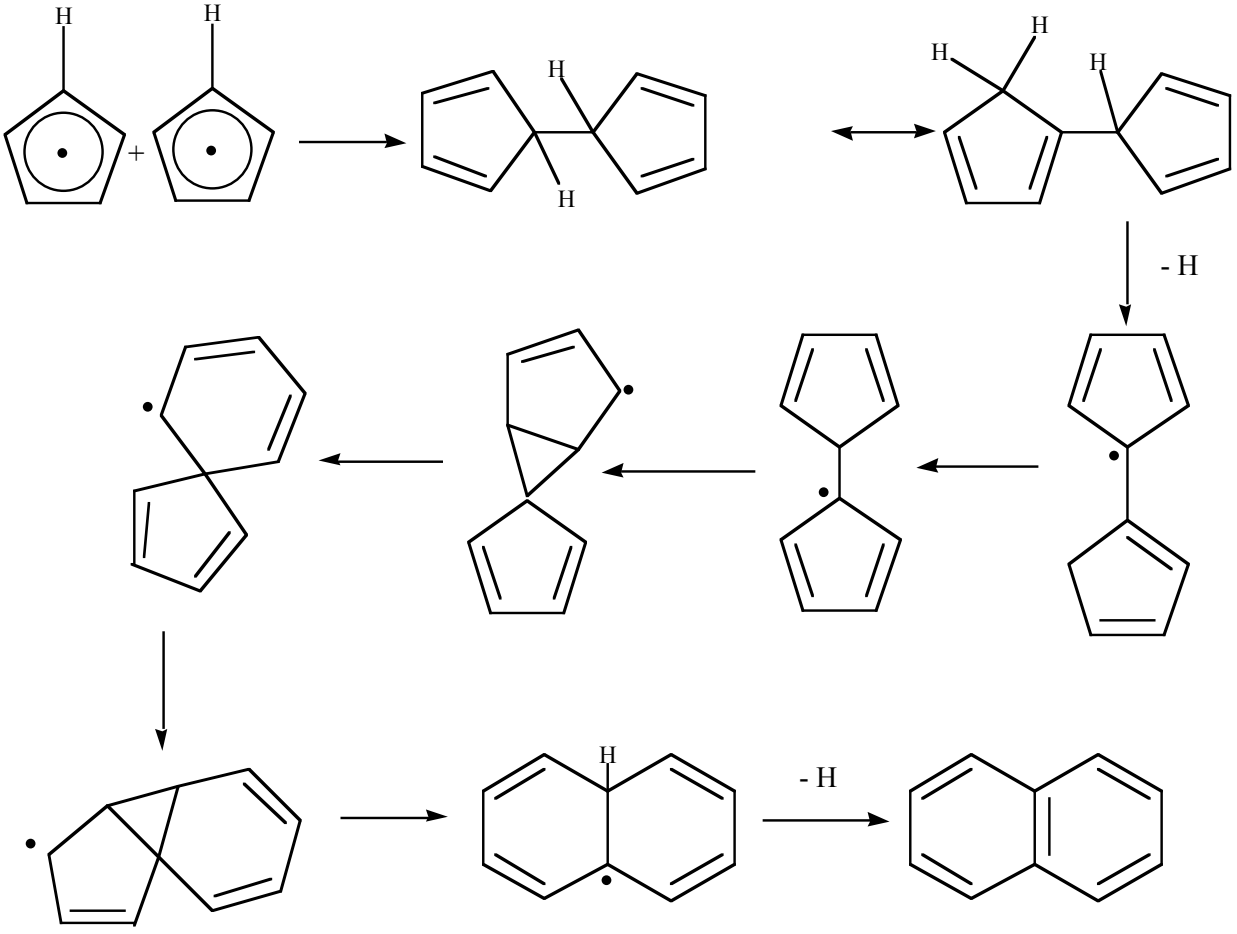

Figure 4.2 Reaction Mechanism for the Formation of Naphthalene from Two Cyclopentadienyl Radicals

would be expected based on the lower carbon-chlorine and carbon-bromine bond strength and thermochemistry [7]. This result also suggests that chlorinated and brominated hydrocarbons may undergo this type of molecular growth reaction more readily than hydrocarbons due to the more favorable elimination of chlorine than hydrogen atoms.

The formation of naphthalene was similar for both individual pyrolysis of 2-MBP and 2-MCP. However, chloronaphthalene is formed in greater yields than bromonapthalene. This is consistent with the elimination of bromine being much faster than chlorine bond as suggested by the weaker carbon-bromine versus carbon-chorine bond [7].

The yield of naphthalene in the mixture of 2-MCP and 2-MBP is 2x greater than for either of the pure compounds, while the yields of chloronaphthalene and bromonaphthalene are similar to their yields as pure compounds. This suggests that both chlorine and bromine facilitate naphthalene formation by an increase in the rate of elimination of Br• and Cl• over that of H• in purely hydrocarbon systems.

Acenapthalene is formed at higher temperatures and lower yields than naphthalene, chloronaphthalene and bromonaphthalene for all results. This suggests that traditional C2 molecular growth pathways form acenaphthalene where 2-MCP and 2-MBP are completely fragmented. It is also possible that part of the high temperature yields of naphthalene, chloronaphthalene and bromonaphthalene also are due to these molecular growth pathways.

4.1.5 Mechanisms for Formation of PCDD/Fs and PBDD/Fs

For the pyrolysis of 2-MCP, it is notable that DF forms at higher temperatures than DD and 1-MCDD. It also forms as phenol begins to decompose. Thus we believe that DF is a recombination of unchlorinated phenoxyl radical formed from decomposition of phenol via Figure 4.3 [18]. In this scheme, the phenoxyl radical converts to the keto-mesomer that then

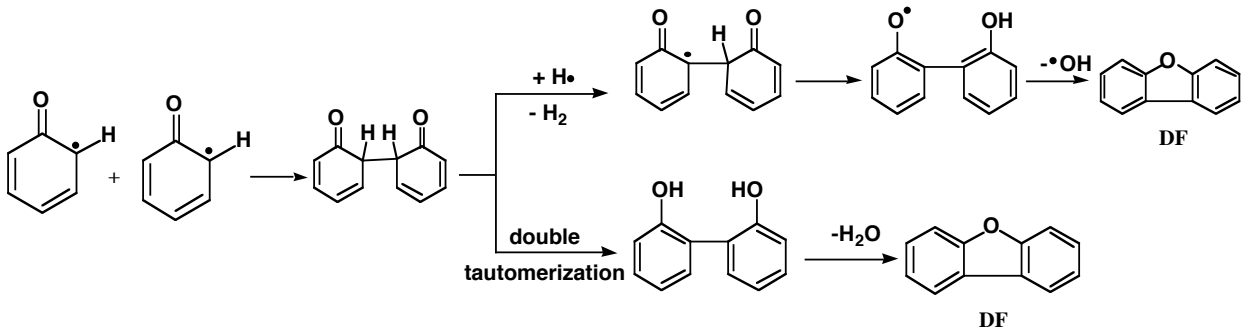

Figure 4.3 Radical-Radical Recombination of Unchlorinated Phenoxyl Radicals to form DF

recombines with another keto-mesomer to form a diketo-dimer. Single proton tautomerization followed by displacement of a hydroxyl radical forms DF. Alternatively, double tautomerization converts the diketo-dimer to the dihydroxy biphenyl (DHB)-dimer which can them eliminate water to form DF. The pyrolysis of 2-MBP uses a similar mechanism for DF formation with the recombination of unbrominated phenoxyl radicals formed from the decomposition of phenol.

Interestingly, the formation of DF from 2-MBP occurs at lower temperatures (600°C) than from 2-MCP (700°C). The Br• concentration in the 2-MBP system is higher than the Cl• concentration in the 2-MCP system due to decomposition temperature of HBr being lower than HCl [5]. The higher Br• concentration leads to faster rates of hydrogen abstraction and DF formation. The yields of DF for both 2-MCP and 2-MBP are the same lending further evidence that they are formed by the same reaction pathway from the unhalogenated phenoxy radical, but with different rates as discussed above.

However results from the mixture of 2-MCP and 2-MBP on the formation of DF, the maximum yield occurs at a later temperature and at a slightly higher yield. This higher yield is largely due to the increase in Br• and Cl• present. With the additional presence of BrCl, there is an increase in Cl• and Br• present and thus the rate of abstraction of H• from the diketo dimer will be faster (figure 4.3) [8].

As expected, DD and 1-MCDD were formed for the pyrolysis of 2-MCP; analogously, DD and 1-MBDD were formed for the pyrolysis of 2-MBP. 4,6-DCDF and the analogous 4,6-DBDF were also expected but not observed [19-20]. However in the case where 2-MCP and 2-MBP were mixed, 4,6-DCDF and 4-B-6-CDF were detected.

The fact that DD and 1-MCDD form at lower temperatures than DF, suggests that they are formed directly from the chlorinated phenoxyl radical of 2-MCP. Figure 4.4 depicts possible reaction pathways to DD, 1-MCDD, and 4,6-DCDF from the reaction of the different mesomers of 2-chlorophenoxyl radical. The pathways for the formation of DD, 1-MBDD and 4,6-DBDF from the pyrolysis of 2-MBP are analogous to the pathways suggested for 2-MCP shown in Figure 4.4.

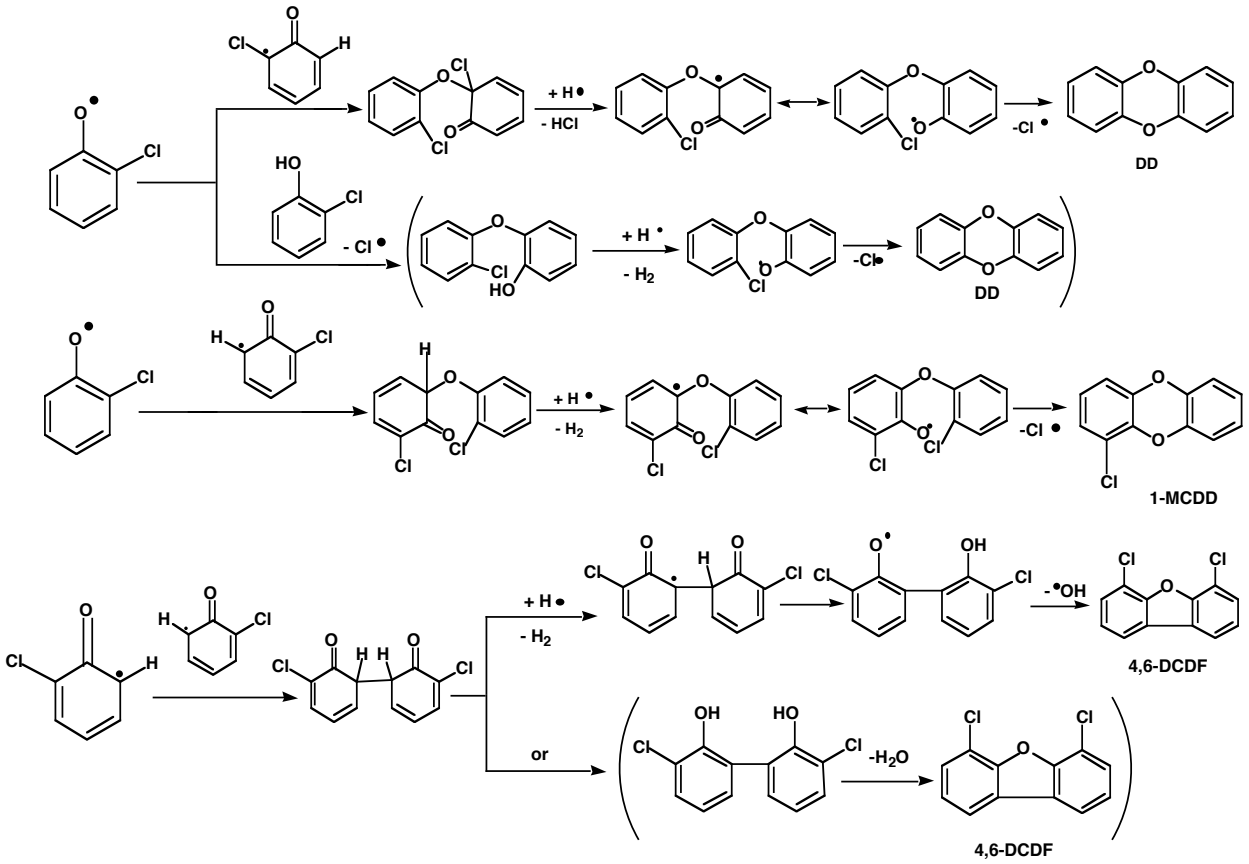

Figure 4.4 Postulated Pathways for the Formation of DD, 1-MCDD and 4,6-DCDF

In the uppermost pathway, the oxygen-centered radical mesomer recombines with the carbon (chlorine substituted) centered radical mesomer to form a keto-ether. Following the abstraction of Cl• by H•, DD is formed by intra-annular elimination of Cl•. Another possible pathway for the formation of DD is through a radical-molecule reaction shown in parentheses below the radical-radical pathway in Figure 4.4. This reaction depicts the oxygen centered radical mesomer reacting with 2-MCP via Cl• displacement to form a chlorohydroxy diphenyl ether (HDE) followed by the abstraction of H• by H•. Finally, DD is formed by intra-annular displacement of Cl•. However it has been previously suggested that this radical-molecule reaction is too slow to account for the observed yields of the DD [10].

Formation of 1-MCDD, shown as the third pathway in figure 4.4, is initiated by the recombination of the oxygen-centered radical mesomer and the carbon-hydrogen- centered radical mesomer to form a keto-ether. Following loss of hydrogen to form the phenoxyl diphenyl ether (PDE), ring closure to form 1-MCDD occurs through intra-annular displacement of Cl•.

The last two pathways in figure 4.4 depict the possible pathways to 4,6-DCDF formation. Initially for both pathways, two carbon-hydrogen centered radical mesomers react to give the diketo-dimer. The dimer can then follow the upper pathway by the abstraction of H• by H•, then undergo tautomerization followed by the displacement of •OH to form 4,6-DCDF. The other possibility is the lower pathway where the diketo-dimer double tautomerizes and then eliminates H_2O to from 4,6-DCDF.

The lack of formation of 4,6-DCDF from the pyrolysis of 2-MCP was surprising based on previous studies in the literature that reported dibenzofuran as the preferred product of reaction of unchlorinated phenoxyl radicals through the carbon-centered radical mesomer and chlorinated dibenzofurans as the preferred product from the reaction of various chlorinated

phenols under oxidative conditions [3, 19-24]. The observed formation of dibenzofurans as the dominant product was justified on the basis that the carbon centered radical mesomer, which leads to the dibenzofuran, was more stable than the oxygen centered mesomer [18].

However the lack of formation of 4,6-DBDF was not as surprising because 4,6-DCDF was not formed for the pyrolysis of 2-MCP. Also in a previous study of the pyrolysis of 2-MBP for a reaction time of 1 hour reported DD as the main product at 600°C without report of 4,6-DBDF as a product [25]. Under pyrolytic conditions, the abstraction of hydrogen by H• to from 4,6-DBDF or 4,6-DCDF is slower than the abstraction of bromine or chlorine by H• to form DD. This is in contrast to oxidative conditions where the hydroxyl radical should rapidly abstract hydrogen and form 4,6-DBDF or 4,6-DCDF from 2-MBP or 2-MCP, respectively [19-20,22-24].

Born, Louw and Mulder reported results from the pyrolysis of 2-MCP where the residence time was 100 seconds and the temperature was 500°C [19]. The detected dioxin products were DD, 4,6 DCDF and 4-MCDF with yields in μmol/h of 16.5, 5.2, and 0.7 at 500°C, respectively. Yang, Mulholland, and Akki also reported the pyrolysis of 2-MCP with a residence time of 10 seconds over a temperature range of 350 to 750°C [20]. Yields of dioxin products were reported only at 700°C. DD, 4,6 DCDF, MCDF and DF were observed, with percent yields, on a carbon feed basis, of 0.218, 0.024, 0.04 and 0.092, respectively.

Based on all these results, it appears that oxidative conditions favors 4,6-DCDF formation, while pyrolysis favors DD formation. This is attributed to the relative rates of the formation of the intermediates in each pathway in Figure 4.4. Under pyrolytic conditions, hydrogen atom is the dominant reactive radical in this system. It readily abstracts Cl• from the intermediate in the upper pathway in Figure 4.4, resulting in the formation of DD [26]. Under oxidative conditions, hydroxyl radical is the dominant reactive radical. It readily abstracts H• in

the fourth pathway in Figure 4.4, to form 4,6-DCDF. Without the assistance of the hydroxyl radical, the abstraction of H• by a hydrogen atom is an order of magnitude slower than the first pathway for our experimental temperatures [26]. Although the carbon-centered mesomer of phenoxyl radical is more stable than the oxygen-centered mesomer [18], pyrolytic conditions create a bottle-neck in the formation of 4,6-DCDF by slowing the necessary abstraction of H• in the intermediate.

However with the pyrolysis of the mixture of 2-MCP and 2-MBP, 4,6-DCDF and the mixed 4-B-6-CDF are detected. 4-B-6-CDF results in the recombination of one 2-chlorophenoxyl radical and one 2-bromophenoxyl radical simlar to the fourth pathway in Figure 4.4. It was previously stated that the presence of bromine increases the Cl• concentration [8]. Chlorine atoms facilitate the abstraction of hydrogen atoms in scheme 3 to form 4,6-DCDF and 4-B-6-CDF. However, hydrogen atoms, not chlorine atoms are involved in the pathways to formation of DD. Thus the presence of bromine increases the formation of 4,6-DCDF and 4-B-6-CDF by increasing the concentration of chlorine atoms. The Br• does not assist as greatly to this formation because of the less energetically favorable HBr that is formed. The 4-B-6-CDF forms the highest yields of all the furans. This result was also seen for previous works with other authors [8, 27]. The results of the AM1 calculations yield very similar ΔH_{rxns} for pathway to 4-B-6-CDF, 4,6-DCDF, and 4,6-DBDF. Brominated phenoxyl radicals predominantly react to form DD instead of 4,6-DBDF. However, a significant fraction also react with chlorinated phenoxyl radicals that can now form 4-B-6-CDF due to the increase in reactive chlorine atoms that facilitates ring closure.

The pyrolysis data for 2-MCP also differs from other reported studies, in that 1-MCDD was observed but not 4,6-DCDF, while the other studies report 4,6-DCDF but not 1-MCDD [19-

20]. However, both studies were at 5-50 x longer reaction times. Their longer times may have favored 4,6-DCDF formation via gas-phase pathways or reactions at the wall. Previously observed yields of 4,6-DCDF were detected that are comparable to DD with low yields of 1-MCDD, for 2-MCP over a CuO/silica surface under pyrolytic conditions [28]. The similarity of product distributions for the surface catalyzed reaction study and the product distribution for the long residence time studies, suggests that the contributions of surface reactions may be significant in these earlier studies, and may responsible for the differences observed in our shorter residence time studies. In fact, it appears that the formation of 1-MCDD should be favored over 4,6-DCDF based on thermochemical kinetic arguments. The abstraction of hydrogen atoms by H• to form 1-MCDD and 4,6 DCDF, respectively, are both slow versus the abstraction of chlorine by H• [26]. Thus the product distribution may be determined by the relative rates of intra-annular displacement of Cl• and •OH, respectively (ΔH_{rxn} =18 kcal/mol for Cl• displacement and 48 kcal/mol for •OH displacement), and the formation of 1-MCDD should be favored over 4,6-DCDF if the rates of formation of the intermediates are similar.

1-MBDD had slightly lower yields but occurred over the same temperature range as formation of 1-MCDD from 2-MCP. Clearly 2-MBP and 2-MCP undergo very similar formation mechanisms with the halogen having little effect on the formation of the product. This suggests that the radical-radical recombination step is rate limiting, rather than the ring closure by halogen displacement. The slightly lower yield of 1-MBDD versus 1-MCDD may be due to competition with formation of DD.

For the mixture of 2-MCP and 2-MBP, formation of 1-MBDD is seen at much lower yields than DD as well as the other PBDD/Fs. The lack of formation of 1-MCDD is surprising. With the pyrolysis of solely 2-MCP, 1-MCDD was observed in yields slightly higher than the

yields seen for 1-MBDD in the pyrolysis of just 2-MBP. The maximum yield of 1-MBDD is similar to the yield of 1-MBDD seen of pyrolysis of soley 2-MBP. These observations suggest that formation of 1-MBDD is not effected by the addition of chlorine as 2-MCP, but the formation of 1-MCDD is affected by the addition of bromine as 2-MBP. Instead, 4,6-DCDF and 4-MCDF were observed, neither of which were detected during the pyrolysis of pure 2-MCP.

Based on all past and present results, it appears that oxidative conditions favors 4,6-DBDF formation, while pyrolysis favors DD formation [19-20, 22, 24-25]. It is also notable that the maximum yield for DD formation from 2-MBP is 20x higher than for 2-MCP. This is reasonable since the ΔH_{rxn} for the second displacement of Br to form DD is exothermic (-12 kcal/mol) and the ΔH_{rxn} displacement of Cl is endothermic (11 kcal/mol), resulting in formation of DD being more favorable for 2-MBP.

With the mixture of 2-MCP and 2-MBP, the highest yield PCDD/F and PBDD/F observed was DD which is similar to the results with the individual pyrolysis of 2-MBP. The yield of DD was 5x less than for pure 2-MBP and 4x greater than for pure 2-MCP. It is believed that the formation of DD is due largely to the recombination of brominated phenoxyl radicals because AM1 calculations for the reactions to form DD show the ΔH_{rxn} for the second displacement of Br to form DD is exothermic (-12 kcal/mol) and the ΔH_{rxn} displacement of Cl is endothermic (11 kcal/mol). The 5x lower yield of DD in the mixture is attributed to the 50% lower concentration of 2-MBP in the mixture. If the rate of formation of DD is approximately second order in the concentration of bromophenoxyl radicals, as it should be based on the recombination mechanism, then the yield of DD should be approximately a factor of 4 lower in the mixture than for the pure 2-MBP.

4-MBDF was the only product formed where the chlorinated analog was not observed in our study of 2-MCP. Figure 4.5 depicts reasonable pathways for the formation of 4-MBDF. Two pathways are depicted: 1); the carbon (hydrogen)-centered radical mesomer can recombine with the carbon (bromine)-centered radical mesomer or 2) the carbon (hydrogen)-centered radical mesomer can recombine with an unbrominated carbon-centered phenoxyl radical to form a diketo-dimer. For the first pathway, H• abstracts bromine and, in the second, H• abstracts another hydrogen. Both pathways then undergo tautomerization followed by displacement of

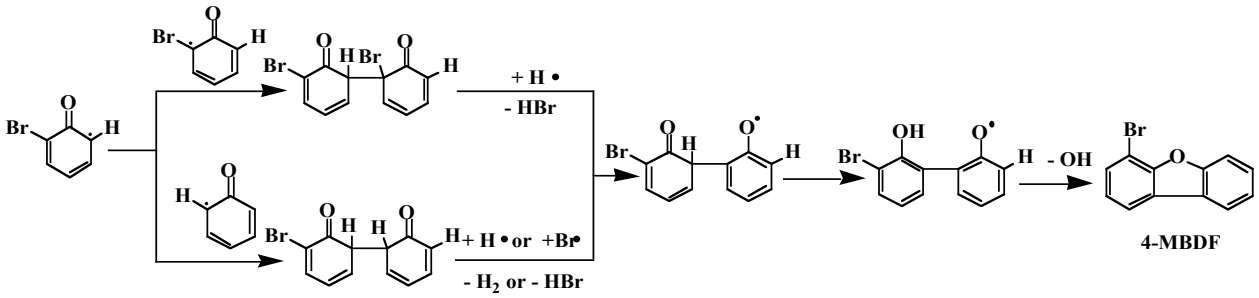

Figure 4.5 Proposed Pathways for Formation of 4-MBDF

hydroxyl to form 4-MBDF. Based on comparisons to simple alkane reactions for the abstraction of bromine by H• and the abstraction of hydrogen by H•, the upper pathway is a much more favorable route for the 4-MBDF formation [29-31].

Both 4-MBDF and 4-MCDF were observed in the mixture of 2-MBP and 2-MCP. However in our study with the individual pyrolysis of 2-MCP, 4-MCDF was not detected but 4-MBDF was seen for 2-MBP. Formation of 4-MCDF follows similar pathways shown in Figure 4.5 with the chlorophenoxyl radicals instead of the bromophenoxyl radicals. The upper pathway in Figure 4.5 seems the more reasonable route for the formation of 4-MBDF and 4-MCDF because of the ease of abstraction of chlorine or bromine by H• over the abstraction of hydrogen by H• [29-31]. Again with the surprising formation of 4-MCDF, it is clear that bromine plays a

roll in the assistance to the formation of the PCDD/Fs by assisting in formation of more Cl• facilitate reactions requiring hydrogen abstraction. The increase in Cl• present lowers the activation energy for hydrogen abstraction in the lower pathway in Figure 4.5 whereas Br• do not have this effect. Also when looking at the ΔH_{rxn} of the final step for 4-MBDF and 4-MCDF formation, the displacement of •OH to form 4-MBDF is 38 kcal/mol less endothermic than the displacement of •OH to form 4-MCDF. So the likelyhood for forming 4-MBDF for the pyrolysis of 2-MBP is more likely than the formation of 4-MCDF from 2-MCP.

4.2 Mechanisms from the Gas-Phase Oxidation of 2-Chlorophenol and 2-Bromophenol[3]

The formation of dioxin products (DD, 1-MCDD, 1-MBDD, 4,6-DBDF and 4,6-DCDF) indicates that stable phenoxyl radicals are formed in significant yields through loss of the hydroxyl-hydrogen. The addition of oxygen also plays a role in the increase in PCDFs and PBDFs formation. Additionally the yields of the PCDFs decreased significantly for the oxidation of the mixture of 2-MBP and 2-MBP compared to the individual oxidation studies of 2-MCP and indicating bromine and oxygen lower the concentration of •OH and Cl• which assests the the PCDF and PBDF formation. The formation of aromatics (phenol, chlorobenzene, and benzene) indicates that simple substitution reactions are occurring. The formation of 2,4-dichlorophenol and 2,6-dichlorophenol and the formation of 2,4-dibromophenol and 2,6-dibromophenol indicate evidence of chlorination of 2-MCP and bromination of 2-MBP. The formation of larger aromatic molecules at low temperatures (naphthalene and chloronaphthalene) is the result of reactions involving the release of CO from the phenoxyl radicals that will then recombine to form naphthalenes. All the heats of reaction, ΔH_{rxn}, AM1 semiempirical calculations for all key steps

[3] Reproduced in part with permission from Environmental Science and Technology, submitted for publication. Unpublished work copyright 2004 American Chemical Society.

in the product formation pathways are located in appendix 1. Psuedo-equilibrium calculations performed to estimate the concentrations of H•, •OH, O•, Cl• and Br• are located in appendix 2.

4.2.1 Decomposition of 2-Chlorophenol and 2-Bromophenol

The addition of oxidative destruction pathways with the addition of molecular oxygen results in the rapid destruction of 2-MBP and 2-MCP beginning at lower temperatures than the temperature observed under pyrolytic conditions. In fact the rapid destruction of 2-MCP begins at 650°C for oxidation rather than 750°C for pyrolysis and 2-MBP begins as low as 600°C for oxidation. In the case where 2-MCP and 2-MBP are mixed, rapid destruction begins at 600°C as well instead of 700°C for pyrolytic conditions. The decomposition of 2-MBP and 2-MCP can be initiated by the loss of the phenoxyl hydrogen by unimolecular, bimolecular, or possibly other low energy pathways (including heterogeneous reactions). Unimolecular decomposition of the oxygen-hydrogen bond (reaction 1) is rapid with a reported rate coefficient for phenol of k_1(430-930°C) = $3.2 \times 10^{15} \exp(-86{,}500/RT)\ s^{-1}$ [1-2]. The reaction enthalpies for unimolecular decomposition of the phenoxyl-hydrogen bond for 2-MCP and 2-MBP are calculated to be virtually identical.

$C_6H_4XOH \rightarrow C_6H_4XO\bullet + H\bullet$ $\Delta H_{rxn(x= Cl)} = 78$ kcal/mol

$\Delta H_{rxn(x= Br)} = 79$ kcal/mol (Reaction 1)

The direct reaction of O_2 with either 2-MCP or 2-MBP is favorable with a reaction enthalpy of ~30 kcal/mol.

$C_6H_4XOH + O_2 \rightarrow C_6H_4XO\bullet + HO_2\bullet$ $\Delta H_{rxn(X=Cl)} = 28$ kcal/mol

$\Delta H_{rxn(X=Br)} = 31$ kcal/mol (Reaction 11)

However, a surface assisted reaction 1a may be the source of the gradual increase in rate of decomposition of both 2-MCP and 2-MBP from 300 to 600°C.

Bimolecular propagation reactions under oxidative conditions include attack by H•, Cl•, Br•, •OH, and O•. In the previous section 4.1.1 on the thermal degradation of 2-MCP and 2-MBP under pyrolytic conditions, the ΔH_{rxn} for reactions with H•, Br• and Cl• were discussed. It was determined that the most favorable reactions for generating chlorophenoxyl radicals and bromophenoxyl radicals were the abstraction of H• by hydrogen, chlorine or bromine (Reactions 3a,b and 7a,b). With the addition of O_2, one can easily generate •OH and O• that can also abstract H• via highly exothermic reactions (Reactions 11 and 12).

$C_6H_4XOH + \bullet OH \rightarrow C_6H_4XO\bullet + H_2O$ $\Delta H_{rxn(X=Cl)} = -42$ kcal/mol

$\Delta H_{rxn(X=Br)} = -39$ kcal/mol (Reaction 12)

$C_6H_4XOH + O\bullet \rightarrow C_6H_4XO\bullet + \bullet OH$ $\Delta H_{rxn(X=Cl)} = -25$ kcal/mol

$\Delta H_{rxn(X=Br)} = -22$ kcal/mol (Reaction 13)

Rate coefficients based on analogous reactions with phenol for reactions 11 and 12 are k_{11} (1000 – 1150 K) = 6.0×10^{12} $cm^3/mol/s$ [5] and k_{12} (340-870 K) = $1.28 \times 10^{13} \exp(-2900/RT)$ $cm^3/mol/s$ [5]. Thus the addition of reactions 11 and 12 increases the formation of the phenoxyl radicals over pyrolytic conditions.

Based on pseudo-equilibrium calculations of the concentrations of reactive radicals and their rate coefficients for reaction with phenol, the rate of reaction 12 is ~190x faster than reaction 13 and a factor of 30 faster than reaction 1 for the oxidation of 2-MCP. For the oxidation of 2-MBP, using these concentrations and the rate expressions given above (using $E_a(\text{rxn } 1) = \Delta H_{rxn} = 79$ kcal/mol), the rate of reaction 12 is ~200x faster than reaction 13 and a factor of 30 faster than reaction 1. Thus reaction 12 is the dominant source of phenoxyl radical under oxidative conditions for both 2-MCP and 2-MBP. In the case where 2-MCP and 2-MBP were mixed, reaction 12 is 190 times faster than reaction 13 and a factor of 30 faster than

reaction 1. However the reaction for the abstraction of H• by chlorine (reaction 7a) is 2000 times faster than reaction 12. The abstraction of H• by hydrogen is not a major source for the formation of the phenoxyl radicals because the concentrations of the H• were not available until 1000°C and found to be at much lower yields than either •OH or Cl•. Pseudo equilibrium calculations suggest that the concentration of Cl• is higher than the concentration of •OH at both 300 and 1000ºC. The abstraction of hydrogen by H• is not a major source for the formation of the phenoxyl radicals because H• were not available until 1000°C. The addition of oxygen, increases the hydroxyl radical concentration and becomes an important reaction pathway for decomposition of 2-MCP and 2-MBP above 600°C. However the abstraction of hydrogen by Cl• is still the dominant pathway of formation of phenoxyl radicals.

4.2.2 Formation of Phenol, Chlorobenzene, Bromobenzene and Benzene

The formation of phenol is likely due to the exothermic displacement of Cl• by H• (ΔH_{rxn} = - 17 kcal/mol) similar to pyrolytic conditions for 2-MCP. Analogously, for the oxidation of 2-MBP, the formation of phenol is likely due to the exothermic displacement of Br• by H• (ΔH_{rxn} = - 29 kcal/mol). The temperature range at which phenol is detected is much lower than for previous results of 2-MBP under pyrolytic conditions. This is due to the early onset of reaction of 2-MBP under oxidative conditions and the oxidation of phenol at higher temperatures. This comparison is very similar to that observed between the pyrolysis and oxidation of 2-MCP. The yield of phenol for the oxidation of 2-MBP is slightly higher than the yields for 2-MCP, which reflects the relative ease of bromine displacement compared to chlorine displacement due to the 15.5 kcal/mol lower carbon-bromine bond energy [7].

When 2-MCP and 2-MBP were mixed, with the addition of oxygen, the detection of phenol was observed in higher yields, over a narrow temperature range of 400 to 650°C, at

temperatures as low as 400°C, which is 100°C lower than for pyrolytic conditions. All of these observations are due to the early onset of reaction and formation of the radical pool before the rapid oxidation of phenol at higher temperatures.

For the oxidation of 2-MCP, chlorobenzene and benzene are formed with much lower yields and at slightly higher temperatures than phenol. These lower yields are due to the more endothermic displacement of •OH from 2-MCP by hydrogen to form chlorobenzene (ΔH_{rxn} = 0 kcal/mol) and the displacement of •OH from phenol by hydrogen to form benzene (ΔH_{rxn} = 4 kcal/mol). The temperature ranges of formation of all these products are lower than for previous results of 2-MCP under pyrolytic conditions. This is due to the early onset of reaction of 2-MCP under oxidative conditions and the oxidation of the products at higher temperatures.

Similarly for the oxidation of 2-MBP, bromobenzene and benzene are formed with much lower yields than phenol. These lower yields are also due to the more endothermic displacement of •OH by hydrogen to form bromobenzene (ΔH_{rxn} = 2 kcal/mol) and the displacement of •OH from phenol by hydrogen to form benzene (ΔH_{rxn} = 4 kcal/mol). However bromobenzene reaches a maximum at 650°C and at 900°C. The lower temperature maximum is due to the displacement of •OH from 2-MBP by hydrogen. However the higher temperature maximum of bromobenzene is due to molecular growth pathways resulting from fragmentation of 2-MBP into C_2 species, which has been well documented, in literature [11-13]. Similar results for the mixture of 2-MCP and 2-MBP were observed. Thus the formation of chlorobenzene, bromobenzene and benzene are not affected by the addition of Cl• or Br•.

4.2.3 Bromination and Chlorination of 2-Bromophenol and 2-Chlorophenol

With the addition of oxygen, both 2-MCP and 2-MBP form dichlorophenols and dibromophenols respectively. In fact when the two are mixed, mixtures of the halogenated

phenols and tribromophenol are even detected. In our previous work, we suggested that since the displacement of H• by Br• or Cl• is endothermic, the direct reaction of Br• or Cl• with 2-MBP or 2-MCP is unlikely. Therefore, figure 4.6 depicts the formation of all these products dependant on whether 2-MCP or 2-MBP are involved. Pathway 1 in figure 4.6 depicts the formation of either 2,4-dibromophenol, 2,4-dichlorophenol, 2-chloro-4-bromophenol or 2-bromo-4-chlorophenol by

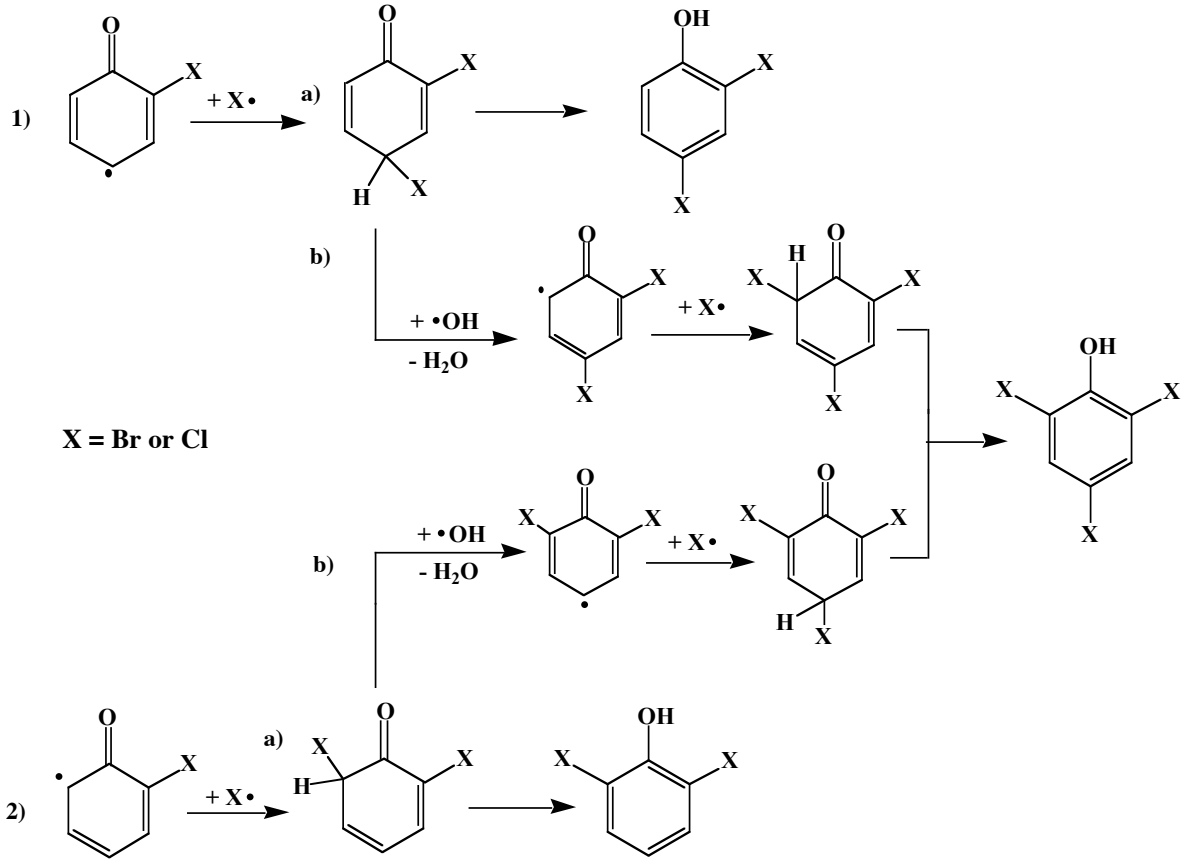

Figure 4.6 Reaction Mechanisms for the Formation of Dihalogenated Phenols and Trihalogenated Phenols from the 2-Bromophenoxyl radical and 2-Chlorophenoxyl Radicals

Br• or Cl• attack at the resonance stabilized, para-carbon centered sites of the bromophenoxyl and chlorophenoxyl radicals followed by tautomerization to yield the respective products. Alternately, pathway 2a in figure 4.6 depicts the Br• or Cl• attack at the resonance stabilized, ortho-carbon centered sites of the bromophenoxyl and chlorophenoxyl radical to form either 2,6-

dibromophenol, 2,6-dichlorophenol or 2-bromo-6-chlorophenol. Formation of 2,4,6-tribromophenol or 2,4,6-trichlorophenol occurs via pathway 1b or 2b in figure 4.6. Before tautomerization, H• can be extracted by a hydroxyl radical and thus form a dibromophenoxyl radical that can then, with the addition of another Br• or Cl• and tautomerization, form 2,4,6-tribromophenol or 2,4,6-trichlorophenol, respectively.

Unlike the results from the pyrolysis of 2-MCP, 2,4-dichlorophenol and 2,6-dichlorophenol were observed for the oxidaiton of 2-MCP. The formation of 2,4-dichlorophenol and 2,6-dichlorophenol by Cl• attack at the resonance-stabilized, ortho- or para- carbon sites of the chlorophenoxyl radicals (ΔH_{rxn} = -43 kcal/mol). Subsequent tautomerization results in the formation of the respective dichlorophenols (ΔH_{rxn} = -20 kcal/mol) (Figure 4.6). Under pyrolytic conditions, HCl is a largely unreactive sink for chlorine. Under oxidative conditions, •OH and HO_2• can react exothermically with HCl to produce a relative abundance of Cl• [8, 32]. Consequently, chlorination reactions are enhanced under oxidative conditions [33-35].

The formation of dibromophenol is instead due to recombination of phenoxyl radicals and Br•. Figure 4.6 depicts the formation of 2,4-dibromophenol and 2,6-dibromophenol by Br• attack at the resonance-stabilized, ortho- or para- carbon sites of the bromophenoxyl radicals (ΔH_{rxn} = -29 kcal/mol). Subsequent tautomerization results in the formation of the respective dibromophenols (ΔH_{rxn} =-17 kcal/mol). The dibromophenols were also detected in our previous study of 2-MBP under pyrolytic conditions. However they were observed over a narrower temperature range and lower yields.

Based on our pseudo-equilibrium calculations at 700°C, the concentrations of Br_2 (9.4 x 10^{-6} mol) and Br• (9.6 x 10^{-7} mol) are respectively 3 and 1 orders of magnitude higher than the concentration of HBr (5.4 x 10^{-8} mol). This is in contrast to the results for 2-MCP where the

concentration of HCl (1.7×10^{-5} mol) was greater than that of Cl_2 (1.3×10^{-6} mol) and Cl• (1.5×10^{-7} mol) and our calculations for the pyrolysis of 2-MBP for which the HBr, Br_2, and Br• concentrations were 4.2×10^{-7} mol, 2.0×10^{-12} mol, and 2.7×10^{-10} mol, respectively. The addition of oxygen creates •OH, which converts HBr into water and Br•, the latter being in equilibrium with Br_2 [5]. The increased yield of brominated products under oxidative conditions is likely due to the release of strong brominating agents, Br•, and as well as the increase in bromophenoxyl radical concentration.

For the mixture of 2-MCP and 2-MBP, formation of 2-chloro-4-bromophenol, 2,4-dibromophenol, 2,6-dibromophenol, and 2,4,6- tribromophenol are due the bromination of 2-MCP and 2-MBP. The formation of 2-bromo-4-chlorophenol is due to the chlorination of 2-bromophenol. Curiously 2,4-dichlorophenol and 2,6-dichlorophenol were not detected which would be products resulting from the chlorination of 2-chlorophenol. With the individual oxidation of 2-MCP, these products were observed.

It has been previously documented that bromination is 10 times more efficient than chlorination [14]. Previous research also suggests that bromine predominantly exists as Br_2 while chlorine is mainly found as HCl [8]. Br_2 decomposes above 300°C into Br• whereas HCl is stable to at least 700°C and does not react to release significant concentrations of Cl•. Since Br• and Cl• are the primary brominating and chlorinating agents under gas-phase conditions, the higher concentration of Br• than Cl• results in more rapid rates of bromination and increased yields of brominated products.

Our pseudo-equilibrium calculations for temperatures between 500 and 1000°C indicate that this is true for our oxidation studies. However, it was found that for the mixture between 500 and 1000°C, the concentration of Br• increased slightly compared to the oxidation of pure 2-

MBP whereas the concentration of Cl• decreased slightly compared to the oxidation of pure 2-MCP. In contrast to our results for the pyrolysis of the mixture of 2-MBP and 2-MCP where the concentration of Cl• is increased with the presence of bromine, the concentration of chlorine, and most notably Cl_2 decreases with the presence bromine. Concentrations of Cl_2 are important because Cl_2 readily dissociates to Cl• with a rate coefficient of k(300-800 K) = 8.51 x 10^{15}exp(-55.84 kcal/RT) cm^3/mol/s [5]. The lower concentration of Cl_2 leads to lower concentrations of Cl•. At 500°C, based the pseudo equilibrium calculations, the percent of total chlorine that is Cl_2 is 1.5x less than for the oxidation of pure 2-MCP. Therefore since the concentration of Br• increases and the concentration of Cl• decreases compared to the oxidation of the pure compounds, bromination of the phenols will dominate over chlorination in the mixture.

The more highly halogenated phenols are detected at higher yields and lower temperatures than for the oxidation of pure 2-MCP due to the increase in bromine concentration via reaction 14.

$HBr + \bullet OH \rightarrow H_2O + Br\bullet$ (Reaction 14)

The rate coefficient for reaction 4 is k_4 (200-420 K) = 6.62x10^{12} cm^3/mol/s versus k (300-700 K) = 1.77x10^{12} exp(-0.89 kcal/RT) cm^3/mol/s [5] for the analogous reaction with HCl. Based on this reaction, the concentration of Cl• also increases with the presence of oxygen compared to pyrolysis.

The presence of Cl• also increases the concentration Br• by also reacting with HBr to form HCl with a rate coefficient of k (228 - 368 K) = 1.2 x 10^{13}exp(-0.71/RT) cm^3/mol/s (Reaction 15) [5].

$Cl\bullet + HBr \rightarrow HCl + Br\bullet$ (Reaction 15)

Therefore, reaction 5 not only increases the concentration of Br• but also decreases the concentration of Cl•, a characteristic confirmed in our pseudo-equilibrium calculations.

4.2.4 Formation of Naphthalene, Chloronaphthalene and Bromonaphthalene

The yields of naphthalene, chloronaphthalene and bromonaphthalene are dramatically decreased with the presence of oxygen. However naphthalene remains present still at low temperatures. In the previous section 4.1.4, a low temperature mechanism was proposed for the formation of naphthalene, chloronaphthalene and bromonaphthalene from the chloro- and bromo-phenoxyl radicals expelling CO to form halogenated cyclopentadienyl radicals with a calculated ΔH_{rxn} of 20 kcal/mol and an assigned rate coefficient of k_{10} (730-1300°C) = $1x10^{11.4}exp(-22100+/-450/T)\ s^{-1}$ [2, 17]. The recombination of two cyclopentadienyl radicals has been previously shown to be a favorable pathway for formation of naphthalene [15]. A similar low temperature route to the formation of naphthalene from the recombination of bromophenoxyl radicals is described in Scheme 2 (*vide infra*) as a competitive pathway to the formation of 4,6-DBDF. This formation of naphthalene is based on a previously proposed pathway of the recombination of two chlorophenoxyl radicals to form naphthalene [36].

The yields of naphthalene and chloronaphthalene are significantly lower under oxidative than pyrolytic conditions, most probably due to the more rapid rate of oxidation of the cyclopentadienyl radical. The oxidation rate of naphthalene is also increased. Thus naphthalene never becomes a major product as it did under pyrolytic conditions. Also with the increase in the concentration of chlorinated phenoxyl radicals, the rate of PCDD/F formation will increase in competition with the elimination of CO. The oxidation rate of naphthalene is also increased. Thus the concentration of naphthalene is dramatically lowered and it never becomes a major

product as it did under pyrolytic conditions. Similar explanations can be said for the formation of naphthalene and bromonaphthalene from the oxidation of 2-MBP.

The formation of naphthalene for both the oxidation of 2-MCP and 2-MBP occurred over a similar temperature range. However, higher yields of naphthalene were observed for the oxidation of 2-MCP than for 2-MBP. This may be due to the higher concentration of bromophenoxyl radicals than chlorophenoxyls radicals, leading to increased rate of formation of PBDD/F by radical recombination processes at the expense of CO elimination leading to naphthalene formation.

In the case where 2-MCP and 2-MBP are mixed, the concentration of naphthalene is even lower in yield for the mixture of 2-MCP and 2-MBP than for the individual oxidation of 2-MCP and 2-MBP. There is a concomitant increase in yield of PBDD/Fs and PCDD/Fs formed.

4.2.5 Mechanisms for Formation of PCDD/Fs and PBDD/Fs

Figure 4.7 summarizes previously identified reaction pathways to DD, 1-MCDD, and 4,6-DCDF from the reaction of the different mesomers of 2-chlorophenoxyl radical with the assistance of •OH. Formation of DD, 1-MBDD, and 4,6-DBDF by the recombination bromophenoxyl radicals from 2-MBP occur by pathways analogous to the pathways shown in figure 4.7.

Pathway 1a in Figure 4.7 depicts the mechanism for DD formation; the oxygen-centered radical mesomer recombines with the carbon (chlorine substituted) centered radical mesomer to form a keto-ether. Following the abstraction of Cl• by H• or •OH, DD is formed by intra-annular elimination of Cl•. Another possible pathway for the formation of DD is through a radical-molecule reaction, 1b, shown in parentheses below the radical-radical pathway in figure 4.7.

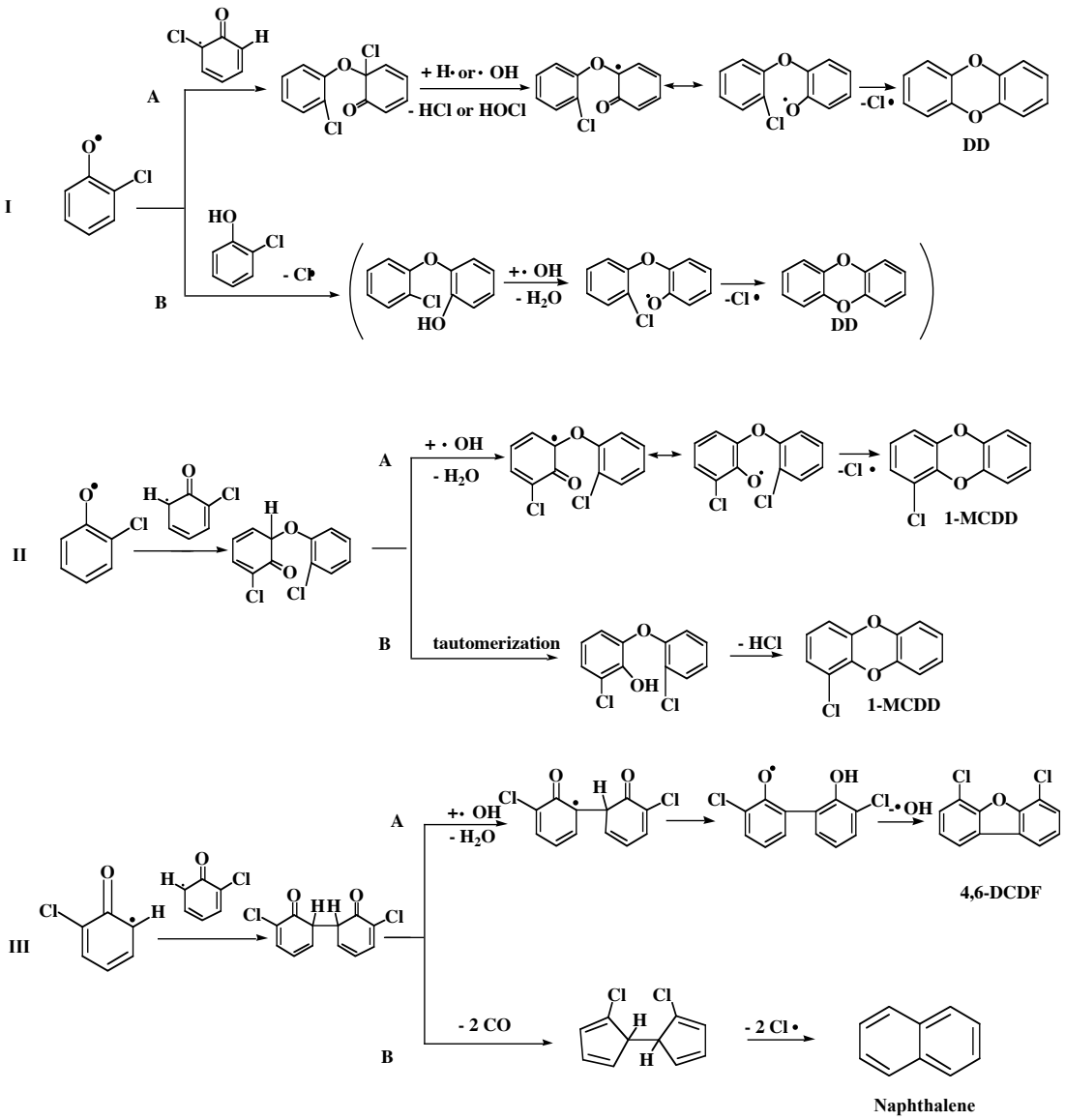

Figure 4.7 Postulated Pathways for the Formation of DD, 1-MCDD and 4,6-DCDF with the Assistance of •OH

This reaction depicts the oxygen centered radical mesomer reacting with 2-MCP via Cl• displacement to form a chlorohydroxy diphenyl ether (HDE) followed by the abstraction of H• by •OH. Finally, DD is formed by intra-annular displacement of Cl•. It has been previously suggested that this radical-molecule reaction is too slow to account for the observed yields of the DD [3, 9-10].

Formation of 1-MCDD, shown as pathway 2a in Figure 4.7, is initiated by the recombination of the oxygen-centered radical mesomer and the carbon-hydrogen- centered radical mesomer to form a keto-ether. Following loss of hydrogen to form the phenoxyl diphenyl ether (PDE), ring closure to form 1-MCDD occurs through intra-annular displacement of Cl•. Pathway 2b depicts an alternate pathway in which ring closure is by unimolecular elimination of HCl.

Pathways 3a and 3b in figure 4.7 depicts the proposed pathway of 4,6-DCDF formation and the competing pathway of naphthalene formation. Initially, for both pathways, two carbon-hydrogen centered radical mesomers react to form a common diketo-dimer intermediate. The dimer can then follow pathway 3a by the abstraction of H• by •OH and undergo tautomerization followed by the displacement of •OH to form 4,6-DCDF. In pathway IIIB the initially formed diketo-dimer forms naphthalene by elimination of two CO molecules followed by a unimolecular isomerization and elimination of two Cl• [15].

Four major differences were observed in the results of oxidation and pyrolysis of 2-MCP:

1. A decrease in non-PCDD/F products under oxidative conditions.
2. An increase in total PCDD/F product yield
3. 4,6-DCDF is the major product under oxidation, while DD and 1-MCDD are the major products for pyrolysis.
4. 1-MCDD is observed at temperatures as low as 400°C under oxidative conditions.

The first two observations are readily explained. The addition of oxygen to the systems results in oxidation of the decomposition products of 2-MCP before they can form the observed aromatic molecular growth products. The addition of oxygen also results in lower temperature

formation of chlorophenoxyl radical where it can react to form PCDD/F products rather than decompose. The explanations of observations 3 and 4 are slightly more subtle.

The maximum yields of DD under oxidative and pyrolytic conditions are 1.32 and 0.28 %, respectively. The maximum yields of 1-MCDD are 0.92 and 0.05 %. In contrast the maximum yields of 4,6-DCDF, which was not detected under pyrolytic conditions was 9.43 % under oxidative conditions. Thus DD only increased by a factor of 4.7, 1-MCDD increased by a factor of 18.4, while 4,6-DCDF increased at least 100x with the addition of oxygen to the system.

Examination of the major pathways to DD, 1-MCDD, and 4,6-DCDF in Figure 4.7 reveals that Cl• is abstracted to form DD, one H• is abstracted to form 1-MCDD, and one of two H• are abstracted to form 4,6-DCDF. H• is the major chain carrier in the 2-MCP system under pyrolytic conditions, while •OH is the major carrier under oxidative conditions. The ΔH_{rxn} for abstraction of Cl• by •OH (pathway 1a in Figure 4.7) is endothermic by 45 kcal/mol. Thus, Cl• abstraction by •OH is not expected to be competitive with the abstraction of Cl• by H•. Addition of oxygen consequently has little effect on the yield of DD. However in pathways 2a and 3a, ΔH_{rxn} for the abstraction of H• by •OH is exothermic by 16 kcal/mol. Thus, the addition of oxygen to the system increases the •OH concentration, which increases the rate of abstraction of H• to form 1-MCDD and 4,6-DCDF. The increase in yield of 4,6-DCDF due to increase in •OH concentration is exponentially larger than for 1-MCDD because the hydrogen abstraction rate coefficient is doubled due to the presence of two sites for hydrogen abstraction in the diketo intermediate involved in 4,6-DCDF formation versus the “single” keto intermediate in formation of 1-MCDD.

Previous studies of the oxidation of 2-MCP over a wide temperature range and longer reaction times have also reported 4,6-DCDF as the major product [19,21-22, 24]. Only the study of Weber and Hagenmaier who studied lower temperature reactions (330-600°C) reports 1-MCDD as a major product at a low temperature of 375°C [22, 24] in addition to DD, 4,6 DCDF, and 4-MCDF. The lower formation temperature is likely due to the longer residence times of 10 minutes of their experiments. Our results also show a low temperature formation of 1-MCDD as well as naphthalene.

The observation of naphthalene and 1-MCDD as the only organic products below 500°C suggests: 1) that a somewhat different mechanism of formation may be operative at these lower temperatures for which the radical pool is not fully developed, and 2) their formation mechanisms have a common intermediate or are at least closely related.

After the recombination of chlorinated phenoxyl radicals to form the diketo intermediate, the formation of naphthalene shown in pathway 3b in figure 4.7, is unimolecular. This can explain the high yields at low temperatures before the radical pool has developed. The observation of significant yields of 1-MCDD at low temperature suggests that it may also be formed by a unimolecular pathway following the formation of the keto-ether intermediate via radical-radical recombination. Alternatively to the abstraction of H• by •OH in pathway 2a in figure 4.7, a simple, intra-ring one proton tautomerization results in the formation of a hydroxy-diphenyl ether intermediate that can then form 1-MCDD by inter-ring elimination of HCl. Above 500°C, the radical pool increases rapidly; and bimolecular pathways involving H• and Cl• abstraction begin to dominate the formation of 1-MCDD and other PCDD/F products.

When looking at the results for the oxidation of 2-MBP, DD is the major product of both pyrolysis and oxidation of 2-MBP. However the yield of DD is 4 times greater for oxidation

than for pyrolysis. This is again primarily due to the increase in bromophenoxyl radicals at lower temperatures for oxidative conditions, which react to form PBDD/Fs. Under pyrolytic conditions, bromophenoxyl radicals form at higher temperatures where their rate of decomposition is greater and yields of PBDD/F are reduced. The yield of 1-MBDD is 5x greater under oxidative conditions than pyrolytic conditions. This again is also due to the increase in bromophenoxyl radicals. However, the presence of •OH facilitates hydrogen abstraction in pathway 2a, which further promotes formation of 1-MBDD.

Detection of 1-MBDD is observed as low as 400°C. This is a dramatically lower than the 650°C formation temperature observed under pyrolytic conditions. This suggests another pathway is involved in the low temperature formation. This is similar to the results seen with the oxidation of 2-MCP where 1-MCDD was detected as low as 400°C. At lower temperatures similar to the formation of 1-MCDD from the oxidation of 2-MCP, 1-MBDD can be formed by a unimolecular pathway following the recombination of the keto-ether intermediate via radical-radical recombination (Pathway 2a in Figure 4.7). The formation of DD and 4-MBDF at 400-450°C is attributed to the lower temperature formation of the bromophenoxyl radical precursor.

One product not observed under pyrolytic conditions, 4,6-DBDF, was detected in high yields under oxidative conditions. This behavior is similar to that observed for 2-MCP. With the addition of oxygen, •OH becomes the major carrier over H•. Hydroxyl radical facilitates highly exothermic hydrogen abstraction reactions in pathways 2a (-46 kcal/mol) and 3a (-47 kcal/mol), resulting in the formation of 1-MBDD and 4,6-DBDF, respectively. However, the abstraction of bromine by •OH is 40 kcal/mol endothermic and not favorable. Thus the increase in •OH concentration increases the rate of 1-MBDD and 4,6-DBDF formations but does not increase the

rate of DD formation, which requires abstraction of bromine. The same explanation stated for the formation of 4,6-DCDF remains true for the formation of 4,6-DBDF.

However, 4,6-DBDF is not the major PBDD/F product like 4,6-DCDF is for the analogous oxidation of 2-MCP. In the competing pathway to formation of DD from 2-MBP or 2-MCP, the final ring closure involves elimination of Br• or Cl•, respectively. For 2-MBP this step is 12 kcal/ mol exothermic, while it is 12 kcal/mol endothermic for 2-MCP. The addition of •OH to the system increases the rates of formation of both 4,6-DBDF and 4,6-DCDF by promoting H• abstraction in pathway 3a in figure 4.7. However, this increase is insufficient to compete with the exothermic formation of DD from 2-MBP whereas it is sufficient to compete with the endothermic formation of DD from 2-MCP. Therefore DD remains the dominant PBDD/F product for 2-MBP.

The yields of 4,6-DBDF and 1-MBDD are ~5x less than the yields of 4,6-DCDF and 1-MCDD. This may be due to the more exothermic abstraction of hydrogen by •OH by 12 kcal/mol for the chlorinated reaction intermediates than the corresponding brominated intermediates as well as the 28 kcal/mol more exothermic abstraction of hydrogen by Cl• than hydrogen by Br•. Based on our pseudo-equilibrium calculations for 2-MBP and similar calculation for the 2-MCP system, the addition of oxygen to the system increases the concentrations of •OH and Br•. However, the hydrogen abstraction reactions necessary for formation of 4,6 DBDF and 1-MBDD from 2-MBP are not as favored by this increase as in the 2-MCP system.

When 2-MCP and 2-MBP were mixed, DD, 1-MBDD, 1-MCDD, 4,6-DCDF, 4,6-DBDF were all detected as well as the 4-B-6-CDF. Formation of 4-B-6-CDF results from the

recombination of a chlorophenoxyl radical and a bromophenoxyl radical to form the diketo-dimer that follows pathway 3a in figure 4.7.

Similar to the results on the pyrolysis of the mixture of 2-MBP and 2-MCP, DD is the major PCDD/F and PBDD/F product detected. The maximum yield of DD increased by a factor of 8 over that observed for pyrolysis of the mixture. In addition the maximum yield is 8 times greater than the maximum yield of DD observed for the individual oxidation of 2-MCP and a factor of 2.6 less than the maximum yield for the individual oxidation of 2-MBP. However this result is in contrast to the thermal degradation of the pure compounds for which the maximum yield of DD only increased by a factor of 4 for 2-MBP and a factor of 4.7 for 2-MCP for oxidation versus pyrolysis.

The AM1 calculations for the ΔH_{rxn} for the formation of DD indicate that the pathway is completely exothermic for 2-MBP, whereas for 2-MCP, the final intra-annular displacement of Cl• is endothermic (11 kcal/mol). Because of the lower bond strength of the C-Br over C-Cl, bromine is a better leaving group than chlorine [7]. Thus the formation of DD is more favorable from 2-MBP than 2-MCP. The lower yield of DD in the mixture versus the oxidation of pure 2-MBP is just a reflection of the lower initial concentration of 2-MBP in the mixture.

Unlike the pyrolysis of the mixture of 2-MCP and 2-MBP where only 1-MBDD was detected, both 1-MCDD and 1-MBDD were observed. In fact the maximum yield of 1-MBDD increase by a factor of 4 over the pyrolytic results. This increase in the maximum yield of 1-MBDD is similar to the 1-MBDD results seen for the individual oxidation and pyrolysis of 2-MBP. The maximum yield of 1-MCDD for the oxidation over pyrolysis of pure 2-MCP increased by a factor of 18, but with the mixture of 2-MCP and 2-MBP, 1-MCDD increased by at least a factor of 100. In addition when comparing the oxidation of the mixture of 2-MCP and

2-MBP with the individual oxidation of 2-MCP, the maximum yield of 1-MCDD is a factor of 10 lower. These observations can be explained by examining the effect of the addition of oxygen on Br• and Cl• concentrations.

With the addition of oxygen, the formation of 1-MBDD and 1-MCDD is strongly facilitated by the abstraction of hydrogen by •OH and Cl• depicted in Figure 4.7. The ΔH_{rxn} is lowered for the abstraction of H• with the assistance of •OH and Cl• for the pathway to form 1-MBDD and 1-MCDD. Since the results for 1-MBDD are similar to those seen for the oxidation of pure 2-MBP, the increase in 1-MBDD is primarily due to this reasoning. Though with the presence of oxygen, the yields of 1-MBDD for pure 2-MBP were only 2 times greater unlike the expected 4 times. The yield of 1-MBDD should be approximately a factor of 4 lower in the mixture than for the pure 2-MBP if the rate of formation of 1-MBDD is approximately second order in the concentration of bromophenoxyl radicals, as it should be based on the recombination mechanism. Thus the presence of Cl• assists in the slight increase of 1-MBDD by also assisting in the abstraction of H•.

For 1-MCDD there is a dramatic increase in yields over the pyrolysis of the mixture, but in comparison with the oxidation of pure 2-MCP, the yields of 1-MCDD are significantly lower. While the addition of •OH will increase the formation of 1-MCDD, the presence of bromine lowers the formation of 1-MCDD by reducing the concentration of both Cl• and •OH in comparison with the oxidation of pure 2-MCP (Reactions 14 and 15).

The maximum yields for the PCDFs observed are also observed to be significantly lower than the results seen for the individual oxidation of 2-MCP. The formation of 4,6-DCDF and 4-B-6-CDF were both observed in yields 5 times greater under oxidative than pyrolysis conditions. The 5 times increase for the oxidative conditions over the pyrolytic is due to the addition of •OH

which assists in the abstraction of H• to form 4,6-DCDF and 4-B-6-CDF. Unlike the pyrolysis of the mixture of 2-MCP and 2-MBP, 4,6-DBDF was observed. This result is similar to the results seen for the oxidation and pyrolysis of pure 2-MBP and therefore the increase in 4,6-DBDF is again due to the presence of •OH, which facilitates in the formation of 4,6-DBDF.

The maximum yield of 4,6-DCDF was not nearly as great as expected compared to the results for the oxidation of pure 2-MCP. However the lower yields of 4,6-DCDF compared to the oxidation of pure 2-MCP is attributed to the presence of bromine in the mixture lowering the concentration of Cl• and •OH over the oxidation of pure 2-MCP. The concentration of •OH is considerably lower than Cl• for oxidation because of its rapid reaction with HBr and HCl (Reaction 14). Consequently Cl• is the primary radical or atom responsible for hydrogen abstraction. Thus the lower yields of Cl_2, which lowers the concentration of Cl• for the mixture of 2-MCP and 2-MBP compared to the oxidation of pure 2-MCP, will lower the yields of 4,6-DCDF.

Figure 4.8 depicts reasonable pathways for the formation of 4-MCDF which was observed under oxidative but not pyrolytic conditions for 2-MCP. Two pathways are depicted: 1) the recombination of the carbon (hydrogen)-centered radical mesomer with the carbon (chlorine)-centered radical mesomer and 2) the recombination of the carbon (hydrogen)-centered radical mesomer with an unchlorinated carbon-centered mesomer to form a diketo-dimer.

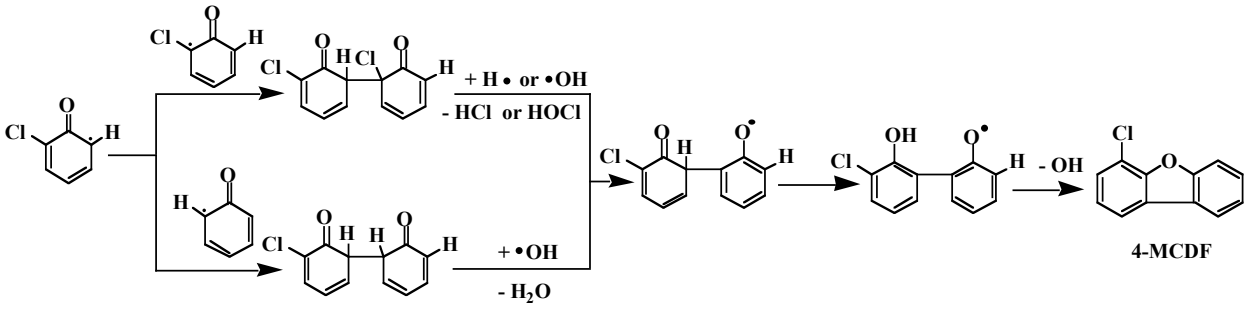

Figure 4.8 Proposed Pathways for the formation of 4-MCDF

For the first pathway, H• abstracts chlorine and, in the second, •OH abstracts another hydrogen. Both pathways then undergo tautomerization followed by displacement of hydroxyl to form 4-MCDF. The pathway to form 4-MBDF from the oxidation of 2-MBP is analogous to the pathways depicted in figure 4.8. Based on comparisons to simple alkane reactions for the abstraction of chlorine or bromine by H• and the abstraction of H• by •OH, the lower pathway is a much more favorable route for 4-MCDF and 4-MBDF formation under oxidative conditions, while the upper pathway of Cl• and Br• abstraction by H• is more favorable under pyrolytic conditions [29-31]. Both 4-MBDF and 4-MCDF were observed in the oxidation of the mixture of 2-MCP and 2-MBP. Since the lower pathway is assisted by the presence of •OH and the yields of both 4-MCDF and 4-MBDF are greater than the yields seen for pyrolysis, the second pathway seems to be the favored pathway for formation of 4-MCDF and 4-MBDF. DF is a simply a recombination product of unchlorinated phenoxyl radical formed from decomposition of phenol [18]. The reaction proceeds by mechanisms shown in figure 4.3.

4.3 Mechanisms from the Surface Mediated Reactions with 2-Bromophenol[4]

Low temperature decomposition of 2-MBP by 500°C indicates that the surface is indeed mediating its reaction. Formation of PBDD/Fs between 250 and 500°C suggest that reaction intermediates, i.e. bromophenoxyl radicals, are stabilized on the CuO/Silica surface. The proposed surface mediated mechanisms for the formation of the PBDD/Fs are the Eley-Rideal for PBDDs and the Langmuir-Hinshelwood mechanisms for PBDFs. The observation of 3-bromo-3,5-cyclohexadiene-1,2-dione (or bromoquinone) and 3,5-dibromo-3,5-cyclohexadiene-1,2-dione (or dibromoquinone) are depicted as intermediates in the formation of PBDDs. The

[4] Reproduced in part with permission from Environmental Science and Technology, submitted for publication. Unpublished work copyright 2004 American Chemical Society.

presence of brominated phenols and brominated benzenes indicate the ease of bromination of the phenoxyl radical when attached to the surface.

4.3.1 Mechanisms Involved for Pyrolytic Conditions

- Destruction of 2-MBP and the absorption 2-MBP to the CuO Silica surface

In order for the oxidation of 2-MBP or further reaction to form PBDD/Fs and other brominated aromatics to occur at low temperatures, 2-MBP must attach to the surface. For chlorinated phenols, this has been shown to occur through chemisorption at copper hydroxide (cf. Figure 4.9) or copper oxide sites through loss of water. This results in a surface adsorbed

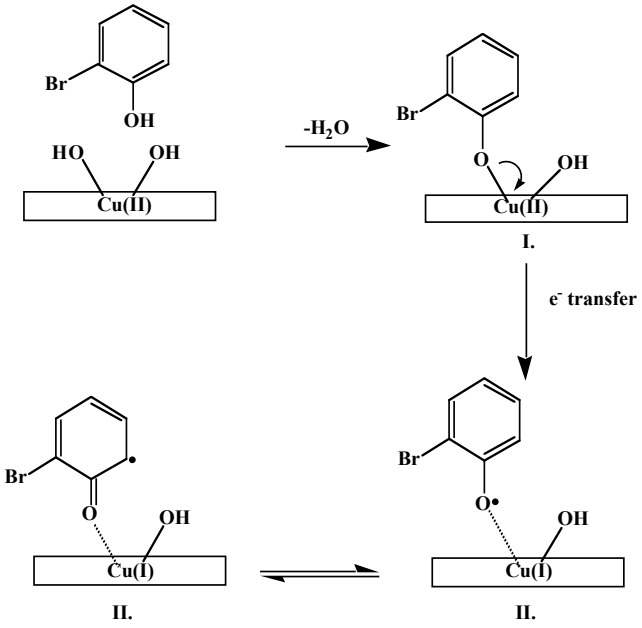

Figure 4.9 Mechanism for Adsorption of 2-MBP to Cu(II)O/Silica Surface

bromophenolate chemically bound to a Cu(II) species (cf. I in figure 4.9). With the assistance of the copper oxide surface, 95% of 2-MBP is destroyed by 350°C. The surface oxygen from the copper oxide surface assists in the oxidation of 2-MBP according to the Mars-van Krevelen mechanism whereby the surface oxygen atoms are consumed by the reagents, leaving oxygen

vacancies. Above 500°C, the Cu(II)O surface assists in the destruction of all PBDD/Fs formed as well as the other products formed at the lower temperatures.

It has been well documented that 2-chlorophenol (2-MCP) can chemisorb to a copper oxide surface [28, 37]. Once 2-MCP is chemisorbed to the Cu(II)O surface, it donates an electron to the copper that is reduced to Cu(I) [37]. The chlorophenolate structure becomes a chlorophenoxylate radical that is resonance stabilized between the ortho- and para- aromatic carbons and the oxygen centered radical mesomers. EPR studies where 2-MCP is absorbed to a copper oxide surface suggests a carbon centered radical [38]. These studies concluded that the carbon-centered radical becomes dominant resonance structure. Figure 4.9 depicts the similar chemisorption of 2-MBP. Since 2-chlorophenol and 2-bromophenol are very similar in structure, it is expected for 2-bromophenol to behave in a similarly to form a carbon centered radical.

- Formation of 2,4-Dibromophenol, 2,6-Dibromophenol and 2,4,6-Tribromophenol

Significant yields of the polybrominated phenols are seen at temperatures as low as 250°C. These products are likely to form from the bromination of 2-MBP once attached to the surface. As shown in figure 4.10, Br• will attack the carbon-centered bromophenoxyl radical at the ortho or para sites and 2,4-dibromophenol and 2,6-dibromophenol are formed via tautomerization. However before the tautomerization, H• can be abstracted by another bromine radical and thus form a dibromophenoxyl radical that can then with the addition of another Br• and tautomerization can form 2,4,6-tribromophenol (Figure 4.10).

The results show that 2,6-dibromophenol has the highest yield of the polybrominated phenols. This can be explained by the relative ease at which the H• can tautomerize in the ortho position being in a close proximity to the oxygen. Also it has previously been suggested that the ortho position for the carbon-centered phenoxyl radical is the most favorable [18, 38].

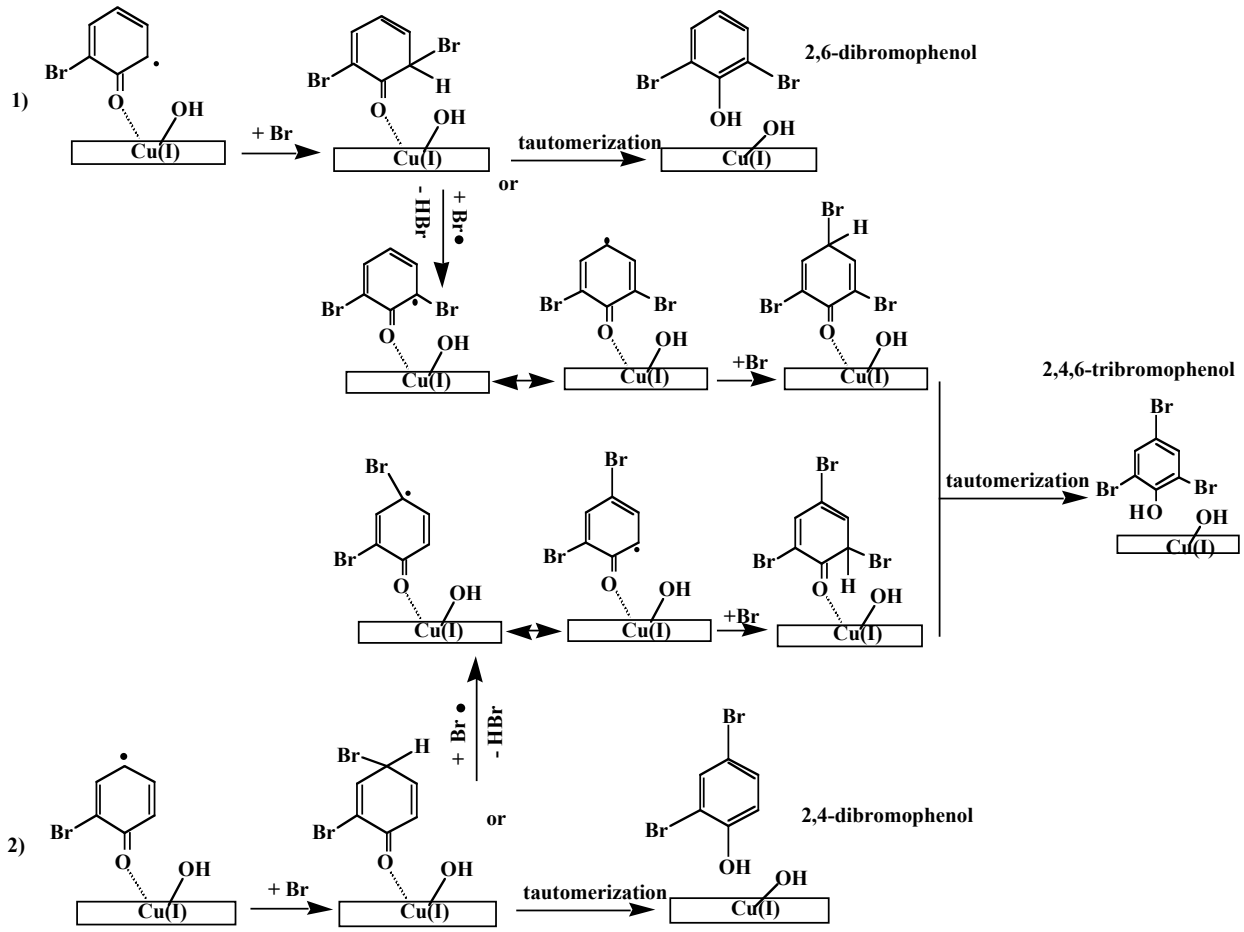

Figure 4.10 Proposed Mechanisms for Formation of 2,4-Dibromophenol, 2,6-Dibromophenol and 2,4,6-Tribromophenol

- Formation of Bromobenzene, 1,2-Dibromobenzene, 1,2,4-Tribromobenzene and 1,2,3,5-Tetrabromobenzene

The formations of the polybrominated benzenes are shown in figure 4.11. Once 2-MBP is attached to the surface, bromination of the phenoxyl radical proceeds by a mechanism similar to that responsible for formation of polybrominated phenols. The polybrominated benzenes observed in the gas phase can then be formed by the displacement by hydrogen or bromine. The yields of brominated benzenes are lower than for brominated phenols as result of displacement via attack at the phenyl-oxygen bond be slower than at the phenoxyl-surface bond.

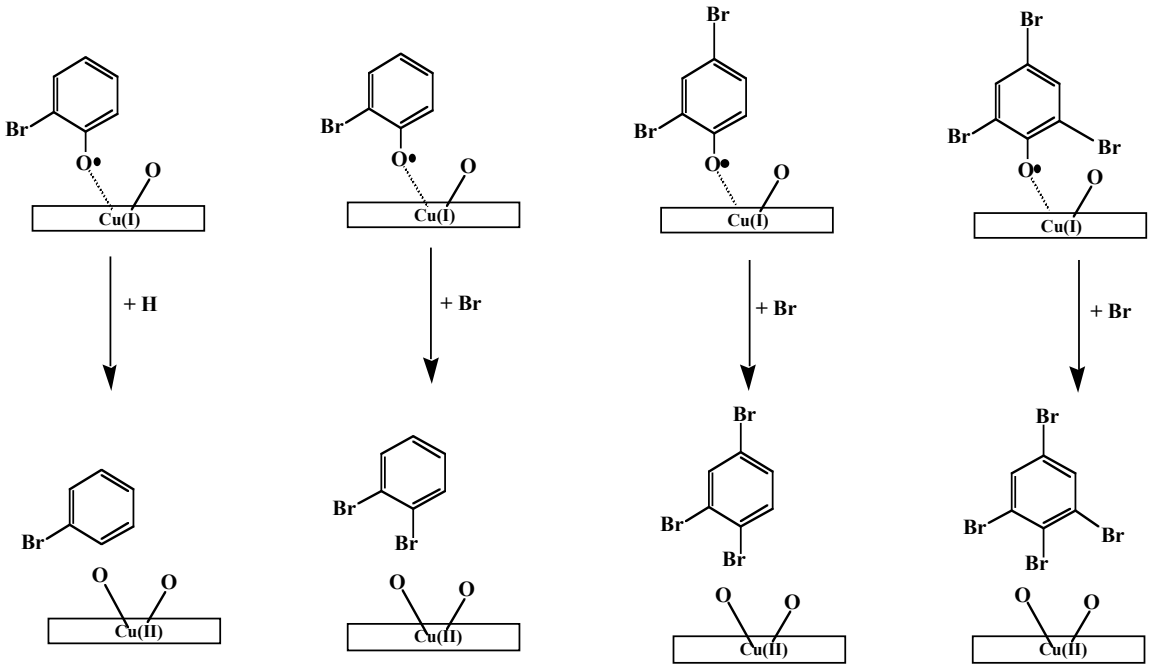

Figure 4.11 Mechanisms for Formation of Brominated Benzenes

It is noticeable that the polybrominated benzenes are formed at lower yields than the polybrominated phenols. This could be due to the fact that displacement of •O by bromine is not as favorable of a reaction, due to the aromaticity of the phenoxyl radical, as tautomerization is for the formation of brominated phenols. As well as the fact that the carbon centered bromophenoxyl radical is the dominant mesomer structure over the oxygen centered radical [37]. In the formation of the polybrominated benzenes, tetrabromobenzene is detected with the highest yield at the lowest temperature of 250°C. 1,2-dibromobenzene is also formed as low as 300°C as well but at slightly lower yields. However surprisingly only one tribromobenzene isomer is detected. One explanation is that this reaction is in direct competition to the formation of the dibromophenols. 2,6-dibromophenol is observed as the dominant dibromophenol and its tribromobenzene counterpart, 1,2,3 tribromobenzene, is not detected in significant yields at all. Whereas the tribromobenzene counterpart to 2,4-dibromophenol, 1,2,4-tribromobenzene, is detected at much lower yields. The ease at which 2,6-dibromophenol versus the slight difficulty

for tautomerization, due to the location, to occur for the formation of 2,4-dibromophenol gives way to allow for 1,2,4-tribromobenzene to be formed. Bromobenzene is formed at higher temperatures than the other brominated benzenes detected. This is due to the fact that the formation of bromobenzene requires the displacement of •O by hydrogen which is a much more unfavorable reaction than the displacement of •O by bromine.

- Formation of Bromoquinone and Dibromoquinone

Based on the results, once 2-MBP attaches to the surface, reaction to the surface oxygen from the copper oxide is also possible. This is depicted in the mechanism to form 3-bromo-3,5-cyclohexadiene-1,2-dione (or bromoquinone) and 3,5-dibromo-3,5-cyclohexadiene-1,2-dione or (dibromoquinone) (Figure 4.12). The ortho carbon centered phenoxyl radical will react with the

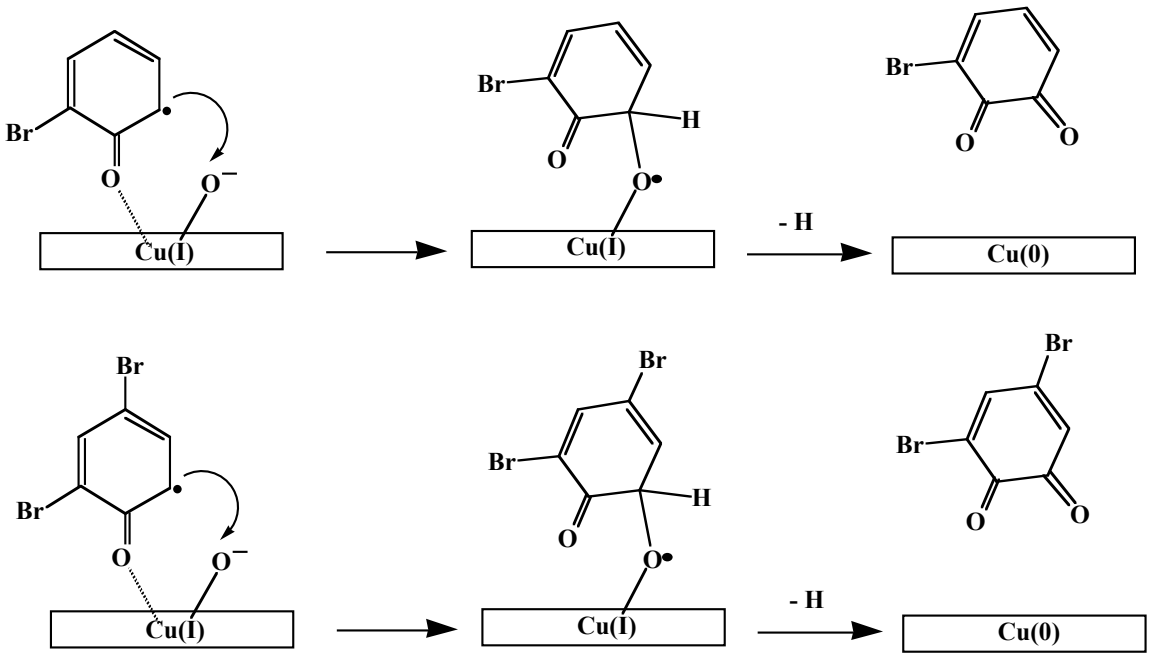

Figure 4.12 Mechanisms for Bromoquinone and Dibromoquinone Formation

terminal oxygen and thus with the elimination of H• the copper is reduce to copper(0) and the quinone detaches from the surface. These pathways are proposed based on previous work for 2-MCP that implies further reduction of Cu(I) (formed after electron transfer from the adsorbed 2-

MCP) to Cu(0) and a gas phase quinone [39]. These products, bromoquinone and dibromoquinone, are possible intermediates to PBDD formation.

- Formation of Dibenzo-p-dioxin, 1-Bromodibenzo-p-dioxin, Dibromodibenzo-p-dioxin, 4-Bromodibenzofuran and Dibenzofuran

There are two general schemes for surface mediated reactions: Langmuir-Hinshelwood and the Eley-Rideal. It has previously been proposed that formation of PCDDs from chlorophenols occurs by the Eley-Rideal mechanism, in which the reaction occurs between an absorbed species and a gas-phase species, and formation of PCDFs from chlorophenols occurs by the Langmuir-Hinshelwood mechanism, which is the reaction between two absorbed species [28, 38]. Because of the similarity in structure between 2-MCP and 2-MBP, these statements can be held true for surface catalyzed reactions with 2-MBP to form PBDD/Fs.

Figure 4.13 represents the Langmuir-Hinshelwood mechanism to form PCDF. Even though DBDF was not detected, the unbrominated DF was observed at 450°C. Once 2-MBP is absorbed to the surface and forms the carbon centered radical structure seen in figure 4.9, two of these surface bond carbon centered phenoxyl radical undergo recombination and tautomerization to form intermediate 2 in figure 4.13. Intermediate 2 then eliminates hydrogen and copper (I) is

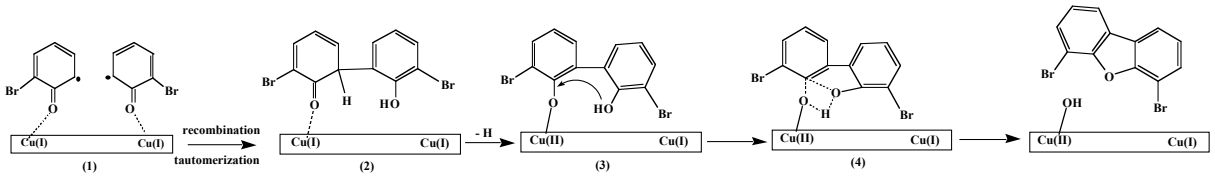

Figure 4.13 Proposed Langmuir-Hinshelwood Mechanism for 4,6-DBDF Formation

oxidized back to copper (II) (Intermediate 3 in Figure 4.13). 4,6-DBDF is then formed by ring closer through a cyclic transition state that results in the regeneration of Cu(II) hydroxide. It is believed that unbrominated phenols follow a similar pathway to form DF. The formation of 4-MBDF occurs by reaction of one brominated phenoxyl radical and an unbrominated phenoxyl

radical or the recombination of the 2 bromophenoxyls to form intermediate 2 in Figure 4.13, which will eliminate to bromine instead of hydrogen. It is likely that the recombination of the 2 surface bound bromophenoxyl radicals is the favorable route in that the elimination of bromine is more favorable than hydrogen due to the lower bond strength of the carbon-bromine bond [7]. In fact 4-MBDF is more likely to form than 4,6-DBDF because bromine plays a role in the formation of 4-MBDF whereas it does not for the formation of 4,6-DBDF.

PBDFs were formed in very low yields, indicating that the Langmuir-Hinshelwood pathways are not favorable for 2-MBP. In contrast to the Eley-Rideal mechanism and the formation of PBDDs, bromine has very little effect on the formation of PBDFs. Bromine acts as a better leaving group than chlorine due to the lower bond strength of the carbon-bromine bond [7]. In addition the abstraction of bromine by H• to form the PBDDs is more favorable than the abstraction of hydrogen by H•. Also the formation of PBDFs requires the presence of 2 surface-bound bromophenolates whereas the formation of PBDDs requires one surface-bound bromophenolate and a gas-phase bromophenoxyl radical. Under pyrolytic conditions, the surface oxygen acts in the oxidation of 2-MBP and thus leaves vacancies. This lowers the number of available sites and thus lowers the potential for the Langmuir-Hinshelwood mechanism to form PBDFs.

Formation of 1-MBDD can occur in one of two pathways. The first pathway seen in Figure 4.14 represents the first of the two plausible Eley-Rideal pathways. As it was shown before with the formation of bromoquinone, the absorbed bromophenoxyl radical can react with another terminal oxygen and 1) eliminate a hydrogen and desorb to form bromoquinone (Figure 4.12) or 2) tautomerize and to the surface intermediate 1 seen in figure 4.14. Once intermediate

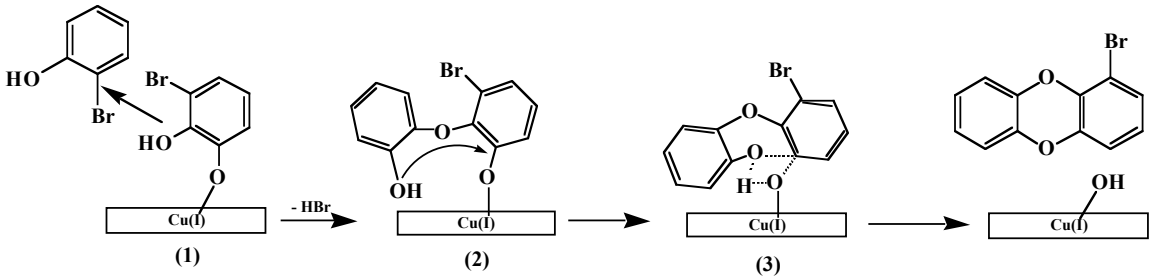

Figure 4.14 Proposed Eley-Rideal Mechanism for 1-MBDD Formation

1 in figure 4.14 is formed, 2-MBP can react with intermediate 1 at one of two places the bromine site or the hydroxyl site. In the case to form 1-MBDD, 2-MBP reacts with intermediate 1 at the hydroxyl site and forms surface bound intermediate 2 via HBr elimination. Intermediate 2 then forms a non-surface bound 1-MBDD through a cyclic transition state.

The remaining PBDDs, DD, DBDD and TrBDD, as well as 1-MBDD can be formed by the second plausible Eley-Rideal pathway seen in figure 4.15. Instead of 2-MBP reacting with

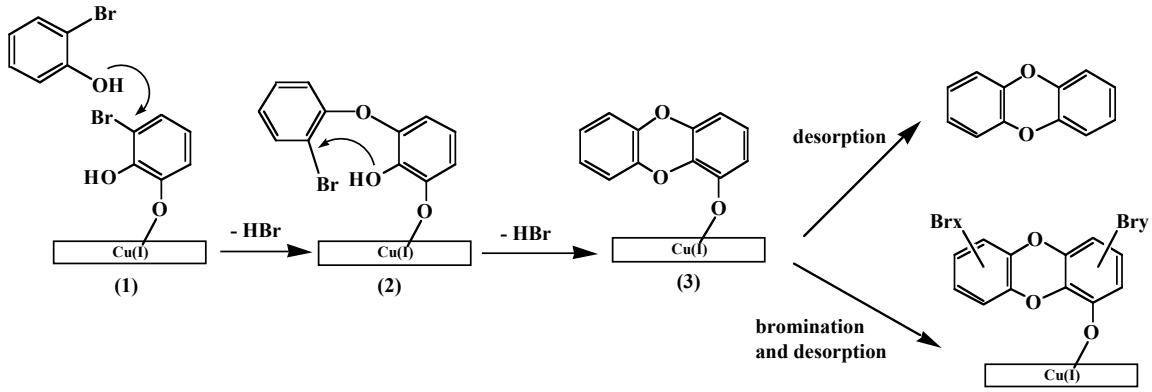

Figure 4.15 Proposed Eley-Rideal Mechanism for DD and PBDDs Formation

intermediate 1 at the hydroxyl substituted site, it reacts at the bromine substituted site, eliminating HBr to form Intermediate 2 in Figure 4.15. Intermediate 2 undergoes ring closure via HBr elimination to form a surface-bound DD. DD can then be desorbed or undergo bromination and desorption to form higher brominated PBDDs, DBDD and TBDD. Higher brominated PBDDs can also be formed by reaction of more highly brominated phenols.

The formation of DBDD exhibits two maxima, 350°C and 450°C. Based on the higher yields of dibromophenols and tribromophenols at lower temperatures, they can contribute to the PBDD formation at the lower temperatures whereas bromination of initially formed may be responsible for the higher temperature PBDDs. Similar observations were made in our previous work on 2-MCP; however, the contributions to PCDD formation from higher chlorinated phenols were small due to their low yields. It is well documented that bromination is 10 times more efficient than chlorination [14]. This is attributable to the dominant halogen for bromine systems being Br_2 versus HCl for chlorine systems [8]. In addition, based on our pseudo-equilibrium gas-phase calculations for the pyrolysis of 2-MBP, the concentration of Br• for temperatures between 300 and 1000°C is at least 100 times greater than the concentration of Cl• for the analogous 2-MCP. In fact at 700°C, Cl• and Cl_2 have not even become present whereas Br• and Br_2 achieve concentration of 3.4×10^{-10} mol and 2.5×10^{-12} mol respectively. In the presence of a surface the radical pool of Br• should only increase since the surface assists in the decomposition of 2-MBP thereby increasing the radicals present in the system. Br_2 readily dissociates to form Br•, whereas HCl (the highest concentration chlorine containing molecule in the 2-MCP system) is a more stable sink of Cl• [7]. Therefore the higher yields of polybrominated phenols and PBDDs is expected because of the higher concentration of Br_2/Br• than Cl_2/Cl. for 2-MCP.

When comparing the surface catalysis studies of 2-MCP with 2-MBP, the maximum yield of DD for 2-MBP is 16 times greater than for 2-MCP. This result was also observed in the gas-phase comparison of 2-MCP and 2-MBP, in the fact that the maximum yield of DD for gas-phase pyrolysis of 2-MBP was 20 times higher than 2-MCP. Clearly bromine is a major contributing factor to the increase in the formation of DD due to the lower bond strength of the C-Br bond over the C-Cl bond strength [7]. Other comparisons between the surface catalyzed

pyrolysis studies between 2-MCP and 2-MBP show that 1) the maximum yield of 1-MBDD is 30 times higher than the maximum yield of 1-MCDD formation and that 2) 4,6-DCDF is observed for 2-MCP whereas 4,6-DBDF is not detected at all in the 2-MBP system. However, 4-MBDF and DF were observed, but at much lower yields than PBDDs. Figures 4.14 and 4.15 demonstrate how bromine plays a major role in the formation of PBDDs. However bromine does not contribute to the formation of the observed PCDFs. Therefore one would expect that the PBDD to PBDF ratio would be much greater than the PCDD to PCDF ratio.

Clearly by looking at the difference between 2-MCP and 2-MBP, the increase in brominated dioxins is extremely significant. Not only are the PBDDs increased but the PBDFs decrease in yield for 2-MBP over the PCDFs for 2-MCP. With the change in halogen from chlorine to bromine, the rate of the reactions to form dioxins is greatly increased and dominates over the surface bound reactions or Langmuir-Hinshelwood reactions to form PBDFs. The formation of DD and 1-MBDD competes with the formation of 4,6-DBDF. The rate of formation of dioxins is so fast in the brominated system that it virtually eliminates the formation of furans that was observed in the surface-mediated reactions in chlorine-containing systems.

4.3.2 Mechanisms Involved for Oxidative Conditions

- Destruction of 2-MBP and the absorption 2-MBP to the CuO Silica surface

With the addition of oxygen, the destruction of 2-MBP dramatically increases over a shorter temperature range than for pyrolytic conditions. At 250°C, 2-MBP has already been reduced to 18% of its initial concentration, versus 69% at 250 C under pyrolytic conditions. There is also a 10% increase in the yields of DBDD/Fs and polybrominated phenols at 250°C for the oxidative conditions over pyrolytic conditions. The increase in PBDD/F formation indicates that while 2-MBP may be decomposed at a greater rate under oxidative conditions, the rate at

which 2-MBP is adsorbed to the surface is increased with the addition of oxygen as well. The copper(II) oxide sites on the silica can be regenerated by O_2 after the consumption of oxygen from previous reactions and therefore allow for the increase in rate of formation of PBDD and polybrominated phenols and benzenes formation. As stated in Section 4.3.1, 2-MBP will chemisorb to the Cu(II)O surface. This will then cause the copper to reduce to Cu(I) and the radical is resonance stabilized to the surface (Figure 4.9).

- Formation of 2,4-Dibromophenol, 2,6-Dibromophenol and 2,4,6-Tribromophenol

Significant yields of the polybrominated phenols are seen at temperatures as low as 250°C. These products are likely to form from the bromination of 2-MBP once attached to the surface. As shown in figure 4.16, Br• will combine with the carbon-centered bromophenoxyl radical at the ortho (1) or para (2) sites and then through tautomerization, 2,4-dibromophenol and 2,6-dibromophenol are formed similar to figure 4.10. However with O_2 present before the tautomerization, H• can be extracted by an hydroxyl radical and thus form a dibromophenoxyl radical that can then with the addition of another Br• and tautomerization can form 2,4,6-tribromophenol (Figure 4.16).

In comparison with 2-MBP under pyrolytic conditions, there is an increase in percent yield for the formation of the polybrominated phenols under oxidative conditions. The dibromophenols reach maximum yields between 300 and 350°C for both conditions. Interestingly, for the oxidative conditions, 2,4-dibromophenol has the highest yield of 48.9% over the other polybrominated phenols, whereas 2,6-dibromophenol achieves the highest yield for pyrolytic conditions. It is also important to note that the maximum yield for 2,4-dibromophenol increases by 5x whereas 2,6-dibromophenol and 2,4,6-tribromophenol only increase by a factor of 1.5 for oxidative conditions. Under pyrolytic conditions, the formation of

2,4-dibromophenol and 2,6-dibromophenol is largely dependant on the final tautomerization eliminating the dibromophenol from the surface. 2,6-Dibromophenol will form the higher yields because of the close proximity of the hydrogen and the oxygen for the conversion from the keto

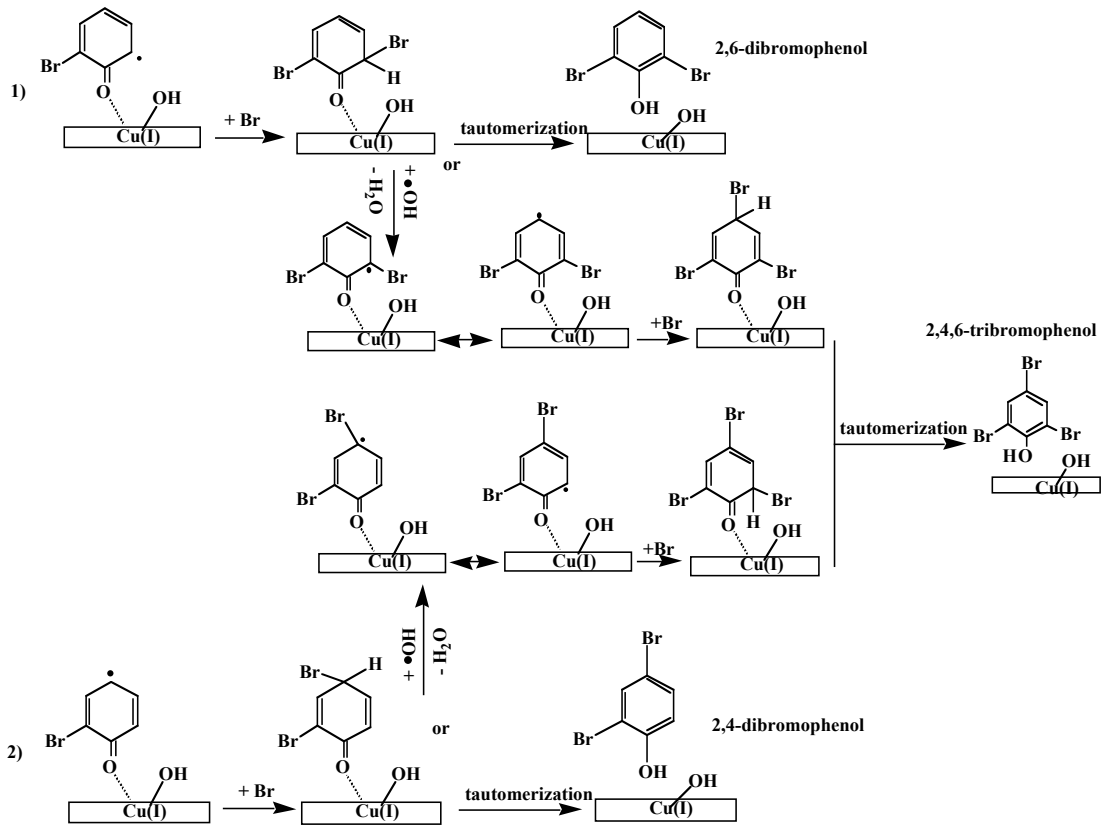

Figure 4.16 Proposed Mechanisms for Formation of 2,4-Dibromophenol, 2,6-Dibromophenol and 2,4,6-Tribromophenol with the Assistance of •OH

to the enol tautomer. However with the addition of oxygen, there is also a higher concentration of •OH that can assist in the formation of the dibromophenols. 2,4-dibromophenol dramatically increases in yield under oxidative conditions because the para-aromatic hydrogen is easier to abstract by •OH due to its location away from the steric hindrance of the surface.

2,4,6-Tribromophenol achieves a maximum yield at 450°C whereas for pyrolytic conditions the maximum yield was seen at 350°C. This shift in the maximum yield is also seen

for the PBDDs. The addition of oxygen increases the rate of bromination that allows it to compete with desorption at higher temperatures.

- Formation of Bromobenzene, 1,2-Dibromobenzene, 1,2,3-Tribromobenzene, 1,2,4-Tribromobenzene and 1,2,3,5-Tetrabromobenzene

The formations of the polybrominated benzenes result from the adsorption of polybrominated phenols. Once 2-MBP or the polybrominated phenols are attached to the surface and then each polybrominated benzene can then be formed by the displacement of •O attached to the surface by bromine and thus removing the polybromobenzene from the surface. However for the formation of bromobenzene, the •O is displaced by hydrogen to detach bromobenzene from the surface (Figure 4.11).

Under pyrolytic conditions, brominated benzenes are formed by displacement of the chemisorbed phenyl ring from the surface through ipso- attack at the aromatic carbon-oxygen bond by H•. With the addition of oxygen, the polybrominated benzenes only increase in yield slightly and, with the exception of bromobenzene, are still much lower in yields than the polybrominated phenols. Clearly the formation of the brominated benzenes are not as favorable as the phenols and the addition of oxygen does not have much of an effect on their formation. This is likely due to intermolecular tautomerization being much faster than ipso attack and the concentration of H• is slightly decreased under oxidative conditions. The slight increase in polybrominated benzenes is due to the increase in Br• with the addition of oxygen. Hydroxyl radicals (which increases with the addition of oxygen) will react with HBr to increase the concentration of Br•. The effect is less dramatic than chlorine systems where HCl is a stronger resevoir of Cl• and the increase in •OH concentration with the addition of oxygen dramatically increases the Cl• concentration and the rate of chlorination [8, 14, 27].

- Formation of Bromoquinone and Dibromoquinone

The formations of bromoquinone and dibromoquinone are previously explained in Section 4.3.1. Figure 4.12 depicts the formation of the two. Bromoquinone and dibromoquinone increase in yield with the addition of oxygen, probably due to the replenishment of terminal oxygen groups as well as an increase in the hydroxyl radical concentration that supports hydrogen abstraction. Bromoquinone decreases in yield as PBDDs increase in yield suggesting that they are intermediates in the formation of PBDDs.

- Formation of Dibenzo-p-dioxin, 1-Bromodibenzo-p-dioxin, Dibromodibenzo-p-dioxin, Tribromodibenzo-p-dioxin and 4-Bromodibenzofuran

There are two general schemes for surface catalyzed reactions: Langmuir-Hinshelwood and the Eley-Rideal. Previously in Section 4.3.1, the formation of PBDDs from bromophenols occurs by the Eley-Rideal mechanism, in which the reaction occurs between an absorbed species and a gas-phase species, and formation of PBDFs from bromophenols occurs by the Langmuir-Hinshelwood mechanism, which is the reaction between two absorbed species.

Figure 4.17 represents the Langmuir-Hinshelwood mechanism to form 4-MBDF. 2-MBP is absorbed to the surface and forms the carbon centered radical structure seen in figure 4.9.

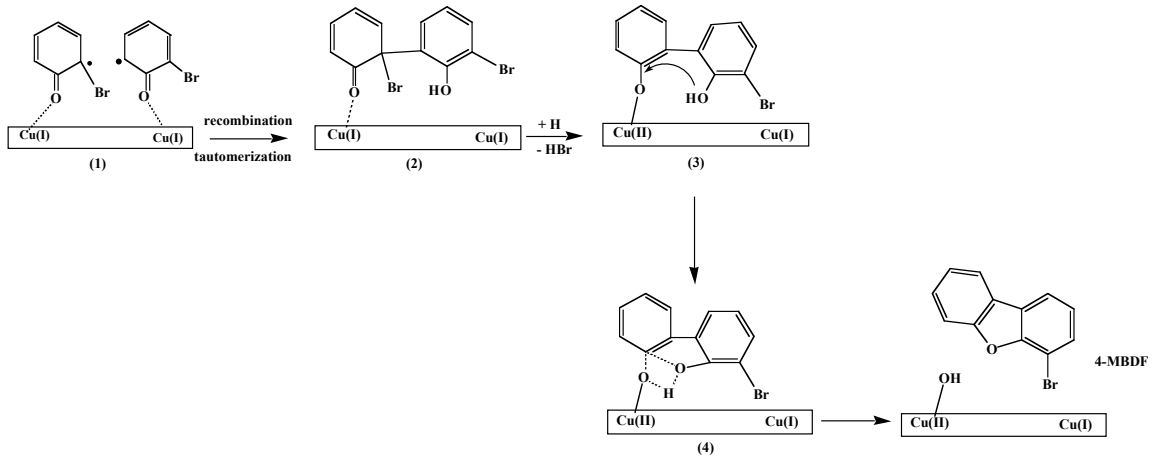

Figure 4.17 Proposed Langmuir Hinshelwood Mechanism for Formation of 4-MBDF

There are two types of these surface bond carbon centered phenoxyl radicals, one where the radical is located near the ortho carbon hydrogen bond and the other where the radical is located near the ortho carbon bromine bond. The ortho carbon hydrogen centered radical can recombine with the other carbon-centered radical and undergo tautomerization to form intermediate 2 in figure 4.17. Intermediate 2 then eliminates bromine and copper (I) is oxidized back to copper (II) (Intermediate 3 in Figure 4.17). 4-MBDF is then formed by ring closer through a cyclic transition state that results in the regeneration of the OH group on copper (II) (Figure 4.17). 4-MBDF was formed under the pyrolytic conditions in ~50x lower yields. The increase with the addition of oxygen can be explained by the increase in the reoxidation of surface sites at higher temperatures.

4,6-DBDF, which was expected to be formed based on the formation of 4,6-DCDF from 2-MCP, was not observed. 4,6-DBDF would have been formed by the reaction of two ortho-carbon (bromine) centered radicals rather than the dissimilar radicals that react to form 4-MBDF. We believe that the relative ease of displacement or abstraction of bromine (versus chlorine) due to the weak carbon-bromine bond facilitates formation of 4-MBDF over 4,6-DCDF [7].

Formation of 1-MBDD can occur in one of two pathways. The first pathway seen in figure 4.14 represents the first of the two plausible Eley-Rideal pathways. As it was shown before with the formation of bromoquinone, the absorbed bromophenoxyl radical can react with another terminal oxygen and 1) eliminate a hydrogen and desorb to form bromoquinone (Figure 4.12) or 2) tautomerize and to the surface species 1 seen in figure 4.14. Once species 1 in figure 4.14 is formed, 2-MBP can react with species 1 at one of two places 1) the hydroxyl site or 2) the bromine site. In the case to form 1-MBDD, 2-MBP reacts with species 1 at the hydroxyl site and forms surface bound intermediate 2 thus eliminating HBr in the process. Intermediate 2 then

undergoes the same cyclic transition state seen in figure 4.17, which then allows for 1-MBDD to be desorbed from the surface.

The remaining PBDDs, DD, DBDD and TrBDD, as well as 1-MBDD can be formed by the second plausible Eley-Rideal pathway seen in figure 4.15. Beginning with the same surface species 1, instead of 2-MBP reacting with species 1 at the hydroxyl site, it reacts at the bromine site and again eliminating HBr to form species 2 in figure 4.15. Species 2 undergoes ring closer via another HBr elimination and thus forming DD still attached the surface. DD can then be desorbed or undergo bromination and desorption to form any number of PBDDs.

With the addition of oxygen, formations of PBDDs continue to dominate over the formation of PBDFs. There are more PBDDs formed and at maximum yields that are from 5 to 70 times higher than the one PBDF detected. With these results and similar results with the oxidation of 2-MCP, the Eley-Rideal mechanism is essentially the more favorable route for the formation of PBDD/Fs [38]. The Eley-Rideal and the Langmuir-Hinshelwood mechanisms are in direct competition with each other in that they both require an absorbed species to form the final product. However for the Eley-Rideal mechanism only one absorbed species is required and thus will reduce the concentration of the absorbed species to form the PBDFs.

There is a distinctive shift of the maximum yields of PBDDs to higher temperatures under oxidative conditions versus pyrolytic. The dibromophenols are at very high yields at low temperatures and as the temperatures increase, they decrease in yield as the formation of PBDDs increase. Therefore it is more probable the PBDDs are formed after the bromination of 2-MBP rather that bromination of DD.

In the presence of oxygen, the PBDDs detected from 2-MBP increase by 5x in yield over the pyrolysis of 2-MBP. This is facilitated by the increase in Br• present in the system. Also

with the excess oxygen present, surface copper oxide surfaces can easily be regenerated at higher temperatures, thus allowing for more PBDDs. In comparison with the similar studies with 2-MCP, there is an even greater increase in PCDDs in the presence of oxygen over pyrolysis [38]. The explanation given was the presence of surface hypochlorite species allowing for the increase in chlorination of the aromatics [38, 40] . The lesser effect of oxygen in the bromine system may be due to: 1) Cu-O-Br bonds are not as strong as Cu-O-Cl bonds and this species may not be stable on the surface and 2) the facile brominating agent Br• is already present in high concentrations versus the lower concentration of Cl• analogous chlorinated hydrocarbon systems [7-8]. DD is the major PBDD product observed whereas the 1-MCDD was the major PCDD product observed for 2-MCP [38]. This observation indicates that path 2 in figure 7 is favored over path 1. We attribute this to the relative ease of the second HBr elimination step the produces the surface bound DD. This view is supported by the observation of higher yields of PBDDs than PCDDs, which suggests that bromination of surface-bound DD is occurring.

Comparison of the surface catalytic studies of 2-MCP and 2-MBP shows that 2-MBP forms much higher yields of PBDDs than 2-MCP forms the analogous PCDDs. The yields of DD alone under the surface catalyzed oxidation of 2-MBP are 200 times greater than for 2-MCP [38]. This increase in PBDDs formation for brominated phenols over PCDDs for chlorinated phenols has been documented for gas-phase reactions [14, 41] as well as the gas-phase results seen in sections 4.1 and 4.2.

4.4 References

1. Shaub, W. M.; Tsang, W. *Dioxin Formation in Incinerators*, Environmental Science and Technology, 1983, **17**: 721.

2. Colussi, A.; Zabel, F.; Benson, S.W., *The Very Low-Pressure Pyrolysis of Phenyl Ethyl Ether, Phenyl Allyl Ether and Benzyl Methyl Ether and the Enthalpy of Formation of the Phenoxyl Radical*, Internationl Journal of Chemical Kinetics, 1977, **9**: 161.

3. Louw, R.; Ahonkhai, S. T., *Radical/radical vs Radical/molecule Reactions in the Formation of PCDD/Fs from (Chloro)phenols in Incinerators* Chemosphere, 2002, **46**: 1273.

4. Carlson, G. L.; Fataley, W. G.; Monocha, A. S.; Bentley, F. F. *Torsional Frequencies and Enthalpies of Intramolecular Hydrogen Bonds of o-Halophenols,* Journal of Physical Chemistry, 1972, **76**: 1553.

5. NIST Chemical Kinetics Database 17, Gaithersburg, MD, 1998.

6. Ritter, E.R.; Bozzelli, J.W.; Dean, A. M. *Kinetic Study on the Thermal Decomposition of Chlorobenzene Diluted in Hydrogen*, Journal of Physical Chemistry*,* 1990, **94**(6): 2493.

7. McMillen, D. F.; Golden, D. M. *Hydrogen Bond Dissociation Energies*, Annual Review Physical Chemistry, 1982, **33**: 493.

8. Soderstrom, G.; Marklund, S. *PBCDD and PBCDF from Incineration of Waste-Containing Brominated Flame Retardants*, Environmental Science and Technology, 2002, **36**: 1959.

9. Khachtrayan, L.; Burcat, A.; Dellinger, B. *An Elementary Reaction-Kinetic Model for the Gas-Phase Formation of 1,3,6,8- and 1,3,7,9-Tetrachlorinated Dibenzo-p-dioxins from 2,4,6-Trichlorophenol*, Combustion and Flame, 2003**, 132**: 406.

10. Khachtrayan, L.; Asatrayan, R.; Dellinger, B. *Development of Expanded and Core Kinetic Models for the Gas Phase Formation of Dioxins from Chlorinated Phenols*, Chemosphere, 2003, **52**: 695.

11. Appel, J.; Bockhorn, H.; Frenklach, M. *Kinetic Modeling of Soot Formation with Detailed Chemistry and Physics: Laminar Premixed Flames of C_2 Hydrocarbons*, Combustion and Flame, 2000, **121**: 122.

12. Richter, H.; Howard, J. B.*Formation of Polycyclic Aromatic Hydrocarbons and Their Growth to Soot - A Review of Chemical Reaction Pathways*, Progress in Energy and Combustion Science**,** 2000, **26**(4):565.

13. Richter, H.; Mazyer, O.A.; Sumathi, R.; Green, W. H.; Howard, J. A.; Bozzelli, J. W. *Detailed Kinetic Study of the Growth of Small Polycyclic Aromatic Hydrocarbons, 1. 1-Naphthyl + Ethyne,* Journal of Physical Chemistry A, 2001, **105**(9): 1561.

14. Kanters, J.; Louw, R. *Thermal and Catalysed Halogenation in Combustion Reactions*, Chemosphere, 1996, **32**(1): 87.

15. Melius, C.F.; Calvin, M.; Marinov, N.M.; Ritz, W.J.; Senkan, S.M. *Reaction Mechanisms in Aromatic Hydrocarbon Formation Involving the C_5H_5 Cyclopentadienyl Moiety*, 26th Symposium (International) on Combustion, The Combustion Institute, 1996, 685.

16. Lu, M.; Muholland, J.A. *Aromatic Hydrocarbon Growth from Indene*, Chemosphere 2001, **42**: 623.

17. Lin, C. Y.; Lin, M.C. *Thermal Decomposition of Methyl Phenyl Ether in Shock Waves: The Kinetics of Phenoxyl Radical Reactions*, Journal of Physical Chemistry, 1986, **90**: 425.

18. Waiter, I.; Born, J.G.P.; Louw, R. *Products, Rates and Mechanism of the Gas-Phase Condensation of Phenoxy Padicals between 500-840 K*, European Journal of Organic Chemistry, 2000, 921.

19. Born, J.G.P.; Louw, R.; Mulder, P. *Formation of Dibenzodioxins and Dibenzofurans in Homogeneous Gas-Phase Reactions of Phenols*, Chemosphere, 1989, **19**: 401.

20. Yang, Y.; Muholland, J.A.; Akki, U. *Formation of Furans by Gas-Phase Reactions of Chlorophenols*, 27th Symposium (International) on Combustion, The Combustion Institute, 1998, 1761.

21. Waiter-Protas, I.; Louw, R. *Gas-Phase Chemistry of Chlorinated Phenols – Formation of Dibenzofurans and Dibenzodioxins in Slow Combustions*, European Journal of Organic Chemistry, 2001, 3945.

22. Weber, R.; Hagenmaier, H.; *Mechanism of the Formation of Polychlorinated Dibenzo-p-dioxins and Dibenzofurans from Chlorophenols in Gas Phase Reactions*, Chemosphere, 1999, **38**: 529.

23. Muholland, J.A.; Akki, U.; Yang, Y.; Ryu, J. Y. *Temperature Dependance of DCDD/F Isomer Distributions from Chlorophenol Precursors*, Chemosphere, 2001, **42**: 719.

24. Weber, R.; Hagenmaier, H. *On the Mechanism of the Formation of Polychlorinated Dibenzofurans from Chlorophenols*, Organohalogen Compounds**,** 1997, **31**: 480.

25. Borojovich, E.; Aizenshtat, Z. J. *Thermal Behavior of Brominated and Polybrominated Compounds II: Pyroproducts of Brominated Phenols as Mechanistic Tools*, Analytical and Applied Pyrolysis, 2002, **63**: 129.

26. Bryukov, M.; Slagle, I.; Knyazev,V. *Kinetics of Reactions of H Atoms with Methane and Chlorinated Methanes*, Journal of Physical Chemistry A, 2001, **105**: 3107.

27. Lemieux, P. M.; Ryan, J. V. *Enhanced Formation of Dioxins and Furans from Combustion Devices by Addition of Trace Quantities of Bromine*, Waste Management, 1998, 18: 361.

28. Lomnicki, S.; Dellinger, B. *Formation of PCDD/F from the Pyrolysis of 2-Chlorophenol on the Surface of Dispersed Copper Oxide Particles*, 29th Symposium (International) on Combustion, The Combustion Institute, 2003, in press.

29. Green, J. H. S.; Maccoll, A. *Studies in the Pyrolysis of Organic Bromides. Part V: The Pyrolysis of Cyclohexyl Bromide*, Journal of Chemical Society, 1955, 2449.

30. Price, S.; Shaw, R.; Trotman-Dicksenson, A. *The Thermal Decomposition of Cyclopentyl Bromide*, Journal of Chemical Society, 1956, 3855.

31. Kale, M.; Maccoll, A. *Studies in the Pyrolysis of Organic Bromides. Part VII: The Maximally Inhibited Decomposition of Cyclopentyl Bromide*, Journal of Chemical Society, 1957, 5020.

32. Wilkstrom, E,; Ryan, S.l Touati, A.; Telfer, M.; Gullett, B. K. *Importance of Chlorine Speciation on de Novo Formation of Polychlorinated Dibenzo-p-dioxins and Polychlorinated Dibenzofurans*, Environmental Science Technology, 2003**, 37**: 1108.

33. Procaccini, C.; Bozzelli, J. W.; Longwell, J. P.; Sarofim, A. F.; Smith, K. A. *Formation of Chlorinated Aromatics by Reactions of Cl, Cl_2 and HCl with Benzene in the Cool-Down Zone of a Combustor*, Environmental Science Technology, 2003**, 37**: 1684.

34. Huang, J.; Onal, I.; Senkan, S. M.; *Formation of Trace By-Products in the Premixed Flames of CH_3Cl/C_2H_4*, Environmental Science and Technology, 1997**, 31**: 1372.

35. Satyapal, S.; Werner, J. H.; Cool, T. A. *An Extended Flame Zone in the Combustion of CH_3Cl*, Combustion Science and Technology, 1995**, 106**: 229.

36. Kim, D. H.; Mulholland, J. A.; Ryu, J-Y; *Formation of Polychlorinated Naphthalenes from Chlorophenols*, 30th Symposium (International) on Combustion, The Combustion Institute, 2003, in press.

37. Farquar, G. R.; Alderman, S. L.; Poliakoff, E. D.; Dellinger, B. *X-ray Spectroscopic Studies of the High Temperature Reduction of Cu(II)O by 2-Chlorophenol on a Simulated Fly Ash Surface*, Environmental Science and Technology, 2003, **37**: 931.

38. Lomnicki, S.; Dellinger, B. *A Detailed Mechanism of the Surface-Mediated Formation of PCDD/F from the Oxidation of 2-Chlorophenol on a CuO/Silica Surface*, Journal of Physical Chemistry A, 2003, **107**: 4387.

39. Christoskova, S.; Stoyanova, M.; Georgieva, M. *Low-Temperature Iron-Modified Cobalt Oxide System: Part 2. Catalytic Oxidation of Phenol in Aqueous Phase* Journal of Applied Catalysis A, 2001, **208**: 243.

40. Born, J. G. P.; Louw, R.; Mulder, P. *Fly Ash Catalyzed Oxidation and Oxychlorination of Phenol*, Organohalogen Compound, 1990, **3**: 31.

41. Sidhu, S.S., Maqsud, L., Dellinger, B. *The Homogeneous, Gas-Phase Formation of Chlorinated and Brominated Dibenzo-p-dioxins from 2,4,6-Trichlorophenol and 2,4,6-Tribromophenols*, Combustion and Flame, 1995, **100**: 11.

CHAPTER 5. SUMMARY

The various combustion conditions addressed in this study have resulted in a better understanding of the mechanisms involved in the formation of PCDD/Fs and PBDD/Fs. In fact these studies have demonstrated the dramatic differences in the behavior of chlorine and bromine, the role of catalytic surfaces, and the impact of oxygen. Under the surface mediated conditions, bromine has increased the yields of PBDDs detected. Pathways to the formation of PBDD/Fs and PCDD/Fs were proposed as well as pathways of formation of the intermediates and PAHs detected from the various studies. In comparing all of these studies, some general conclusions can be made.

5.1 Gas Phase Conditions

The observations shown in Figure 5.1 describe the significant difference between 2-MBP

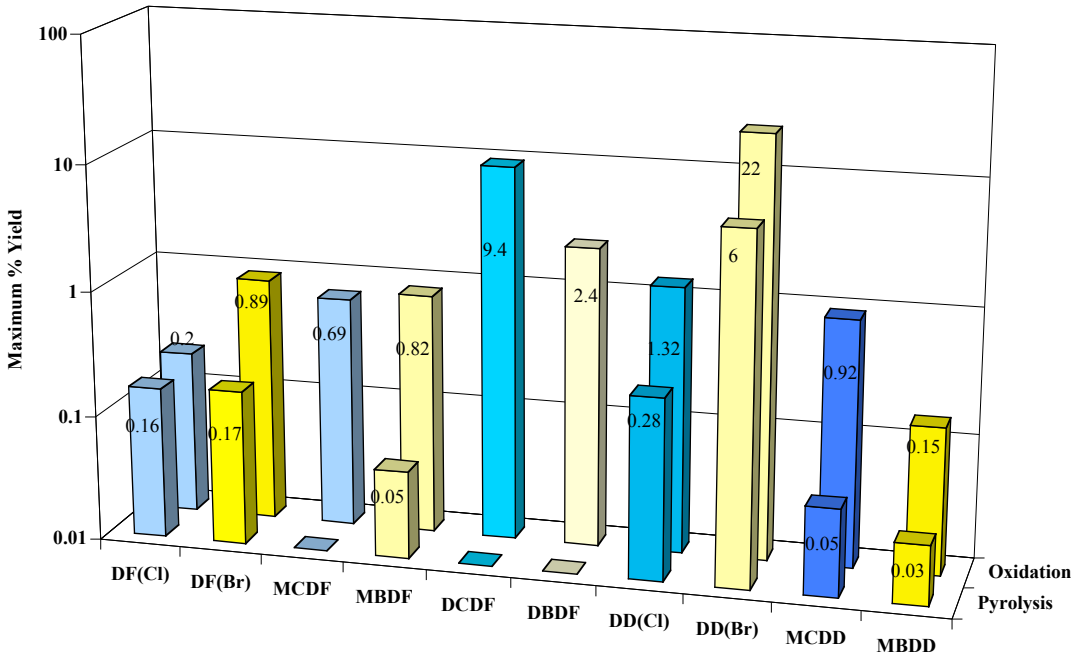

Figure 5.1 Comparison of the PCDD/Fs and PBDD/Fs from the Gas-Phase Pyrolysis and Oxidation of 2-MBP and 2-MCP

and 2-MCP as well as the effect of the presence of oxygen. For all the gas-phase conditions, DD is the major PBDD/F product observed for 2-MBP. However while DD was the major PCDD/F product observed for 2-MCP under pyrolytic gas-phase conditions, 4,6-DCDF was the major PCDD/F product observed under oxidative conditions. In addition, 4,6-DCDF and 4,6-DBDF remained unobserved for the individual pyrolysis of 2-MCP and 2-MBP.

5.1.1 Oxidation versus Pyrolysis

- The overall yields of PCDD/F and PBDD/F are increased by the addition of oxygen due to the increase in the concentration of halogenated phenoxyl radicals, especially at low temperature.

The increase in the formation of these products is due to the increase in the concentration of bromophenoxyl radicals and chlorophenoxyl radicals at lower temperatures formed by the rapid reactions involving •OH and O• with rate coefficients based on analogous reactions with phenol for the abstraction of hydrogen by •OH and O• being k_{OH} (1000 – 1150 K) = $6.0x10^{12}$ $cm^3/mol/s$ and k_O (290-870 K) = $1.7x10^{13}exp(-3060/RT)$ $cm^3/mol/s$ respectively [1-3].

In addition, pseudo equilibrium calculations demonstrate an increase in the concentrations of Cl• and Br• at lower temperatures with the addition of oxygen (Table 5.1). The Cl_2 and Br_2 formed from the oxidation of 2-MCP and 2-MBP readily dissociates to Cl• and Br• with rate coefficients of k_{cl} (300-800 K) = $8.51 \times 10^{15}exp(-55.84$ kcal/RT) $cm^3/mol/s$ and k_{br} (1800 – 2500 K) = $2.35 \times 10^{14}exp(-42.92$ kcal/RT) $cm^3/mol/s$ [1, 4]. The addition of oxygen increases the concentration of Cl• by reaction 1 with a rate coefficient of k_1 (300-700 K) = $1.77x10^{12}$ exp(-0.89 kcal/RT) $cm^3/mol/s$ [1, 5].

•OH + HCl → H_2O + Cl• (Reaction 1)

Table 5.1 Pseudo-Equilibrium Calculations of Major Cl, Br and O Species for Pyrolysis and Oxidation of Pure 2-MCP, 50:50 Mixture of 2-MCP & 2-MBP and Pure 2-MBP

	2-MCP		2-MCP & 2-MBP		2-MBP	
500ºC	**Pyrolysis**	**Oxidation**	**Pyrolysis**	**Oxidation**	**Pyrolysis**	**Oxidation**
	Moles (% Cl)		**Moles (% Cl or Br)**		**Moles (% Br)**	
O	-	ND	-	ND	-	ND
OH	-	2.0×10^{-11}	-	1.8×10^{-11}	-	2.0×10^{-11}
H_2O	1.1×10^{-16}	1.9×10^{-4}	1.02×10^{-16}	2.05×10^{-4}	6.8×10^{-14}	2.24×10^{-4}
2-MCP	8.6×10^{-5} (97 %)	0	0	0	-	-
Cl_2	ND	1.72×10^{-5} (38 %)	ND	5.9×10^{-6} (26.8 %)	-	-
HCl	1.9×10^{-6} (2.2 %)	5.4×10^{-5} (62 %)	4.39×10^{-5} (99.7 %)	3.3×10^{-5} (73.2 %)	-	-
Cl	ND	2.4×10^{-8} (0.03 %)	ND	1.3×10^{-8} (0.018 %)	-	-
2-MBP	-	-	0	0	8.6×10^{-5} (97%)	0
Br_2	-	-	2.50×10^{-12} (1.1×10^{-5}%)	2.2×10^{-5} (99.7 %)	ND	4.4×10^{-5} (99.8 %)
HBr	-	-	4.39×10^{-5} (99.7%)	1.1×10^{-8} (0.03 %)	1.9×10^{-6} (2.2%)	1.7×10^{-8} (0.02 %)
Br	-	-	2.36×10^{-11} (5.4×10^{-5}%)	8.7×10^{-8} (0.2 %)	ND	1.2×10^{-7} (0.14 %)
700ºC	**2-MCP**		**2-MCP and 2-MBP**		**2-MBP**	
O	-	3.5×10^{-11}	-	3.5×10^{-11}	-	3.5×10^{-11}
OH	-	3.2×10^{-9}	-	3.1×10^{-9}	-	3.4×10^{-9}
H_2O	2.21×10^{-18}	1.8×10^{-4}	2.08×10^{-18}	2.0×10^{-4}	7.5×10^{-5}	2.2×10^{-4}
2-MCP	8.5×10^{-5} (96.5 %)	0	0	0	-	-
Cl_2	ND	5.7×10^{-6} (12.8 %)	ND	1.5×10^{-6} (6.8 %)	-	-
HCl	1.99×10^{-6} (2.2 %)	7.7×10^{-5} (86.7 %)	4.3×10^{-5} (99.7%)	4.1×10^{-5} (92.5 %)	-	-
Cl	ND	6.6×10^{-7} (0.75 %)	1.37×10^{-12} (3.1×10^{-6}%)	3.2×10^{-7} (0.70%)	-	-
2-MBP	-	-	0	0	8.5×10^{-5} (96.5 %)	0
Br_2	-	-	3.3×10^{-11} (1.0×10^{-4}%)	2.0×10^{-5} (93 %)	9.09×10^{-12} (2.0×10^{-5}%)	4.2×10^{-5} (95 %)
HBr	-	-	4.3×10^{-5} (99.7%)	1.7×10^{-7} (0.39%)	1.9×10^{-6} (2.2 %)	2.4×10^{-7} (0.27 %)
Br	-	-	3.3×10^{-9} (0.007 %)	2.9×10^{-6} (6.6%)	1.2×10^{-9} (0.001%)	4.3×10^{-6} (4.8 %)

The abstraction of hydrogen is also facilitated by Cl•. The known rate coefficient for the abstraction of hydrogen by Cl• for phenol is k_{Cl} (25°C) = $1.43x10^{14}$ cm^3/mol/s [1]. A similar increase in the concentration of Br• and hydrogen abstraction by Br• is expected. Therefore the increase in the radical pool at lower temperatures increases the lower temperature formation of phenoxyl radicals before decomposition, thereby increasing the yield of PCDD/F and PBDD/F.

- The formation of PCDD/Fs and PBDD/Fs is facilitated by the addition of oxygen due to the abstraction of hydrogen by •OH from reaction intermediates.

The formation of the PCDFs and PBDFs was observed at 100x greater yields in the presence of oxygen. This is largely due to the increased concentration of •OH and Cl• and their facilitation of the formation of PCDFs and PBDFs by hydrogen abstraction from phenoxyl radical recombination products and intermediates (Figure 5.2). A similar effect is implied in the

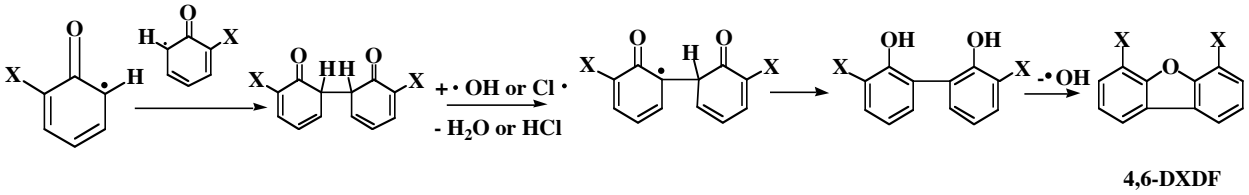

Figure 5.2 Pathway to the Formation of 4,6-DCDF and 4,6-DBDF

formation of 1-MBDD and 1- MCDD (Figure 5.3). The yield of DD is not increased because its

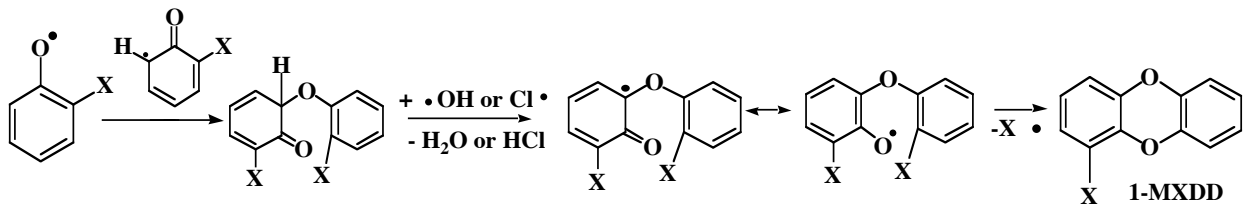

Figure 5.3 Pathway to the Formation of 1-MCDD and 1-MBDD

mechanism involves chlorine or bromine abstraction which is facilitated by H• not •OH. (The ΔH_{rxn} for the abstraction of chlorine or bromine by •OH is highly endothermic (ΔH_{rxn} = 40 kcal/mol))

5.1.2 Bromine Versus Chlorine

- The yields of PBDDs are 20x higher than PCDDs due to the ease of displacement of bromine versus chlorine in the ring closure step.

For both the pyrolysis and oxidation of 2-MBP, maximum yields of DD are ~20 times higher in yield than the maximum yields observed for 2-MCP. This is primarily due to all the steps in the formation of DD for 2-MBP being exothermic whereas the ΔH_{rxn} for the final displacement of chlorine to form DD from 2-MCP is endothermic (ΔH_{rxn} = 12 kcal/mol for chlorine displacement versus –12 kcal/mol for bromine displacement) (Figure 5.4).

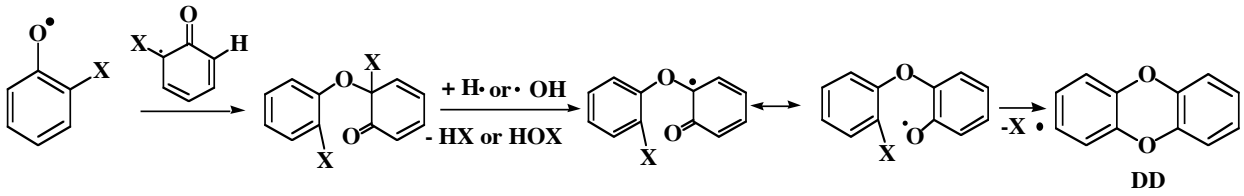

Figure 5.4 Pathway to the Formation of DD

This is consistent with Br• being a better leaving group than Cl• [6].

PBDD to PBDF ratios are greater than PCDD to PCDF ratios due to Br• displacement in the ring closure step to from PBDD being faster than the rate of abstraction of hydrogen by •OH in PBDF formation. 4,6-DCDF is the major product for the oxidation of 2-MCP whereas DD, not the analogous 4,6-DBDF, is the major product for the oxidation of 2-MBP. The addition of oxygen to the system increases the concentrations of •OH and reactive chlorine species that assist in the abstraction of hydrogen to form the 4,6-DCDF and 4,6-DBDF (Table 5.1). However this increase is insufficient to compete with the exothermic formation of DD from 2-MBP whereas it is sufficient to compete with the endothermic formation of DD from 2-MCP. Thus, the hydrogen abstraction reactions necessary for formation of 4,6-DBDF (and 1-MBDD) from 2-MBP are not as favored by this increase as in the 2-MCP system.

- Bromination occurs more readily than chlorination under pyrolytic conditions because the concentration of Br• is greater than that of Cl•.

Under pyrolytic conditions, bromination of 2-MBP is observed whereas; the chlorination of 2-MCP is unobserved. Our pseudo-equilibrium calculations for pyrolytic conditions indicate that Br• is present at temperatures as low as 700°C whereas Cl• remains undetected (Table 5.1). With these higher concentrations of Br•, bromination of 2-MBP is more efficient than the chlorination for the 2-MCP system.

- Chlorination increases significantly and bromination increases only slightly with the addition of oxygen.

The pseudo-equilibrium calculations for the oxidations of pure 2-MCP and 2-MBP indicate that HCl is the dominant form of chlorine and Br_2 is the dominant form of bromine (Table 5.1). This is similar to previously reported calculations [7]. It has also been reported that bromination is 10 times more efficient than chlorination [8]. In comparison to pyrolytic conditions, the concentration of Cl• increases significantly by a factor of at least 100 with the addition of oxygen to the system (Table 5.1). However, Br• is present under both pyrolytic and oxidative conditions and its concentration changes only slightly with the addition of oxygen (Table 5.1). The formation of Br_2 and Cl_2 is important since they readily dissociate to the brominating and chlorinating agents, Br• and Cl• [1, 4]. Oxygen assists in the formation of Cl• by reaction 1. This assistance is not as necessary for bromine since bromine already predominantly exists as Br_2.

5.1.3 Mixed Bromo/Chloro Systems

- The formation of PCDFs is increased with the addition of bromine due to an increase in the concentration of reactive chlorine.

Cl• facilitates the abstraction of hydrogen to form 4,6-DCDF (Figure 5.2). Unlike the pyrolysis of pure 2-MCP, 4,6-DCDF and 4-MCDF were detected from the mixture of 2-MCP and 2-MBP (Figure 5.5). The pseudo-equilibrium calculations indicate an increase in the

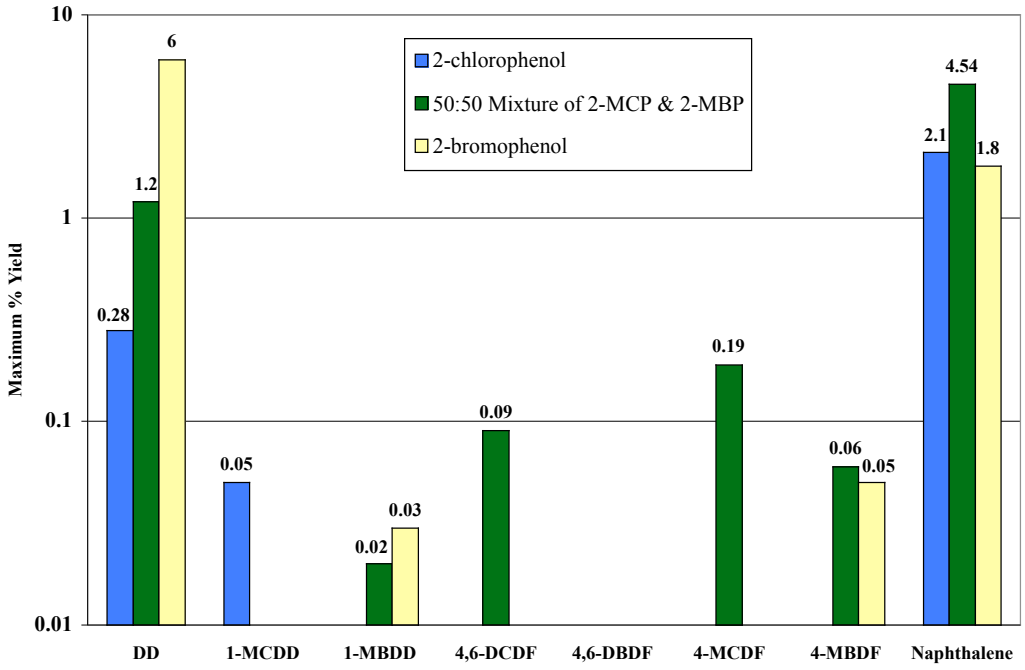

Figure 5.5 Comparison of PBDD/Fs and PCDD/Fs from Individual Gas-Phase Pyrolysis of 2-MBP and 2-MCP with the 50:50 Mixture of 2-MCP and 2-MBP

concentrations of Cl• at 700ºC with the presence of bromine (2-MBP) in the system (Table 5.1). The presence of Br_2 generates more Cl• by reaction 2 with a rate coefficient, k_2 (293-333 K) = $4.5 \times 10^{12}\exp(-6.9\ \text{kcal/RT})\ \text{cm}^3/\text{mol/s}$ [1, 9].

$Br\bullet + Cl_2 \rightarrow BrCl + Cl\bullet$ (Reaction 2)

Since Br_2 readily decomposes to Br•, the reaction of Br• with Cl_2 will form the BrCl and Cl•. In addition, BrCl will generate more Cl• than Cl_2. However 4,6- DBDF remains undetected since

the bromophenoxyl radicals predominately react to form DD due to the exothermicity of the reaction of 2-MBP to form DD (Figure 5.4).

- Chlorination is increased with the addition of oxygen due to the increase in concentration of Cl•.

Chlorination is evident with the presence of 2-bromo-4-chlorophenol for both the oxidation and pyrolysis of the mixture of 2-MBP and 2-MCP. The increase in Cl• via reaction 2 facilitates chlorination.

- The yields of PCDD/Fs are decreased with the addition of oxygen and bromine due to the slight decrease in the concentration of •OH and Cl•, which facilitate hydrogen abstraction reactions.

The yield of 4,6-DCDF and 1-MCDD are decreased for the mixture of 2-MCP and 2-MBP compared to the oxidation of pure 2-MCP (Figure 5.6). The presence of bromine lowers the yields of 1-MCDD and 4,6-DCDF by reducing the concentration of both Cl• and •OH in comparison with the oxidation of pure 2-MCP (Table 5.1). In addition, the concentration of Cl_2 decreases significantly in the presence of oxygen and bromine. This will also lower the availability of Cl• since Cl_2 readily dissociates to Cl• [1, 4]. At 500°C, based the pseudo equilibrium calculations, the percent of total chlorine that is Cl_2 is 1.5x less than for the oxidation of pure 2-MCP (Table 5.1). The presence of Cl• also increases the concentration Br• by also reacting with HBr to form HCl and Br• (Reaction 3) with a rate coefficient of k (228 - 368 K) = $1.2 \times 10^{13} \exp(-0.71/RT)$ $cm^3/mol/s$ [1, 10].

$Cl\bullet + HBr \rightarrow HCl + Br\bullet$ (Reaction 3)

Therefore, reaction 3 not only increases the concentration of Br•, but also decreases the concentration of Cl•, a characteristic confirmed in our pseudo-equilibrium calculations.

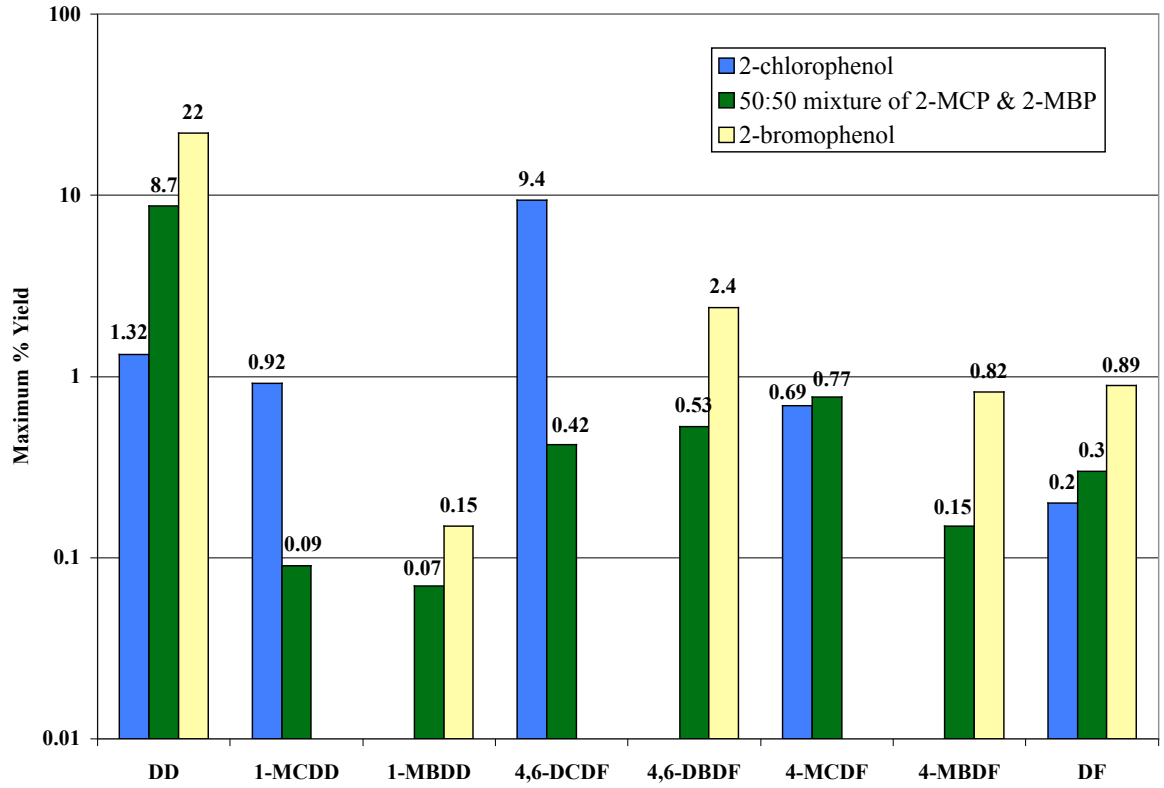

Figure 5.6 Comparison of PBDD/Fs and PCDD/Fs from Individual Gas-Phase Oxidation of 2-MBP and 2-MCP with the 50:50 Mixture of 2-MCP and 2-MBP

The pseudo-equilibrium calculations also reveal a very small decrease in concentration of •OH in comparison with the oxidation of pure 2-MCP (Table 5.1). The calculations also indicate that the concentration of •OH is considerably less than the concentrations of Cl• and Br• for the mixture and thus will play a smaller role in the formation of PCDFs and PBDFs. Bromine can lower •OH by reaction 4.

$HBr + \bullet OH \rightarrow H_2O + Br\bullet$ (Reaction 4)

The rate coefficient for reaction 4 is k_4 (200-420 K) = 6.62×10^{12} $cm^3/mol/s$ versus the slower reaction with HCl (k (300-700 K) = 1.77×10^{12} exp(-3708/RT) $cm^3/mol/s$) [1, 5, 11]. Therefore there is a decrease in the formation of 4,6-DCDF and 1-MCDD because •OH and Cl• play an important role in the formation of 4,6-DCDF and 1-MCDD in the mixture whereas 4,6-DBDF

only exhibits a decrease that is explained by the use of a lower concentration of 2-MBP.

5.2 Surface Mediated versus Gas-Phase Reactions

PBDDs were observed at yields greater than the PBDFs. In fact unlike 2-MCP, the expected 4,6-DBDF for 2-MBP was never detected for the surface-mediated gas-phase conditions (Figure 5.7). In addition PBDDs are observed in greater yields than the analogous PCDDs, with the yields of DD being 200 times greater for 2-MBP than 2-MCP under oxidative conditions. There is also an increase in bromination for 2-MBP compared to 2-MCP with the presence of polybrominated phenols and polybrominated benzenes.

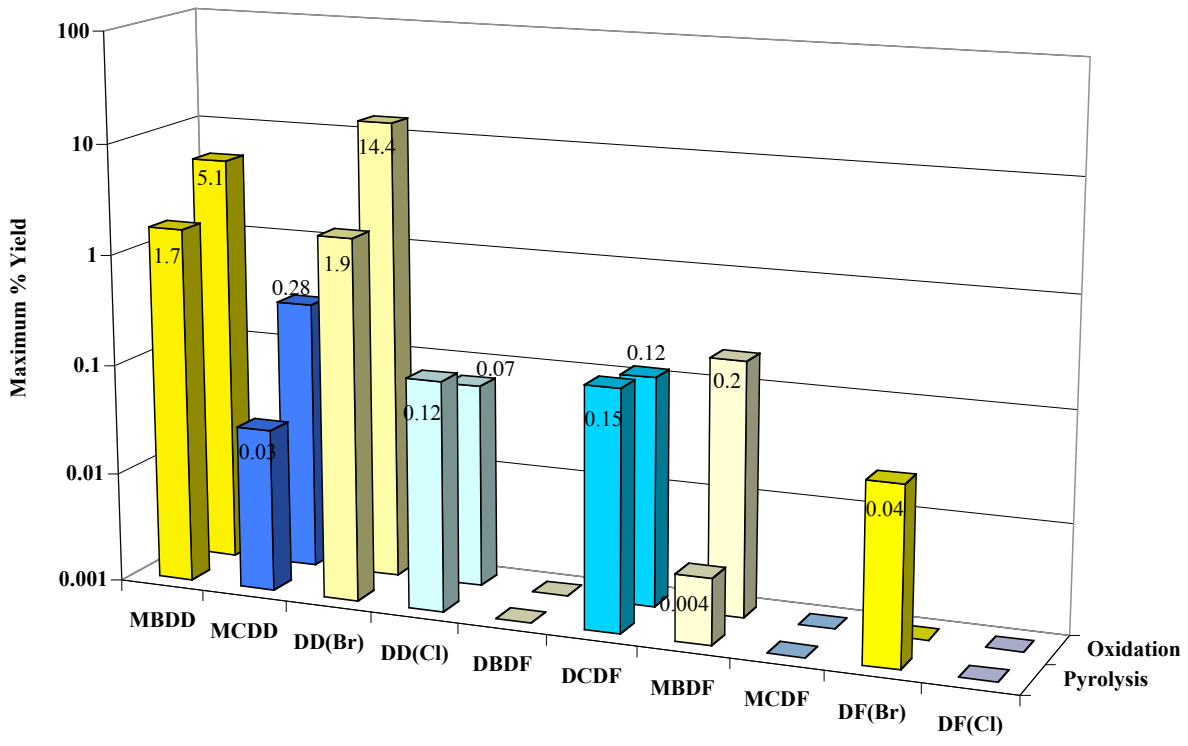

Figure 5.7 Comparison of the PCDD/Fs and PBDD/Fs from the Surface-Mediated Pyrolysis and Oxidation of 2-MBP and 2-MCP

5.2.1 Difference between 2-Chlorophenol and 2-Bromophenol

- PBDDs formed at higher yields than PCDDs due to bromine acting as a better leaving group than chlorine.

The results of the surface-mediated formation of PCDD/Fs are similar to the results for gas-phase PCDD/Fs formation in that 4,6-DCDF was observed and the yields of DD for 2-MCP are significantly lower than the yields observed for 2-MBP [12-13]. The Eley-Rideal mechanism is the favored route to form PBDDs for 2-MBP. For the Eley-Rideal mechanism, bromine greatly assists in the formation of the PBDDs by acting as a good leaving group (Figure 5.8). Since the

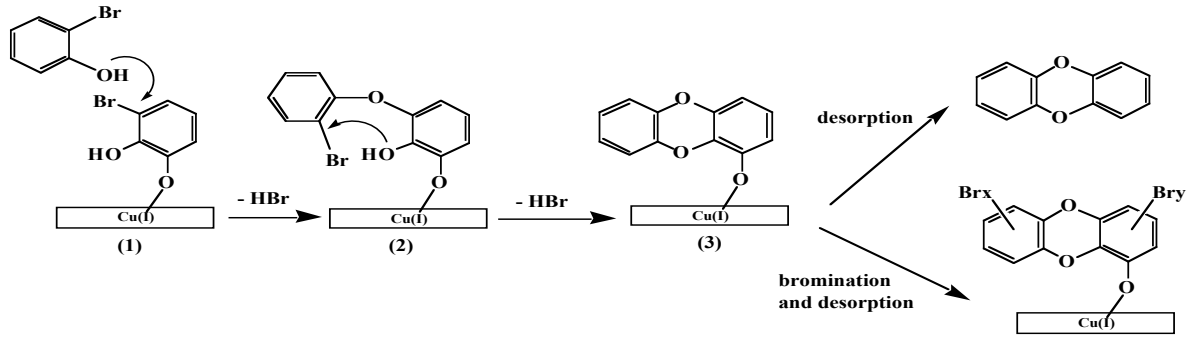

Figure 5.8 Eley-Rideal Mechanism for DD and PBDDs Formation

Carbon-bromine bond strength is lower than the carbon-chlorine bond strength, bromine is a better leaving group than chlorine [6]. PBDDs were formed in higher yields, indicating that the Eley-Rideal pathways to form PBDDs are not favorable for 2-MBP (Figure 5.9).

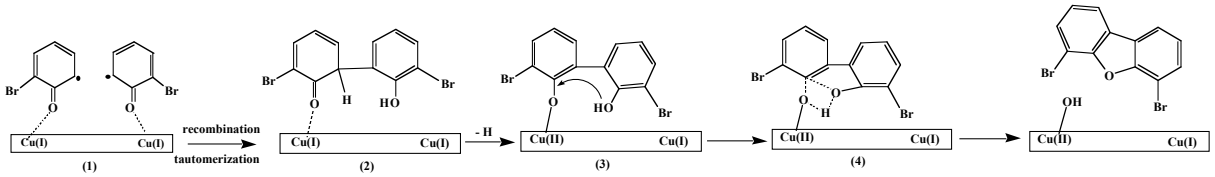

Figure 5.9 Langmuir-Hinshelwood Mechanism for 4,6-DBDF Formation

In contrast, bromine has very little effect on the formation of PBDFs. Bromine does not

play a role in the Langmuir-Hinshelwood mechanism and thus the formation of PBDFs is effected and less likely than formation of PBDDs.

The Eley-Rideal and the Langmuir-Hinshelwood mechanisms are in direct competition with each other in that they both require an adsorbed species to form the final product. However for the Eley-Rideal mechanism, only one adsorbed species is required to form PBDFs. This lowers the number of available sites and thus lowers the potential for the Langmuir-Hinshelwood mechanism to form PBDFs. Therefore one would expect, as observed, that the PBDD to PBDF ratio would be much greater than the PCDD to PCDF ratio.

5.2.2 The Effect of the Addition of Oxygen

- The maximum yields of PBDDs shift to higher temperatures with the addition of oxygen due to the increase in concentration of polybrominated phenols formed by surface bromination by hypobromites that decompose at higher temperatures..

With the addition of oxygen, the yields of PBDDs are increased by 5x over the pyrolysis of 2-MBP. This is due to the increase in Br• concentration and the regeneration of the copper oxide surfaces in the presence of excess oxygen. The dibromophenols are observed in high yields at low temperatures. As the temperatures increase, they decrease in yield and the formation of PBDDs increase. Therefore it is more probable the PBDDs are formed after the bromination of 2-MBP rather than from bromination of DD. However, the increase in PBDDs for 2-MBP under oxidative conditions over pyrolytic is not as great as the increase in PCDDs observed for 2-MCP [12-13]. The possible reasoning for this is that the presence of the surface hypochlorite species (Cu-O-Cl) allows for the increase in chlorination whereas the analogous surface hypobromite species (Cu-O-Br) will not be as effective because the Cu-O-Br species may not be as stable on the surface due to the O-Br bonds not being as strong. In addition, the

presence of reactive bromine species is already in higher concentrations with Br_2 being the dominant source of Br• versus the analogous Cl• whose dominant source is HCl [7].

5.2.3 Difference Between Gas-Phase and Surface-Mediated Gas-Phase Conditions

- The yields of the polybrominated phenols, PBDDs (and analogous chlorine compounds) increase due to surface associated species that increase the rate of bromination.

PBDD/Fs and PCDD/Fs are formed at lower temperatures for the surface-mediated reactions. The yields of DD are lower for the surface-mediated conditions than for the gas-phase. However surface-mediated conditions facilitate the formation of higher brominated PBDDs and higher chlorinated PCDDs. Therefore some of the DD that is formed on the surface is brominated or chlorinated to form the higher PBDDs and PCDDs. This is attributed to surface hypochlorite species (Cu-O-Cl) [12-13] and surface hypbromite (Cu-O-Br). However, the increase in bromination is not as great as chlorination due to surface hypobromite species (Cu-O-Br) being less stable at higher temperatures.

5.3 Summary

In conclusion, bromine plays a very important role in the formation of PBDD/Fs and PCDD/Fs. This study demonstrates some of the effects brominated hydrocarbons have on the overall distribution and formation of PCDD/Fs as well as PBDD/Fs. Clearly, bromine inhibits complete combustion creating more combustion by-products that will lead to the formation of PCDD/Fs and PBDD/Fs as well as PAHs. In addition bromine increases the concentration of Cl• present in the system that facilitates in the formation of the PCDD/Fs. However all of these studies have shown that DD is the major product detected when bromine is present. Since the initial reactant used was a simple precursor to PBDD/F formation, higher brominated phenols will only lead to higher brominated DDs.

Mechanistic rationales have also been identified for the differences in product distribution, PCDD to PCDF branching ratios as well as PBDD to PBDF branching ratios for oxidative versus pyrolytic conditions. These results have implications in the mechanism of molecular growth and particle formation from resonance stabilized radicals such as cyclopentadienyl and phenoxyl radicals and their derivatives. Reaction kinetic models are needed to better understand the competition between molecular growth pathways to form PAH and the relative yield of PCDD/F products and PBDD/F products. These results, mechanisms, and reaction kinetic codes can serve as a model for the formation of PCDD/Fs and PBDD/Fs from the range of chlorinated and brominated phenols present in full-scale combustors.

5.4 References

1. NIST Chemical Kinetics Database 17, Gaithersburg, MD, 1998.

2. He, Y.Z.; Mallard, W.G.; Tsang, W. *Kinetics of Hydrogen and Hydroxyl Radical Attack on Phenol at High Temperatures*, Journal of Physical Chemistry, 1988, **92**:

3. Koch, R.; Stucken, D-V.; Wagner, H.G. *Reactions of Aromatic Ethers with Atomic Oxygen O(3P) in the Gas Phase*, 24th Symposium (International) on Combustion, The Combustion Institute, 1992, 675.

4. Huybrechts, G.; Narmon, M.; Van Mele, B. *The pyrolysis of CCl_4 and C_2Cl_6 in the Gas Phase. Mechanistic Modeling by Thermodynamic and Kinetic Parameter Estimation* International Journal of Chemical Kinetics, 1996, **28:** 27.

5. Husain, D.; Plane, J.M.C.; Xiang, C.C. *Kinetic Studies of the Reactions of OH(X2II) with Hydrogen Chloride and Deuterium Chloride at Elevated Temperatures by Time-Resolved Resonance Fluorescence*, Journal of Chemical Society, Faraday Transition 2, 1984, **80**: 713.

6. McMillen, D. F.; Golden, D. M. *Hydrogen Bond Dissociation Energies*, Annual Review Physical Chemistry, 1982, **33**: 493.

7. Soderstrom, G.; Marklund, S. *PBCDD and PBCDF from Incineration of Waste-Containing Brominated Flame Retardants*, Environmental Science and Technology,

2002, **36**: 1959.

8. Kanters, J.; Louw, R. *Thermal and Catalysed Halogenation in Combustion Reactions*, Chemosphere, 1996, **32**(1): 87.

9. Christie, M.I.; Roy, R.S.; Thrush, B.A. *The Photochemical Reaction between Bromine and Chlorine*, Transaction Faraday Society, 1955, **55**:

10. Dobis, O.; Benson, S.W. *Temperature Coefficients of Rates of Ethyl Radical Reactions with HBr and Br in the 228-368 K Temperature Range at Millitorr Pressures*, Journal of Physical Chemistry A, 1997, **101**: 6030.

11. Atkinson, R.; Baulch, D.L., Cox, R.A.; Crowley, J.N.; Hampson, R.F, Jr.; Kerr, J.A.; Rossi, M.J.; Troe, J. *Summary of Evaluated Kinetic and Photochemical Data for Atmospheric Chemistry*, IUPAC Subcommittee on Gas Kinetic Data Evaluation for Atmospheric Chemistry Web Version December 2001.

12. Lomnicki, S.; Dellinger, B. *Formation of PCDD/F from the Pyrolysis of 2-Chlorophenol on the Surface of Dispersed Copper Oxide Particles*, 29th Symposium (International) on Combustion, The Combustion Institute, 2003, in press.

13. Lomnicki, S.; Dellinger, B. *A Detailed Mechanism of the Surface-Mediated Formation of PCDD/F from the Oxidation of 2-Chlorophenol on a CuO/Silica Surface*, Journal of Physical Chemistry A, 2003, **107**: 4387.

APPENDIX 1. CALCULATED ΔH_{rxns} FOR REACTIONS

1. Decompostion of 2-MCP and 2-MBP

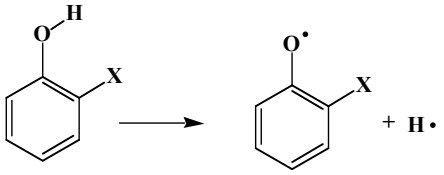

ΔH_{rxns}	
X = Cl	X = Br
78 kcal/mol	79 kcal/mol

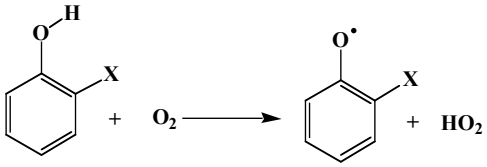

28 kcal/mol	31 kcal/mol

2. Propagation Reactions

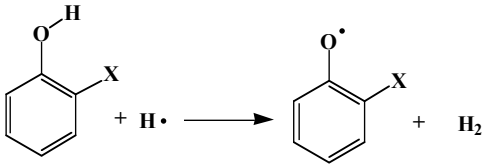

-25 kcal/mol	-23 kcal/mol

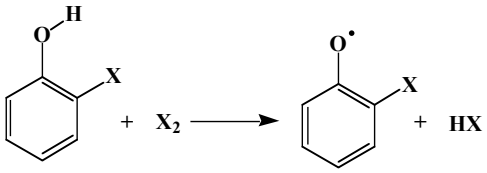

-25 kcal/mol	-8 kcal/mol

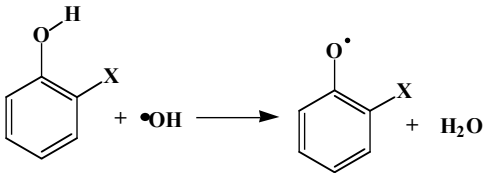

-42 kcal/mol	-39 kcal/mol

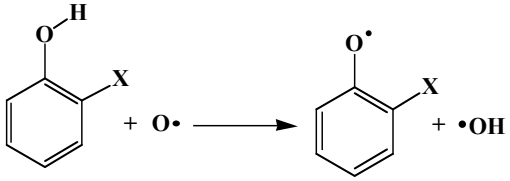

-25kcal/mol	-22 kcal/mol

3. Formation of Phenol and Benzenes

	ΔH_{rxns}	
	X = Cl	X = Br
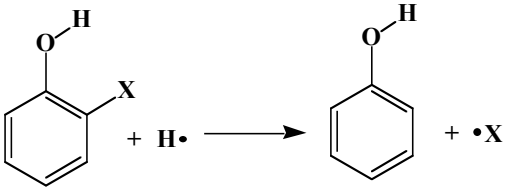	-17 kcal/mol	-29 kcal/mol
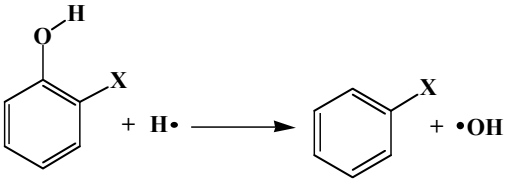	0 kcal/mol	2 kcal/mol
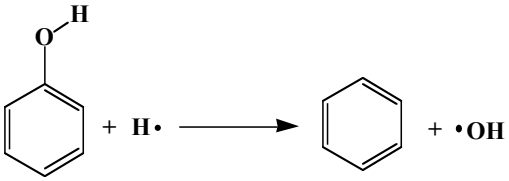	4 kcal/mol	4 kcal/mol

4. Miscelleneous Propagation reactions

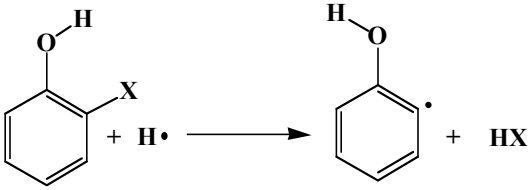	-14 kcal/mol	-11 kcal/mol
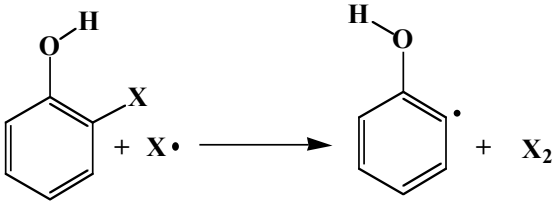	30 kcal/mol	22 kcal/mol
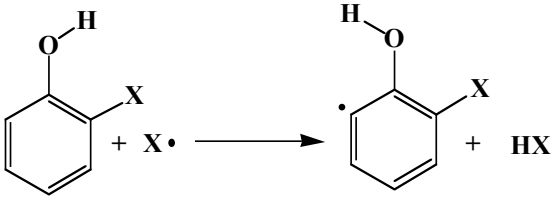	1 kcal/mol	19 kcal/mol

5. Formation of 2,4 and 2,6 – Dibromophenols and Dichlorophenols

ΔH_{rxns}

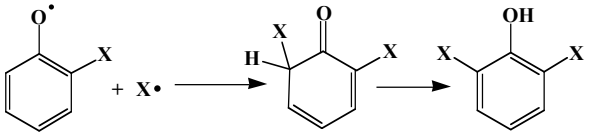

X = Cl	X = Br
-17 kcal/mol	-16 kcal/mol

Cl = -42 kcal/mol
Br = -29 kcal/mol

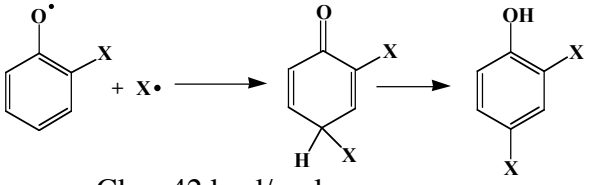

-20 kcal/mol	-18 kcal/mol

Cl = -42 kcal/mol
Br = -29 kcal/mol

6. Formation of DD

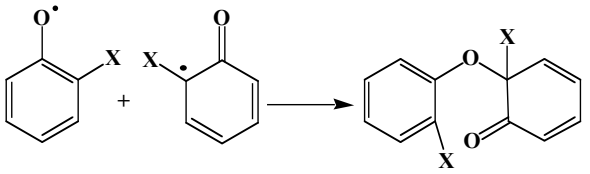

-3 kcal/mol	-1 kcal/mol

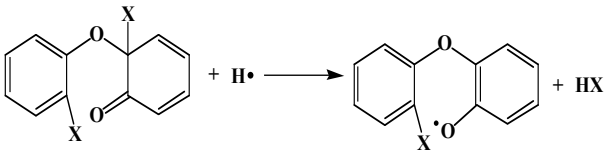

-64 kcal/mol	-56 kcal/mol

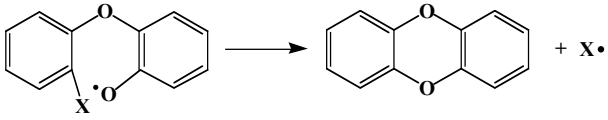

12 kcal/mol	-12 kcal/mol

7. Formation of 1-MCDD and 1-MBDD

	ΔH_{rxns}	
	X = Cl	X = Br
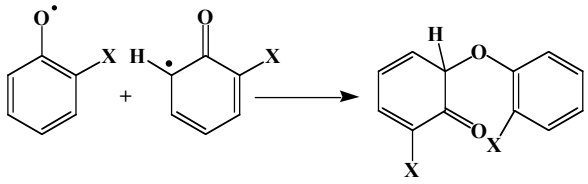	2 kcal/mol	-11 kcal/mol
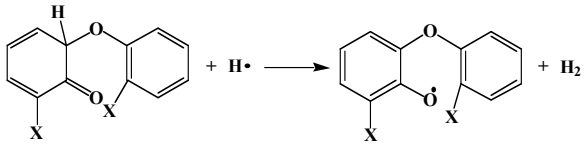	-42 kcal/mol	-30 kcal/mol
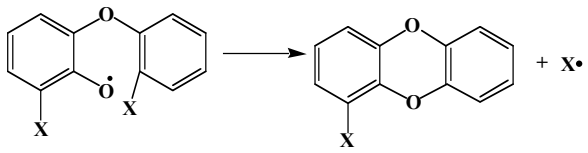	20 kcal/mol	5 kcal/mol

8. Formation of 4,6-DCDF and 4,6-DBDF

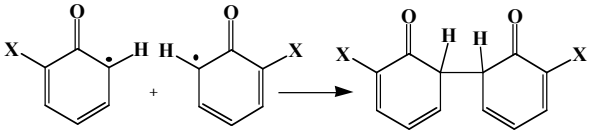	-11 kcal/mol	-12 kcal/mol
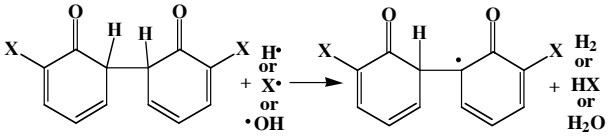	-42 kcal/mol -43 kcal/mol -59 kcal/mol	-30 kcal/mol -15 kcal/mol -46 kcal/mol
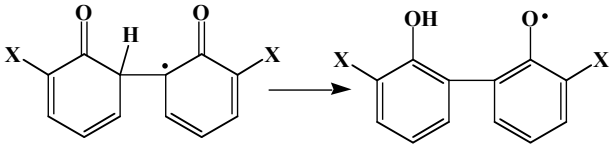	-6 kcal/mol	-17 kcal/mol
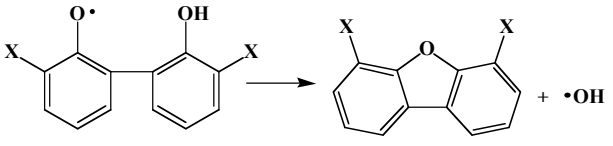	48 kcal/mol	45 kcal/mol

9. Formation of 4-MCDF or 4-MBDF

	ΔH_{rxns}	
	X = Cl	X = Br
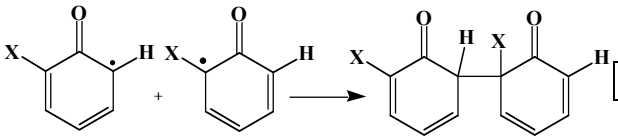	-2 kcal/mol	3 kcal/mol
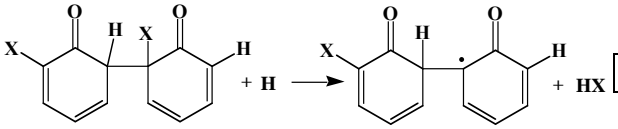	-93 kcal/mol	-61 kcal/mol

OR

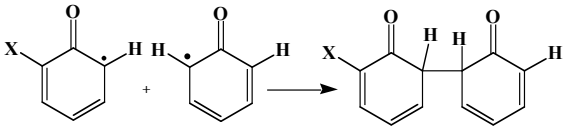	-12 kcal/mol	-13 kcal/mol
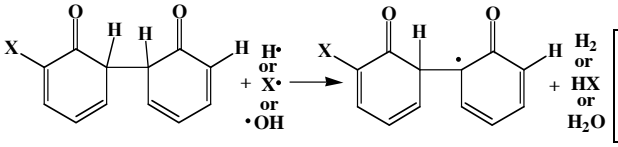	-66 kcal/mol -88 kcal/mol -83 kcal/mol	-30 kcal/mol -15 kcal/mol -46 kcal/mol

TO

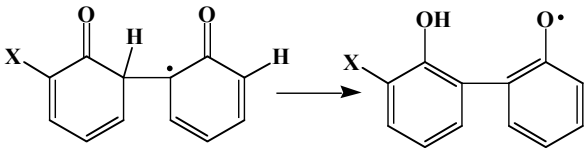	-18 kcal/mol	-17 kcal/mol
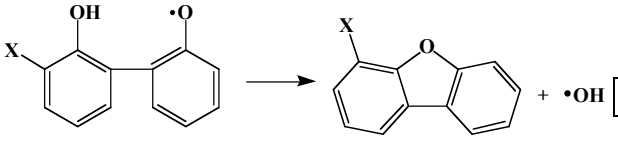	83 kcal/mol	45 kcal/mol

APPENDIX 2. PSEUDO EQUILIBRIUM CALCULATIONS

1. Pseudo Equilibrium Calculations for Pyrolysis of 2-Chlorophenol

$[C_6H_5ClO]$ 8.8E-5
$[N_2]$ 1.0
TEMP 570 K

MIXTURE:	INITIAL STATE:	EQUILIBRIUM STATE:
Mol Fractions		
H_2O	9.9990E-06	8.2244E-14
CO	0.0000E+00	1.1999E-05
CO_2	0.0000E+00	3.0101E-12
H_2	0.0000E+00	1.3998E-05
HCl	0.0000E+00	1.9998E-06
C_6H_5ClO	8.7991E-05	8.5990E-05

TEMP 770 K

MIXTURE:	INITIAL STATE:	EQUILIBRIUM STATE:
Mol Fractions		
H_2O	9.9990E-06	1.1090E-16
CO	0.0000E+00	1.1999E-05
H_2	0.0000E+00	1.3998E-05
HCl	0.0000E+00	1.9998E-06
C_6H_5ClO	8.7991E-05	8.5990E-05

TEMP 970 K

MIXTURE:	INITIAL STATE:	EQUILIBRIUM STATE:
Mol Fractions		
H	0.0000E+00	3.7077E-12
H_2O	9.9990E-06	2.2152E-18
CO	0.0000E+00	1.1999E-05
H_2	0.0000E+00	1.3998E-05
HCl	0.0000E+00	1.9998E-06
C_6H_5ClO	8.7991E-05	8.5990E-05

TEMP 1270 K

MIXTURE:	INITIAL STATE:	EQUILIBRIUM STATE:
Mol Fractions		
Cl	0.0000E+00	3.0769E-10
H	0.0000E+00	2.5346E-09
H_2O	9.9990E-06	6.2981E-20
CO	0.0000E+00	1.1999E-05
H_2	0.0000E+00	1.3997E-05
HCl	0.0000E+00	1.9995E-06
C_6H_5ClO	8.7991E-05	8.5990E-05

2. Pseudo Equilibrium Calculations of the Pyrolysis of 2-Bromophenol

$[C_6H_5BrO]$ 8.8E-5
$[N_2]$ 1.0
TEMP 570 K

MIXTURE:	INITIAL STATE:	EQUILIBRIUM STATE:
Mol Fractions		
H_2O	9.9990E-06	6.8149E-14
CO	0.0000E+00	1.1999E-05
CO_2	0.0000E+00	2.4942E-12
H_2	0.0000E+00	1.3998E-05
HBr	0.0000E+00	1.9998E-06
C_6H_5BrO	8.7991E-05	8.5990E-05

TEMP 770 K

MIXTURE:	INITIAL STATE:	EQUILIBRIUM STATE:
Br	0.0000E+00	9.0959E-12
H_2O	9.9990E-06	9.6172E-17
CO	0.0000E+00	1.1999E-05
H_2	0.0000E+00	1.3998E-05
HBr	0.0000E+00	1.9998E-06
C_6H_5BrO	8.7991E-05	8.5990E-05

TEMP 970 K

MIXTURE:	INITIAL STATE:	EQUILIBRIUM STATE:
Br_2	0.0000E+00	4.0836E-12
Br	0.0000E+00	1.1883E-09
H	0.0000E+00	3.7078E-12
H_2O	9.9990E-06	1.9901E-18
CO	0.0000E+00	1.1999E-05
H_2	0.0000E+00	1.3999E-05
HBr	0.0000E+00	1.9986E-06
C_6H_5BrO	8.7991E-05	8.5990E-05

TEMP 1270 K

MIXTURE:	INITIAL STATE:	EQUILIBRIUM STATE:
Br_2	0.0000E+00	3.5279E-11
Br	0.0000E+00	9.7833E-08
H	0.0000E+00	2.5390E-09
H_2O	9.9990E-06	5.8767E-20
CO	0.0000E+00	1.1999E-05
H_2	0.0000E+00	1.4046E-05
HBr	0.0000E+00	1.9019E-06
C_6H_5BrO	8.7991E-05	8.5990E-05

3. Pseudo Equilibrium Calculations for the Pyrolysis of 2-Chlorophenol and 2-Bromophenol

$[C_6H_5BrO]$ 4.2E-5
$[C_6H_5ClO]$ 4.2E-5
$[N_2]$ 1.0
TEMP 570 K

MIXTURE:	INITIAL STATE:	EQUILIBRIUM STATE:
Mol Fractions		
H_2O	9.9990E-06	7.3351E-14
CO	0.0000E+00	8.8429E-05
CO_2	0.0000E+00	4.3863E-04
H_2	0.0000E+00	1.0535E-03
HBr	0.0000E+00	4.3921E-05
HCl	0.0000E+00	4.3921E-05
C_6H_5BrO	4.3952E-05	3.0969E-31
C_6H_5ClO	4.3952E-05	7.9395E-31

TEMP 770 K

MIXTURE:	INITIAL STATE:	EQUILIBRIUM STATE:
Mol Fractions		
Br_2	0.0000E+00	2.5094E-12
Br	0.0000E+00	2.3625E-11
H_2O	9.9990E-06	1.0205E-16
CO	0.0000E+00	2.1724E-04
CO_2	0.0000E+00	3.0982E-04
H_2	0.0000E+00	9.2472E-04
HBr	0.0000E+00	4.3921E-05
HCl	0.0000E+00	4.3921E-05
C_6H_5BrO	4.3952E-05	0.0000E+00
C_6H_5ClO	4.3952E-05	0.0000E+00

TEMP 970 K

MIXTURE:	INITIAL STATE:	EQUILIBRIUM STATE:
Mol Fractions		
Br_2	0.0000E+00	3.2855E-11
Br	0.0000E+00	3.3045E-09
Cl	0.0000E+00	1.3720E-12
H	0.0000E+00	2.7446E-11
H_2O	9.9990E-06	2.0854E-18
CO	0.0000E+00	3.1295E-04
CO_2	0.0000E+00	2.1410E-04
H_2	0.0000E+00	8.2900E-04
HBr	0.0000E+00	4.3918E-05
HCl	0.0000E+00	4.3921E-05
C_6H_5BrO	4.3952E-05	0.0000E+00
C_6H_5ClO	4.3952E-05	0.0000E+00

TEMP 1270 K

MIXTURE:	INITIAL STATE:	EQUILIBRIUM STATE:
Mol Fractions		
Br_2	0.0000E+00	3.4465E-10
Br	0.0000E+00	3.0217E-07
Cl	0.0000E+00	9.0231E-10
H	0.0000E+00	1.8128E-08
H_2O	9.9990E-06	6.0666E-20
CO	0.0000E+00	3.9190E-04
CO_2	0.0000E+00	1.3516E-04
H_2	0.0000E+00	7.5020E-04
HBr	0.0000E+00	4.3618E-05
HCl	0.0000E+00	4.3920E-05
C_6H_5BrO	4.3952E-05	0.0000E+00
C_6H_5ClO	4.3952E-05	0.0000E+00

4. Pseudo Equilibrium Calculations for the Oxidation of 2-Chlorophenol

$[C_6H_5ClO]$ 8.8E-5
$[O_2]$ 0.2
$[N_2]$ 0.79
TEMP 570 K
PRES 1

MIXTURE:	INITIAL STATE:	EQUILIBRIUM STATE:
Mol Fractions		
O_2	2.0200E-01	2.0138E-01
H_2O	0.0000E+00	2.1358E-04
N_2	7.9791E-01	7.9782E-01
CO_2	0.0000E+00	5.3322E-04
Cl_2	0.0000E+00	3.5835E-05
HCl	0.0000E+00	1.7202E-05
Cl	0.0000E+00	4.6494E-11
C_6H_5ClO	8.8881E-05	0.0000E+00

TEMP 770 K

MIXTURE:	INITIAL STATE:	EQUILIBRIUM STATE:
Mol Fractions		
O_2	2.0200E-01	2.0139E-01
OH	0.0000E+00	1.9067E-11
H_2O	0.0000E+00	1.9504E-04
N_2	7.9791E-01	7.9781E-01
CO_2	0.0000E+00	5.3322E-04
Cl_2	0.0000E+00	1.7292E-05
HCl	0.0000E+00	5.4262E-05
Cl	0.0000E+00	2.2941E-08

C_6H_5ClO	8.8881E-05	0.0000E+00

TEMP 970 K

MIXTURE:	INITIAL STATE:	EQUILIBRIUM STATE:
Mol Fractions		
O_2	2.0200E-01	2.0140E-01
O	0.0000E+00	3.5125E-11
OH	0.0000E+00	3.1139E-09
HO_2	0.0000E+00	2.6875E-11
H_2O	0.0000E+00	1.8380E-04
N_2	7.9791E-01	7.9780E-01
CO_2	0.0000E+00	5.3322E-04
Cl_2	0.0000E+00	5.7283E-06
HCl	0.0000E+00	7.6753E-05
Cl	0.0000E+00	6.5978E-07
C_6H_5ClO	8.8881E-05	0.0000E+00

TEMP 1270 K

MIXTURE:	INITIAL STATE:	EQUILIBRIUM STATE:
Mol Fractions		
H_2	0.0000E+00	2.3546E-11
H	0.0000E+00	3.7122E-12
O_2	2.0200E-01	2.0139E-01
O	0.0000E+00	5.2260E-08
OH	0.0000E+00	3.4044E-07
HO_2	0.0000E+00	1.2524E-09
H_2O	0.0000E+00	1.8372E-04
N_2	7.9791E-01	7.9780E-01
H_2O_2	0.0000E+00	3.9659E-12
CO	0.0000E+00	1.1431E-10
CO_2	0.0000E+00	5.3321E-04
Cl_2	0.0000E+00	1.0294E-06
HCl	0.0000E+00	7.6571E-05
Cl	0.0000E+00	1.0239E-05
C_6H_5ClO	8.8881E-05	0.0000E+00

5. Pseudo Equilibrium Calculations for the Oxidaiton of 2-Bromophenol

$[C_6H_5BrO]$ 8.8E-5
$[O_2]$ 0.2
$[N_2]$ 0.79
TEMP 570 K
PRES 1

MIXTURE:	INITIAL STATE:	EQUILIBRIUM STATE:
Mol Fractions		
O_2	2.0200E-01	2.0138E-01

H_2O	0.0000E+00	2.2218E-04
N_2	7.9791E-01	7.9782E-01
CO_2	0.0000E+00	5.3323E-04
Br_2	0.0000E+00	4.4435E-05
HBr	0.0000E+00	1.8191E-10
Br	0.0000E+00	3.0166E-10
C_6H_5BrO	8.8881E-05	0.0000E+00

TEMP 770 K

MIXTURE:	INITIAL STATE:	EQUILIBRIUM STATE:
Mol Fractions		
O_2	2.0200E-01	2.0138E-01
OH	0.0000E+00	2.0494E-11
H_2O	0.0000E+00	2.2217E-04
N_2	7.9791E-01	7.9782E-01
CO_2	0.0000E+00	5.3323E-04
Br_2	0.0000E+00	4.4365E-05
HBr	0.0000E+00	1.6993E-08
Br	0.0000E+00	1.2319E-07
C_6H_5BrO	8.8881E-05	0.0000E+00

TEMP 970 K

MIXTURE:	INITIAL STATE:	EQUILIBRIUM STATE:
Mol Fractions		
O_2	2.0200E-01	2.0138E-01
O	0.0000E+00	3.5374E-11
OH	0.0000E+00	3.4383E-09
HO_2	0.0000E+00	2.9649E-11
H_2O	0.0000E+00	2.2205E-04
N_2	7.9791E-01	7.9782E-01
CO_2	0.0000E+00	5.3323E-04
Br_2	0.0000E+00	4.2175E-05
HBr	0.0000E+00	2.4486E-07
Br	0.0000E+00	4.2763E-06
C_6H_5BrO	8.8881E-05	0.0000E+00

TEMP 1270 K

MIXTURE:	INITIAL STATE:	EQUILIBRIUM STATE:
Mol Fractions		
H_2	0.0000E+00	2.8382E-11
H	0.0000E+00	4.0797E-12
O_2	2.0200E-01	2.0137E-01
O	0.0000E+00	5.2317E-08
OH	0.0000E+00	3.7382E-07
HO_2	0.0000E+00	1.3749E-09
H_2O	0.0000E+00	2.2119E-04

N_2	7.9791E-01	7.9780E-01
H_2O_2	0.0000E+00	4.7769E-12
CO	0.0000E+00	1.1446E-10
CO_2	0.0000E+00	5.3321E-04
Br_2	0.0000E+00	1.2565E-05
HBr	0.0000E+00	1.5796E-06
Br	0.0000E+00	6.2158E-05
C_6H_5BrO	8.8881E-05	0.0000E+00

6. Pseudo Equilibrium Calculations of the Oxidation of the Mixture of 2-Chlorophenol and 2-Bromophenol

$[C_6H_5BrO]$ 4.4E-5
$[C_6H_5ClO]$ 4.4E-5
$[O_2]$ 0.2
$[N_2]$ 0.79
TEMP 570 K

MIXTURE:	INITIAL STATE:	EQUILIBRIUM STATE:
Mol Fractions		
O_2	2.0200E-01	2.0138E-01
H_2O	0.0000E+00	2.1632E-04
N_2	7.9791E-01	7.9782E-01
CO_2	0.0000E+00	5.3323E-04
Br_2	0.0000E+00	2.2218E-05
HBr	0.0000E+00	1.2654E-10
Br	0.0000E+00	2.1246E-10
C_6H_5BrO	4.4440E-05	0.0000E+00
C_6H_5ClO	4.4440E-05	0.0000E+00
Cl_2	0.0000E+00	1.6363E-05
HCl	0.0000E+00	1.1710E-05
Cl	0.0000E+00	3.1546E-11

TEMP 770 K

MIXTURE:	INITIAL STATE:	EQUILIBRIUM STATE:
Mol Fractions		
O_2	2.0200E-01	2.0139E-01
OH	0.0000E+00	1.9655E-11
H_2O	0.0000E+00	2.0587E-04
N_2	7.9791E-01	7.9781E-01
CO_2	0.0000E+00	5.3322E-04
Br_2	0.0000E+00	2.2168E-05
HBr	0.0000E+00	1.1540E-08
Br	0.0000E+00	8.6857E-08
C_6H_5BrO	4.4440E-05	0.0000E+00
C_6H_5ClO	4.4440E-05	0.0000E+00
Cl_2	0.0000E+00	5.9081E-06

HCl	0.0000E+00	3.2606E-05
Cl	0.0000E+00	1.3444E-08

TEMP 970 K

MIXTURE:	INITIAL STATE:	EQUILIBRIUM STATE:
Mol Fractions		
O_2	2.0200E-01	2.0139E-01
O	0.0000E+00	3.5243E-11
OH	0.0000E+00	3.2679E-09
HO_2	0.0000E+00	2.8192E-11
H_2O	0.0000E+00	2.0154E-04
N_2	7.9791E-01	7.9781E-01
CO_2	0.0000E+00	5.3322E-04
Br_2	0.0000E+00	2.0643E-05
HBr	0.0000E+00	1.6299E-07
Br	0.0000E+00	2.9868E-06
C_6H_5BrO	4.4440E-05	0.0000E+00
C_6H_5ClO	4.4440E-05	0.0000E+00
Cl_2	0.0000E+00	1.4969E-06
HCl	0.0000E+00	4.1103E-05
Cl	0.0000E+00	3.3784E-07

TEMP 1270 K

MIXTURE:	INITIAL STATE:	EQUILIBRIUM STATE:
Mol Fractions		
H_2	0.0000E+00	2.5907E-11
H	0.0000E+00	3.8949E-12
O_2	2.0200E-01	2.0138E-01
O	0.0000E+00	5.2274E-08
OH	0.0000E+00	3.5711E-07
HO_2	0.0000E+00	1.3136E-09
H_2O	0.0000E+00	2.0207E-04
N_2	7.9791E-01	7.9780E-01
H_2O_2	0.0000E+00	4.3625E-12
CO	0.0000E+00	1.1435E-10
CO_2	0.0000E+00	5.3321E-04
Br_2	0.0000E+00	4.0813E-06
HBr	0.0000E+00	8.6018E-07
Br	0.0000E+00	3.5411E-05
C_6H_5BrO	4.4440E-05	0.0000E+00
C_6H_5ClO	4.4440E-05	0.0000E+00
Cl_2	0.0000E+00	2.4251E-07
HCl	0.0000E+00	3.8979E-05
Cl	0.0000E+00	4.9705E-06

APPENDIX 3. COPYRIGHT PERMISSIONS

ACS PUBLICATIONS DIVISION GUIDELINES FOR THESES AND DISSERTATIONS

ATTENTION: STUDENTS, STUDENT ADVISORS, AND TEACHERS

Permission is automatically granted to include your **paper(s) or portions of** your **paper(s) in your thesis; please pay special attention to the implications paragraph below. The Copyright Subcommittee of the Joint Board/Council Committees on Publications approved the following:**

> Copyright permission for published and submitted material from theses and dissertations
> ACS extends blanket permission to students to include in their theses and dissertations their own articles, or portions thereof, that have been published in ACS journals or submitted to ACS journals for publication, provided that the ACS copyright credit line is noted on the appropriate page(s).
>
> Publishing implications of electronic publication of theses and dissertation material
> Students and their mentors should be aware that posting of theses and dissertation material on the Web prior to submission of material from that thesis or dissertation to an ACS journal may affect publication in that journal. Whether Web posting is considered prior publication may be evaluated on a case-by-case basis by the journal's editor. If an ACS journal editor considers Web posting to be "prior publication", the paper will not be accepted for publication in that journal. If you intend to submit your unpublished paper to ACS for publication, check with the appropriate editor prior to posting your manuscript electronically.

If your paper has **not** yet been published by ACS, we have no objection to your including the text or portions of the text in your thesis/dissertation in **print and microfilm formats**; please note, however, that electronic distribution or Web posting of the unpublished paper as part of your thesis in electronic formats might jeopardize publication of your paper by ACS. Please print the following credit line on the first page of your article: "Reproduced (or 'Reproduced in part') with permission from [JOURNAL NAME], in press (or 'submitted for publication'). Unpublished work copyright [CURRENT YEAR] American Chemical Society." Include appropriate information.

If your paper has already been published by ACS and you want to include the text or portions of the text in your thesis/dissertation in **print or microfilm formats**, please print the ACS copyright credit line on the first page of your article: "Reproduced (or 'Reproduced in part') with permission from [FULL REFERENCE CITATION.] Copyright [YEAR] American Chemical Society." Include appropriate information.

Note: If you plan to submit your thesis to UMI or to another dissertation distributor, you should not include the unpublished ACS paper in your thesis if the thesis will be disseminated electronically, until ACS has published your paper. After publication of the paper by ACS, you may release the entire thesis (**not the individual ACS article by itself**) for electronic dissemination; ACS's copyright credit line should be printed on the first page of the ACS paper.

SUMMARY: The inclusion of your ACS unpublished or published manuscript is permitted in your thesis in print and microfilm formats. If ACS has published your paper you may include the manuscript in your thesis on an intranet that is not publicly available. Your ACS article cannot be posted electronically on a publicly available medium, such as but not limited to, electronic archives, Internet, intranet, library server, etc. The only material from your paper that can be posted on a public electronic medium is the article abstract, figures, and tables and you may link to the article's DOI.

Questions? Please contact the ACS Publications Division Copyright Office at copyright@acs.org or at 202-872-4368.

August 1998, March 2003, October 2003

VITA

Catherine Spearing Evans was born on September 10, 1976, in Shreveport, Louisiana. She earned a bachelor of science degree from the University of the South in Sewanee, Tennessee, in 1998. Immediately she went on to pursue a doctoral degree in environmental physical chemistry at Lousisana State University in Baton Rouge, Louisiana. Her research studies entailed the study of the mechanistic gas-phase formation of PCDD/Fs and PBDD/Fs in combustion processes under the direction of Dr. Barry Dellinger. She will receive her doctor of philosophy degree in December 2004.